ISTANBUL TECHNICAL UNIVERSITY ★ INSTITUTE OF SCIENCE AND TECHNOLOGY

PREPARATION OF ACRYLATE AND SULFONAMIDE BASED POLYMERIC SORBENTS FOR SEPARATION OF BIOMOLECULES

Ph.D. Thesis by
Erdem YAVUZ

Department : Polymer Science and Technologies

Programme : Polymer Science and Technologies

SEPTEMBER 2010

ISTANBUL TECHNICAL UNIVERSITY ★ INSTITUTE OF SCIENCE AND TECHNOLOGY

PREPARATION OF ACRYLATE AND SULFONAMIDE BASED POLYMERIC SORBENTS FOR SEPARATION OF BIOMOLECULES

**Ph.D. Thesis by
Erdem YAVUZ
(515042011)**

SEPTEMBER 2010

İSTANBUL TEKNİK ÜNİVERSİTESİ ★ FEN BİLİMLERİ ENSTİTÜSÜ

BİYOMOLEKÜLLERİN AYRILMASI İÇİN SÜLFONAMİD VE AKRİLAT BAZLI POLİMERİK SORBENTLERİN HAZIRLANMASI

DOKTORA TEZİ
Erdem YAVUZ
(515042011)

Tezin Enstitüye Verildiği Tarih :	**06 Temmuz 2010**
Tezin Savunulduğu Tarih :	**16 Eylül 2010**

Tez Danışmanı :	**Prof. Dr. B. Filiz ŞENKAL (İTÜ)**
Eş Danışman :	**Prof. Dr. M. Yakup ARICA(GÜ)**
Diğer Jüri Üyeleri :	**Prof. Dr. Candan Erbil (İTÜ)**
	Doç. Dr. Yeşim GÜRSEL (İTÜ)
	Doç. Dr. Ayfer Saraç (YTÜ)
	Prof.Dr. Ümit Tunca (İTÜ)
	Prof.Dr. Ülker Beker (YTÜ)

EYLÜL 2010

FOREWORD

This study has been carried out at Istanbul Technical University, Chemistry Department of Science & Letter Faculty.

First and foremost I want to thank my supervisor, Prof.Dr. B. Filiz ŞENKAL. It has been an honor to be her first Ph.D. student. She has taught me, both consciously and unconsciously, how good experimental chemistry is done. I am heartily thankful for her gracious support, encouragement and guidance throughout my whole academic career and for providing me a peaceful environment to work at Istanbul Technical University.

I express my appreciation to my co-supervisor Prof. Dr. M. Yakup ARICA for sharing his deep knowledge, experience and continuous encouragement throughout my research and for having contributed immensely to my personal and professional time at Kırıkkale University and Gazi University.

Assoc. Prof. Dr. Gülay BAYRAMOĞLU, whom I like to give my special thanks for giving me an opportunity to share her knowledge and invaluable support.

Also special thanks go to Assoc. Prof. Dr. Yeşim Hepuzer GÜRSEL and Res. Assist. Argun Talat GÖKÇEÖREN for their support and help.

Finally, words are not enough to express my gratitude towards my family. They have been exceptionally supportive and loving during all stages of my life.

July 2010   Erdem YAVUZ
                                                                    (Chemical Engineer)

TABLE OF CONTENTS

LIST OF TABLES

LIST OF FIGURES

xiv

PREPARATION OF ACRYLATE AND SULFONAMIDE BASED POLYMERIC SORBENTS FOR SEPARATION OF BIOMOLECULES

SUMMARY

To perform the isolation, purifcation or analysis of substances, at scales ranging from tonnage quantities to picograms is an important feature of our modern life.

The polymeric sorbents are very important for separation of biomolecules, organic and inorganic wastes.

In this thesis, Hydrazine, amine, carboxylic acid and methane sulfonic acid containing resins were prepared and were characterized by using spectroscopic and analytical methods.

Hydrazine containing resin was prepared starting from crosslinked polyvinyl benzyl chloride resin (PVBC). The resin was reacted excess of hydrazine. And, CORE-SHELL type resin was synthesized by using PVBC resin as initiator for SI-ATRP graft polymerization of poly (glycidiyl methacrylate). The grafted resin was interacted with excess of hydrazine to obtain hydrazine functionality (Figure 1).
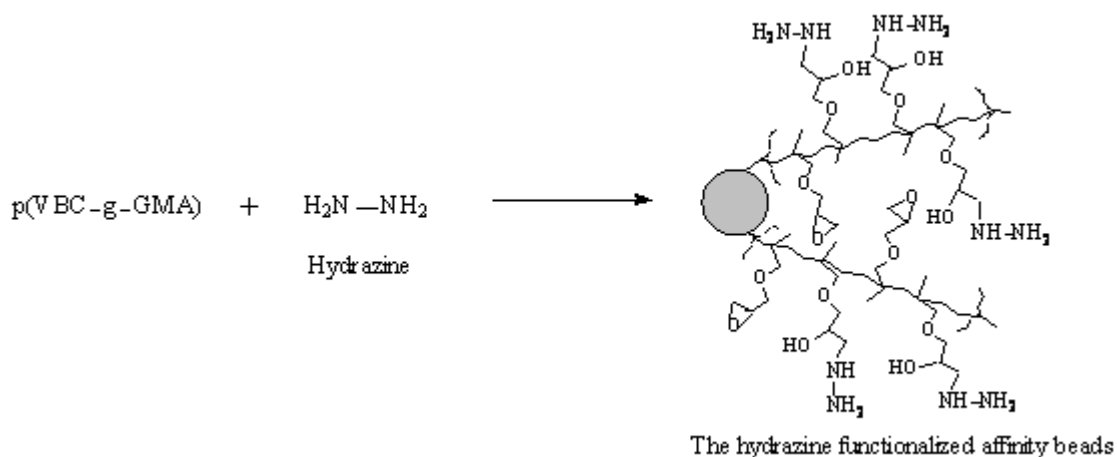
Figure 1: Preparation of the Resin1.

The hydrazine function may react with aldehydes to form hydrazone (Figure 2).
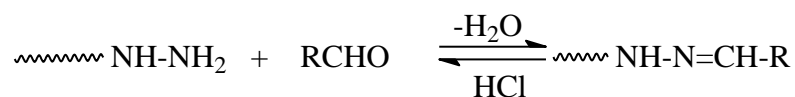
Figure 2: Hydrazine interaction with aldehyde.

Invertase enzyme has aldehyde function therefore; the resin was used to separate the enzyme selectively. Sorption properties of the Resin1 were given in Table1.

Table.1 The D–R and Freundlich isotherm constants and correlation coefficients of isotherm models for the adsorption of invertase on hydrazine-functionalized beads.

| Temperature (K) | Dubinin–Radushkevich (D–R) models constant | | | | | | Freundlich constant | model |
	q_{exp} (mg/g) R^2	q_m (mg/g)	$Kx10^5$ (mol^2/kj^2)	E(kj/mol)	n	K_F	R^2
279	54.68 0.989	59.15	9,3	2.32	0.8	51.94	0.970
289	72.86 0.989	85.88	7.7	2.55	0.9	83.93	0.944
298	86.70 0.969	87.67	5.5	3.02	1.11	111.05	0.924
308	102.10 0.950	103.54	1.5	5.72	2.13	114.16	0.957

Also, aldehyde sorption of the beads was investigated and the results were given in Table 2.

Table 2. The aldehyde sorption capacity of the Resin 1 in methanol.

Aldehyde	Capacity (mmol / g. resin)	Regeneration(mmol / g. resin)
Salicyl aldehyde	0.205	0.200
Acetaldehyde	1.756	1.746
Benzaldehyde	0.448	0.417

The methane sulfonic acid containing resin was prepared reaction with crosslinked chlorosulfonated resin and aminomethane sulfonic acid (Figure 3).
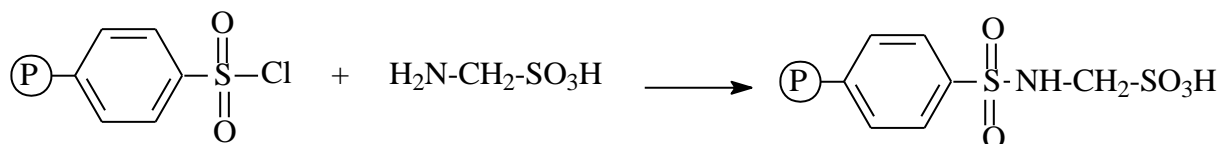
Figure 3: Preparation of aminomethane sulfonic acid containing resin.

The resin was interacted with basic dyes (crystal violet and methylene blue). The sorption properties of the resin depending on pH were given in Table 3.

Table 3. Maximum dye sorption capacites of the resin 2 depending on pH

Dye	pH	Capacity (g dye / g resin)
Methylene Blue	2	0.16
	4	0.26
	8	0.37
Crystal violet	2	-
	4	0.30
	8	0.40

Trypsin was used as a basic protein. Adsorption capacities of the Resin 2 were investigated for different pH (Figure 4) and ionic strength (Figure 5). Experimental results were well fitted with Langmiur isotherm model.
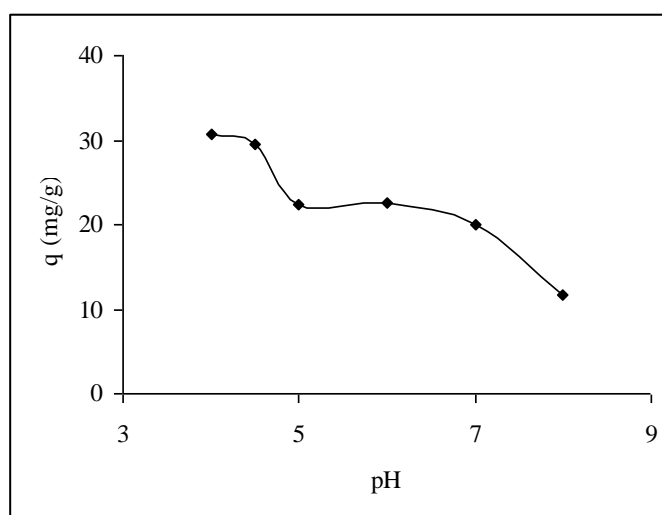
Figure 4: Effects of pH on trypsin adsorption on the Resin 3.
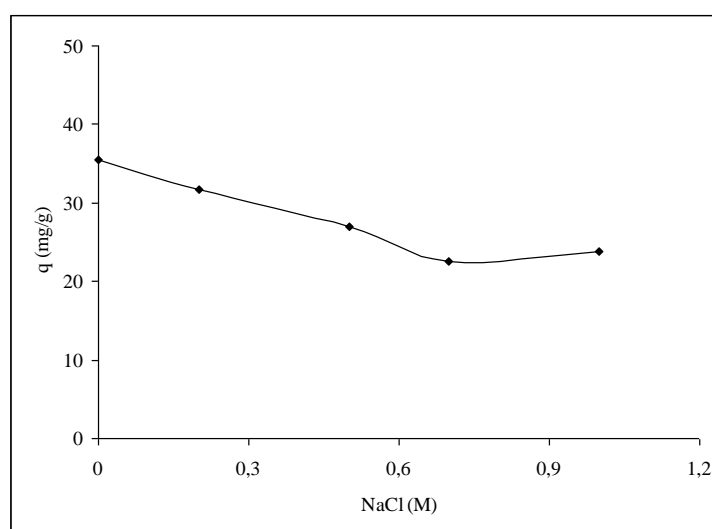
Figure 5: Effects of ionic strength on trypsin adsorption on the Resin2.

Poly (ethyl acrylate) was grafted onto PVBC by using SI-ATRP method. And, grafted resin was hydrolyzed in KOH and H_2SO_4 solutions respectively (Figure 6).
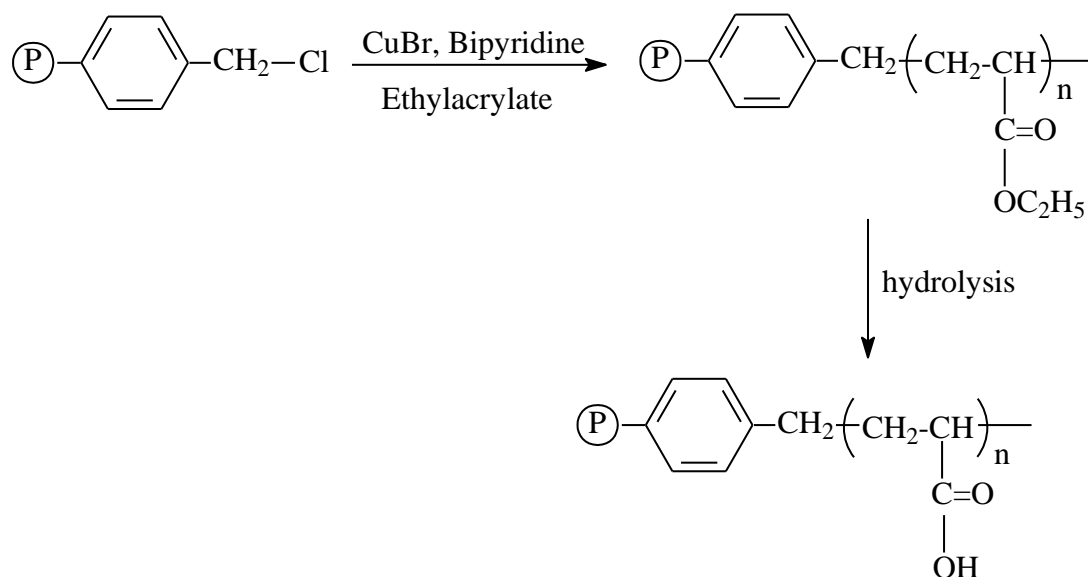
Figure 6: Preparation of the poly (acrylic acid) grafted onto PVBC resin.

The resin was interacted basic dyes. Sorption properties were given in Table 4.

Table 4: pH depending on dye sorption of the resin 3

Dye	pH	Capacity (mg dye / g resin)
Methylene Blue	4.0	210
	6.0	250
	7.0	300
	8.0	200
Crystal violet	4.0	-
	6.0	190
	7.0	250
	8.0	200

BİYOMOLEKÜLLERİN AYRILMASI İÇİN SÜLFONAMİD VE AKRİLAT BAZLI POLİMERİK SORBENTLERİN HAZIRLANMASI

ÖZET

Eser miktarlardan tonlara varan miktarlardaki maddeleri ayırmak, saflaştırmak ve analiz etmek çevre ve insan sağlığı bakımından çok önemlidir.

Polimerik sorbentler biyomoleküllerin, inorganik ve organik atıkların ayrılmasında oldukça önemlidir.

Bu tezde hidrazin, amin, karboksilik asit ve metansülfonik asit içeren reçineler hazırlanmış spektroskopik ve analitik yöntemler kullanılarak karekterize edilmiştir.

Hidrazin içeren reçine çapraz bağlı poli (vinil benzil klorür) (PVBC) reçineden başlayarak hazırlanmıştır. Reçine hidrazinin fazlasıyla reaksiyona sokulmuştur. Çekirdek-saçak tipindeki reçine, poli(glisidil metakrilat) (PGMA)' ın aşı polimerizasyonunda başlatıcı olarak PVBC'deki halojen başlatıcı grupları üzerinden SI-ATRP yöntemi kullanılarak sentezlenmiştir. PGMA aşılanmış reçine hidrazin ile modifiye etmek için hidrazinin fazlasıyla reaksiyona sokulmuştur (Şekil 1).
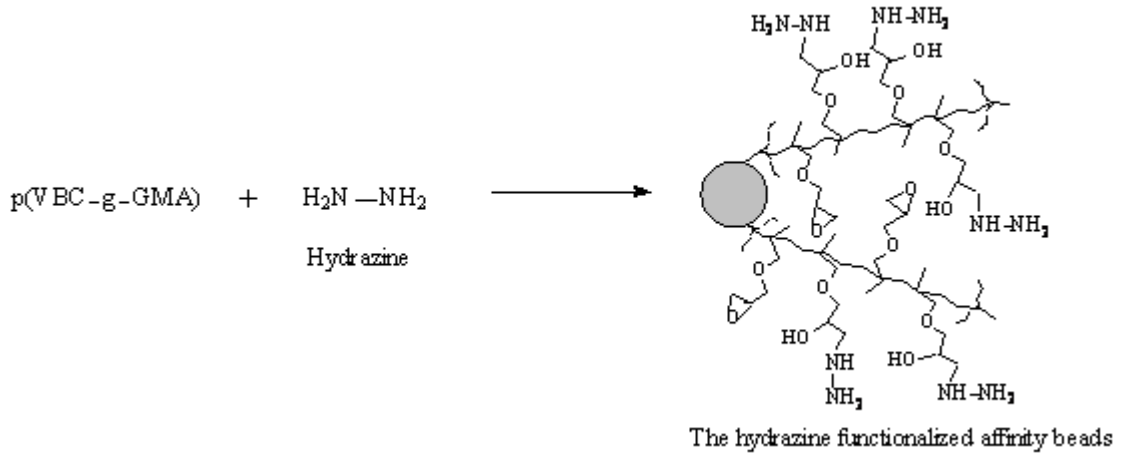
Şekil 1: Reçine 1'in hazırlanması

Hidrazin fonksiyonlu gruplar aldehidlerle hidrazon oluştururlar (Şekil 2).
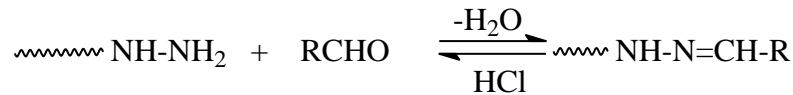
Şekil 2: Hidrazinin aldehidle etkileşimi

İnvertaz enzimi aldehid fonksiyonuna sahip olduğundan reçine invertaz enzimini seçici olarak ayırmak için kullanılmıştır. Reçine1'in adsorpsiyon özellikleri Çizelge 1'de verilmiştir.

Çizelge 1: Hidrazin fonksiyonel küreler üzerine inveraz adsorpsiyonu için izoterm modellerinin düzeltme faktörleri ve D–R ve Freundlich izoterm sabitleri.

Sıcaklık (K)	Dubinin–Radushkevich (D–R) model sabitleri				Freundlich sabitleri		model
	q_{exp} (mg/g) R^2	q_m (mg/g)	$Kx10^5$ (mol^2/kj^2)	E(kj/mol)	n	K_F	R^2
279	54.68 0.989	59.15	9.3	2.32	0.8	51.94	0.970
289	72.86 0.989	85.88	7.7	2.55	0.9	83.93	0.944
298	86.70 0.969	87.67	5.5	3.02	1.11	111.05	0.924
308	102.10 0.950	103.54	1.5	5.72	2.13	114.16	0.957

Aynı zamanda kürelerin aldehid adsorplaması incelenmiş ve sonuçlar Çizelge 2'de verilmiştir.

Çizelge 2: Reçine 1'in metanoldeki aldehid adsorplama kapasiteleri

Aldehid	Kapasite (mmol / g. reçine)	Geri kazanım (mmol / g. reçine)
Salisil aldehid	0,205	0.200
Asetaldehid	1,756	1.746
Benzaldehid	0,448	0,417

Metansülfonik asit içeren reçine (Reçine 2) klorosülfolanmış reçine ile aminometan sülfonik asitin reaksiyonuyla hazırlanmıştır (Şekil 3).
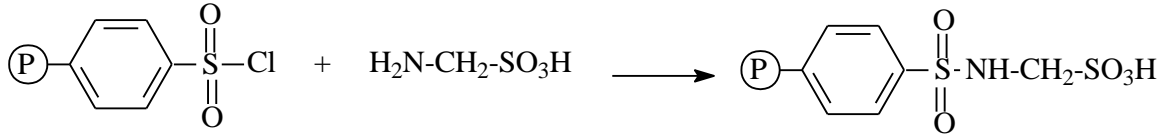
Şekil 3: Aminometan sülfonik asit içeren reçinenin hazırlanması.

Boya protein etkileşimi benzer özelliktedir. Bu nedenle Reçine 3 bazik boyalarla etkileşime sokulmuştur (Kristal violet ve metilen blue). Reçinenin pH'a bağlı adsorpsiyon özellikleri Çizelge 3'de verilmiştir.

Çizelge 3. Reçine2'ün pH'a bağlı maksimum boya adsorplama kapasiteleri

Boya	pH	Kapasite (g boya / g reçine)
Metilen Blue	2	0.16
	4	0.26
	8	0.37
Kristal violet	2	-
	4	0.30
	8	0.40

Bazik protein olarak tripsin kullanılmıştır. Reçinenin tripsin adsorplama kapasitesi farklı pH (Şekil 4) ve iyonik (şekil 5) ortamda incelenmiştir Ayrıca reçinenin adsorpsiyon izotermleri de elde edilmiş ve deneysel sonuçların Langmuir izoterm modeliyle uyumluluk gösterdiği tespit edilmiştir.
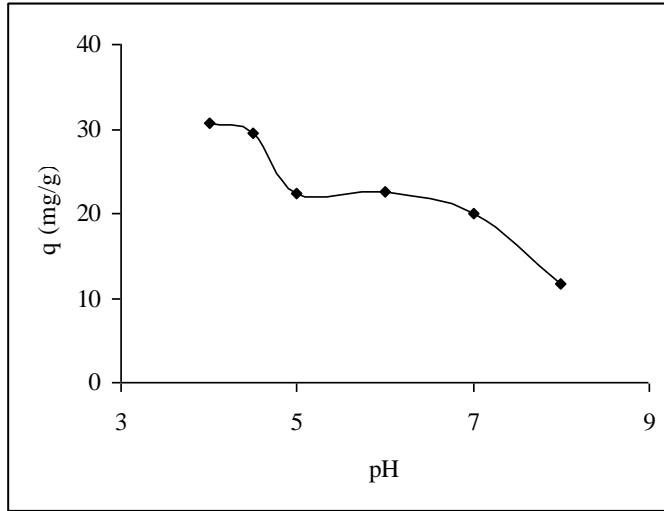
Şekil 4: Reçine 3 için pH'ın tripsin adsorpsiyonuna etkisi.
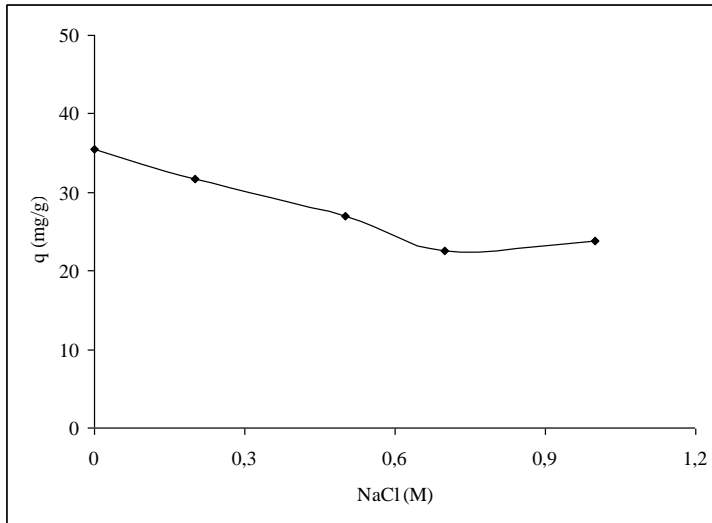
Şekil 5: Reçine 3 için iyonik gücün tripsin adsorpsiyonuna etkisi.

Diğer karboksilik asit grubu taşıyan reçinede poli(Etil akrilat)'ın PVBC üzerine SI-ATRP yöntemiyle aşılanıp daha sonra KOH ve H_2SO_4 çözeltileri ile hidroliz edilmesiyle (Şekil 6) hazırlanmıştır.
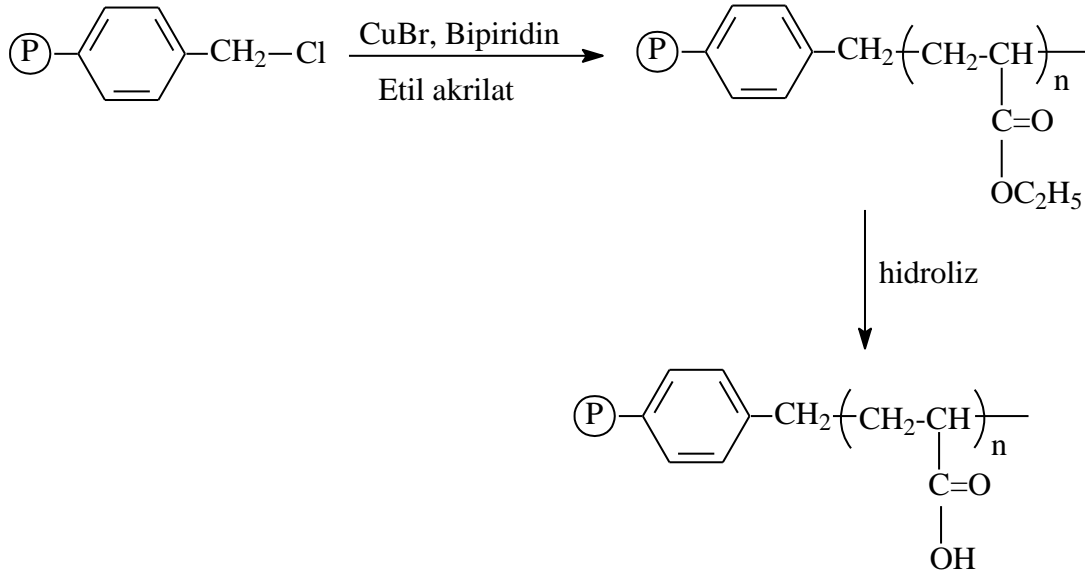
Şekil 6: Poli(akrilik asit) aşılanmış PVBC reçine.

Reçine bazik boyalarla etkileştirilmiştir. Sonuçlar Çizelge 4'de verilmiştir.

Çizelge 4: Reçine 3 için pH'a bağlı boya adsorplanması.

Boya	pH	Kapasite (mg boya / g reçine)
MetilenBlue	4.0	210
	6.0	250
	7.0	300
	8.0	200
Kristal violet	4.0	-
	6.0	190
	7.0	250
	8.0	200

1. INTRODUCTION

To perform the isolation, purification or analysis of substances, at scales ranging from tonnage quantities to picograms is an important feature of our modern life. These separations support all aspects of research and commerce and indeed a vast industry has arisen to provide the equipment to perform and control these important processes. To provide these capabilities a whole family of techniques has evolved to exploit differences in the physical or chemical properties of the compounds of interest, and to accommodate the scales on which the separations are performed. After all, a separation that works on the picogram scale based perhaps on capillary electrophoresis may not easily be transferred to the gram scale and will be utterly impossible on the kilogram scale. In such instances an alternative type of separation, based on a totally different principle must be sought.

Basically, all separation techniques rely on thermodynamic differences between components to differentiate one component from another, while kinetic factors determine the speed at which separation can be achieved. This applies most obviously to distillation, chromatography and electrophoresis, but is also obvious in most of the other techniques; even particle size separation by sieving can be classified in this way [1].

The rapid development of biotechnology, pharmaceutical science and, medicine requires more reliable and efficient separation techniques for the isolation and purification of biomolecules such as proteins, enzymes, hormones and nucleic acids .

All of these applications are based on the phenomenon of adsorption, in which one or more substances are retained on the surface of a solid adsorbent. Several types of adsorbent materials have been prepared and used in the various biotechnological and biomedical applications. The poly disperse beaded particles as solid supports, produced by suspension polymerization in the size range of 50–1000μm, are mostly used in the chromatographic area as a support materials for the immobilization of various ligands.

Immobilization of active biomolecules on solid supports for applications in biosensors and biotechnology is of great interest [2]. For these applications, active biomolecules, such as enzymes and antibodies, are generally employed as recognition elements because of their specific affinity for the adsorbates. The main considerations for immobilization of biomolecules are their stability, activity and concentration. Their stability is known to be elevated by covalent binding to a substrate [3-4].

Tethering a bioactive compound or molecule to a solid substrate by an effective spacer can improve its bioactivity by reducing steric restrictions [3]. Various types of functional spacers, such as self-assembled monolayers and polymer brushes, have been used as supports for covalent immobilization of biomolecules. Polymer brushes have well-defined structures, excellent mechanical stability, and functional groups suitable for further surface functionalization. ATRP has been used to prepare polymer brushes of different functionalities for binding of active biomolecules [5-19].

Carboxylic acids, epoxides, aldehydes, hydroxyls and primary amines are of common functional groups used for immobilization of biomolecules.

Carboxyl polymer brushes have higher protein-binding capacities due to high concentrations of –COOH groups at the brush interface. In the case of reversible binding of biomolecules in bioseparation, the well-defined poly(acrylic acid) (PAA) and poly (methacrylic acid) brushes are generally used as the negatively charged polyelectrolytes, which can electrostatically bind positively charged enzymes, such as lysozyme [20] and pectinase [15]. PAA brushes have also been used for covalent coupling of both positively and negatively charged biomolecules [17, 21-22]. Well-defined PAA brushes prepared via

ATRP has been used to covalently bind different biomolecules including BSA [9], avidin [9], anti-C-reactive protein (anti-CRP) antibody [14], and ribonuclease A (RNase A) [16]. As expected, with the increase in the thickness of the PAA brush, the surface density of immobilized biomolecules also increases.

Although PAA brushes have been widely used in the immobilization of biomolecules, it should be pointed out that pH is a major factor contributing to the dissociation of key functional groups within the active sites of enzymes [23-24]. At high concentration of the surface-grafted AAc polymer, the activity of enzymes

immobilized on the PAA brush-modified surfaces was affected adversely by the low pH value of PAA surfaces. The negative effects of pH on the enzyme activity can be avoided by using other neutral polymer brushes containing reactive groups, such as epoxides [17].

The epoxide groups can react readily and irreversibly with nucleophilic groups, such as $-NH_2$, $-SH$, and $-COOH$. Thus, the epoxide group-containing polymers can serve as surface linkers for biomolecules [25–27]. The most common epoxide polymer brushes are based on poly (glycidyl methacrylate) (PGMA).Well-defined PGMA brushes can be prepared via surface-initiated ATRP of glycidyl methacrylate (GMA) from various substrate surfaces, including silicon wafers [17,28-29], silica particles [30], Fe_3O_4 particles [19] and polymer films [31-32].

In this thesis, firstly poly (VBC) beads were prepared by suspension polymerization and the beads were modified with poly (GMA), and PAA, using surface-initiated atom transfer radical polymerization, SI-ATRP, aiming to construct the material surface with a fibrous polymer. The epoxy groups of the fibrous polymer were reacted with hydrazine and ammonia. Consequently, a hydrazine functional and a carboxylic acid functional core-shell type polymer supported reagents were obtained. The hydrazine and amine functionalized poly (VBC-g-GMA) beads were used as an affinity support for adsorption of invertase from solution and yeast crude extract. The influence of pH, equilibrium time, ionic strength and initial invertase concentration on the adsorption capacities of both hydrazine and amine functionalized beads has been investigated. It was shown that the relative activity of immobilized invertase was higher than that of the free enzyme over broader pH and temperature ranges. After inactivation of enzyme, poly (VBC-g-GMA) beads can be regenerated easily and re loaded with the enzyme for repeated use.

These polymers and a sulfonic acid functional chlorosulfonated poly (styrene-divinyl benzene) beads were also used for adsorption of textile dyes. Because dyes undergo same reactions like proteins, it was shown that these supported materials could be used for removal of textile dyes.

Finally, because invartese has aldehyde functionality and hydrazines forms hydrazones with aldehydes it was shown that hydrazine functionalized poly (VBC-g-GMA) beads and poly (VBC) beads showed affinity through both aliphatic and aromatic aldehydes.

2. THEORETICAL PART

2.1 Separation Techniques

2.1.1 Chromatography

Chromatography is a separation technique used in chemical laboratories to a wide extent, where it is used in analysis, isolation and purification. In terms of scale, at one extreme minute quantities of less than a nanogram are separated and identified during analysis, while hundreds of kilograms of material per hour are processed into refined products. It is the versatility of chromatography in its many variants that is behind its ubiquitous status in separation science, coupled with simplicity of approach and a reasonably well-developed framework in which the different chromatographic techniques operate. Chromatography is a physical method in which the components of a mixture are separated by their distribution between two phases; one of these phases in the form of a porous bed, bulk liquid, layer or film is generally immobile (stationary phase), while the other is a fluid (mobile phase) that percolates through or over the stationary phase. A separation results from repeated sorption/desorption events during the movement of the sample components along the stationary phase in the general direction of mobile-phase migration. Useful separations require an adequate difference in the strength of the physical interactions for the sample components in the two phases, combined with a favorable contribution from system transport properties that control sample movement within and between phases. Several factors are responsible to produce an acceptable separation. Individual compounds are distinguished by their ability to participate in common intermolecular interactions in the two phases, which can generally be characterized by equilibrium constant, and is thus a property predicted from chemical thermodynamics. Interactions are mainly physical in type or involve weak chemical bonds, for example dipole- dipole, hydrogen bond formation, charge transfer, etc., and reversible, since useful separations only result if the compound spends some time in both phases. During transport through or over the stationary phase,

differential transport phenomena, such as diffusion and flow anisotropy, result in dispersion of solute molecules around an average value, such that they occupy a finite distance along the stationary phase in the direction of migration. The extent of dispersion restricts the capacity of the chromatographic system to separate and, independent of favorable thermodynamic contributions to the separation, there is a finite number of dispersed zones that can be accommodated in the separation. Consequently, the optimization of a chromatographic separation depends on achieving favourable kinetic features if success is to be obtained.

2.1.1.1 The Classification of chromatographic techniques

The chromatographic techniques can be classified in terms of the phases employed for the separation (Figure 2.1) [1], with a further subdivision possible by the distribution process employed. In addition, for practical utility transport processes in at least one phase must be reasonably fast; for example, solid-solid chromatography, which may occur over geological time spans, is impractical in the laboratory because of the slow migration of solutes through the crystal lattice. Two distinct phases are required to set up the distribution component of the separation mechanism, which explains why gas-gas chromatography does not exist and liquid-liquid separations are restricted to immiscible solvents. When the mobile phase is a gas, the stationary phase can be a liquid or a solid and the separation techniques are called gas-liquid chromatography (GLC) and gas-solid chromatography (GSC). The simple term GC encompasses both techniques but, unless otherwise specified, it usually means GLC since this is the most common arrangement. Separations in GLC occur because of differences in gas-liquid partitioning and interfacial adsorption. In GSC, the retention mechanism is governed by interfacial adsorption or size exclusion, if a solid of controlled pore size, such as a zeolite, is used as the stationary phase. When the mobile phase is a supercritical fluid (SFC) the stationary phase can be a liquid or a solid, and the distribution process may be interfacial adsorption or absorption.
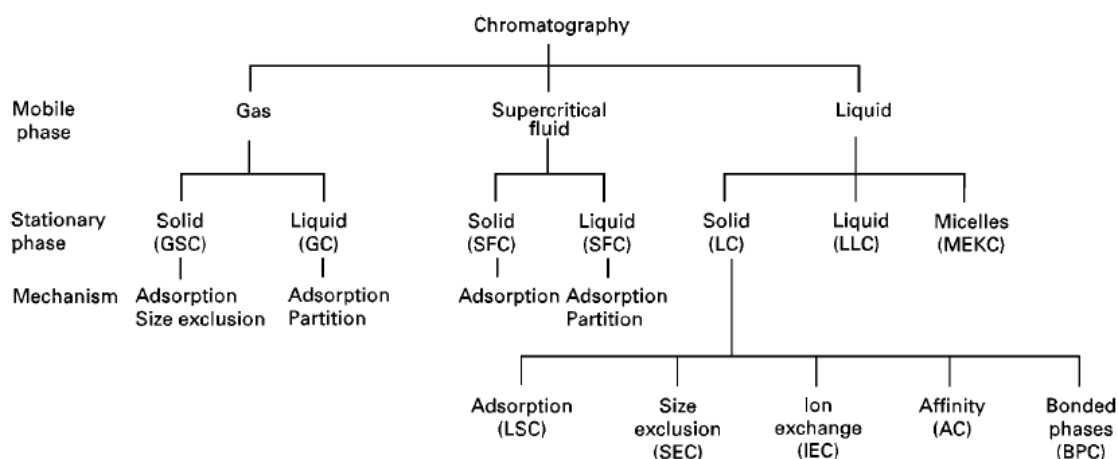
Figure 2.1: Family tree of chromatographic methods.

When the mobile phase is a liquid the stationary phase can be a solid (liquid-solid chromatography, LSC) with interfacial adsorption as the dominant distribution process; a solid of controlled pore size (size exclusion chromatography, SEC), in which the distribution constant is characteristic of the ratio of the solute size to the dimensions of the stationary phase pore sizes; a solid with immobilized ionic groups accessible to solutes in the mobile phase with electrostatic interactions as the dominant distribution process (ion exchange chromatography or ion chromatography, IEC or IC); a solid with immobilized molecular recognition sites accessible to the analyte in the mobile phase (affinity chromatography, AC) in which the dominant distribution process process is the three-dimensional specificity of the molecular interactions between the receptor and the analyte (a technique used in biotechnology); a porous solid coated with a film of immiscible liquid (liquid-liquid chromatography, LLC) in which the dominant distribution process is partitioning; or a solid with a surface containing organic groups attached to it by chemical bonds (bonded-phase chromatography, BPC) in which the dominant distribution processes are interfacial adsorption and partitioning.

2.1.1.2 Mode of zone displacement

In nearly all chromatographic systems, transport of solute zones occurs entirely in the mobile phase. Transport is an essential component of the chromatographic system since the most common arrangement for the experiment employs a sample inlet and a detector at opposite ends of the column, with sample introduction and detection occurring in the mobile phase (GC, SFC, LC). In planar chromatographic systems (TLC, PC), sample introduction and detection is performed in the stationary phase,

but the detection is of solute zones that have been transported different distances by the mobile phase. In GC the movement of solute molecules from the stationary to the mobile phase is controlled by the vapor pressure of the solutes in the column, and is usually manipulated by varying temperature. At an optimum temperature sample, molecules will spend some of their time in the mobile phase, where they will be transported through the column, and sometime in the stationary phase, where they are differentiated by their capacity for intermolecular interactions with the stationary phase. Displacement of solute zones can be achieved in three distinct ways: frontal analysis, elution and displacement (Figure 2.2) [1].
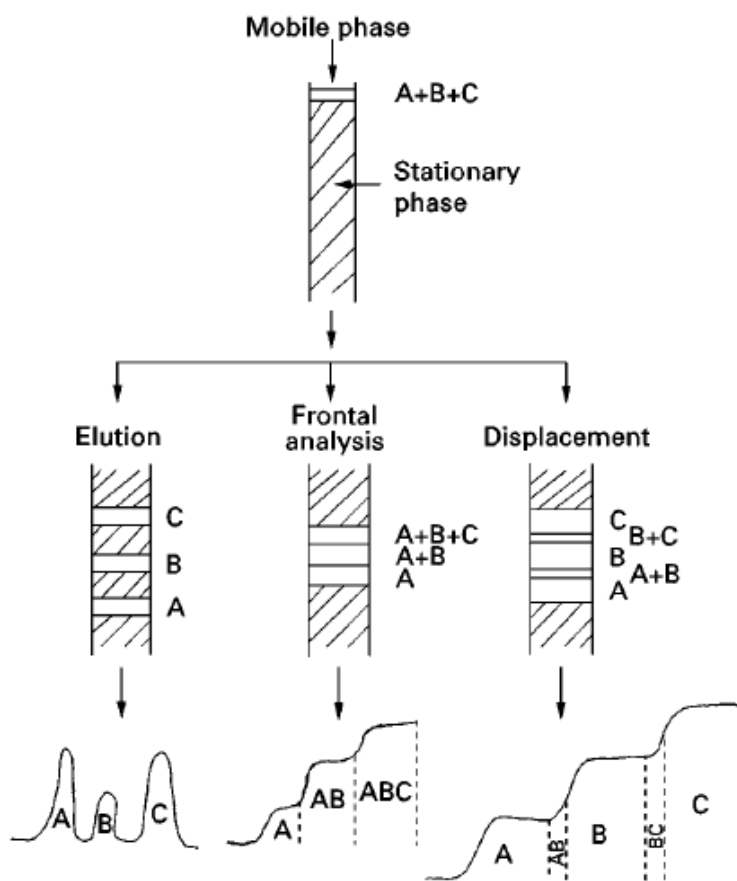
Figure 2.2: Mode of zone displacement in chromatography.

2.1.1.3 Instrumentation

Modern chromatographic methods are instrumental techniques in which the optimal conditions for the separation are set and varied by electromechanical devices controlled by a computer external to the column or layer. Separations are largely automated with important features of the instrumentation being control of the Sow

8

and composition of the mobile phase, provision of an inlet system for sample introduction, column temperature control, online detection to monitor the separation, and display and archiving of the results. Instrument requirements differ significantly according to the needs of the method employed. Unattended operation is usually possible by automated sample storage or preparation devices for time-sequenced sample introduction.

2.1.2 Electrophoresis

Electrophoresis is a basically analytical method in which separations are based on the differing mobilities (i.e. speed and direction of movement) of two or more charged analytes (ionic compounds) or particles held in a conducting medium under the influence of an applied direct current electric field (Figure 2.3).
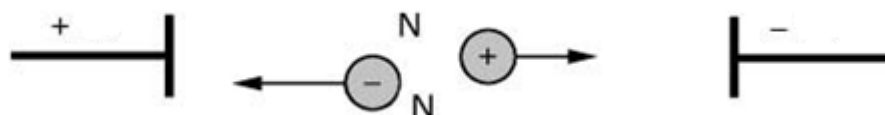
Figure 2.3: The basic principle of all electrophoretic separations is that charged ions attempt to move in an electric field towards the electrode of opposite polarity. Neutral compounds do not move.

Electrophoresis therefore contrasts to chromatography, which, is defined as a method, used primarily for the separation of two or more components of a mixture, in which the components are distributed between two phases, one of which is stationary while the other moves. Another difference is that in chromatography the modeling of the separation from first principles is complex, dificult and imprecise whereas a relatively simple theoretical background to electrophoresis has been developed.

In electrophoresis, the movement is towards the electrode of opposite charge to that of the particle or ion being separated. Cations are positively charged ions and move towards the negative electrode (the cathode). Anions are negatively charged ions and move to the positive electrode (the anode). It is important to note that neutral species do not move under the influence of the electric field, although they may diffuse from the load position or be carried by electro osmotic flow. The rate of migration (velocity) of any charged particle in an electric field can, at its simplest, be considered to be the vector sum of a driving force (the electrical force) and any

resisting or aiding forces. Any ion, compound or body carrying an overall charge at a given pH value will move in solution under appropriate conditions. In simple solutions, ions will move freely toward the electrode of opposite charge and the product of the charge on the ion and the applied electric field (E) gives the electric force experienced by the ion. However, since even a simple ion can be considered as a particle this movement is opposed by a frictional drag given by Stokes' law [1].

2.1.3 Extraction

Extractions are common in the world around us. Each time we brew a cup of tea or a pot of coffee, and each time we launder our clothes, we are performing a chemical extraction process. Perhaps because of this familiarity, extraction processes in chemical laboratories are often not fully appreciated, or fully understood. Quite simply, an extraction is the process of moving one on more compounds from one phase to another. However behind this simple definition lies a great deal of subtlety: separations are contrary to thermodynamic intuition, because entropy is gained through mixing, not separation; extraction methods are developed based on a drive towards equilibrium, but the kinetics of mass transfer cannot be ignored.

Extractions are carried out for a variety of reasons, for example when distillation is either impractical (e.g., distillations are favorable when the relative volatility of the compounds to be separated is greater than about 1.2) or is too expensive, to isolate material for characterization, to purify compounds for subsequent processing, etc. Extractions can be classified according to a number of schemes:

- analytical versus preparative (depending on the quantity of pure compound to be separated);
- batch versus continuous (depending on the mode offending the material to be separated into the extraction apparatus)
- based on the types of phases involved (called liquid-liquid extraction, gas-solid extraction, etc.).

2.1.4 Ion exchange

Ion exchange has been described as the oldest scientific phenomenon known. This claim arises from descriptions that occur in the Bible and in the writings of Aristotle, but the first scientific explanation to ion exchange is attributed to two English

agricultural chemists in 1850. These were J. T. Way and H. S. Thompson, who independently observed the replacement of calcium in soils by ammonium ions. This discovery was the precursor to the study of inorganic materials capable of 'base' exchange, and in 1858 C. H. Eichorn showed that natural zeolite minerals (chabazite and natrolite) could reversibly exchange cations. H. Gans who, at the turn of the century, patented a series of synthetic amorphous aluminosilicates for this purpose recognized the importance of this property in water softening. He called them 'permutites', and they were widely used to soften industrial and domestic water supplies until recent times, as well as being employed in nuclear waste treatment. Permutites had low ion Exchange capacities and were both chemically and mechanically unstable.

This early work has generated some myths commonly stated in elementary texts, namely that zeolite minerals are responsible for the 'base' exchange in soils and that permutites are synthetic zeolites. The presence of clay minerals in soils accounts for the majority of their exchange capacity, and zeolites by definition must be crystalline.

2.1.4.1 What is ion exchange?

A basic definition of ion exchange is that it is the transfer of ions across a boundary; this would then cover movement of ions from one liquid phase to another. A simple representation of the process, when univalent cations are being transferred is given in the chemical equation below:

$$M^- A_c^+ + B_s^+ \Leftrightarrow M^- B_c^+ + A_s^+$$

(2.1)
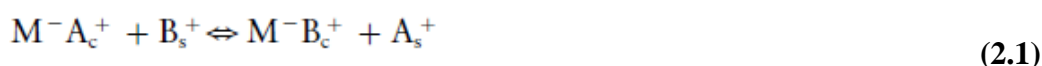
Here $M^- A_c^+$ represents a solid carrying a negative charge ('solid anion', sometimes described as a 'fixed ion') neutralized by the A^+ ions inside its structure.

The A^+ ions are replaced by B^+ originally in the solution phase (normally aqueous). The subscripts 'c' and 's' refer to the solid and solution phase, respectively.

2.1.4.2 General properties of exchange media

An ideal ion exchange medium is one that fulfils the following criteria:

1. A regular and reproducible composition and structure;

2. High exchange capacity;

3. A rapid rate of exchange (i.e. an open porous structure);

4. Chemical and thermal stability and resistance to 'poisoning' as well as radiation stability when used in the nuclear industry;

5. Mechanical strength stability and attrition resistance;

6. Consistency in particle size, and compatibility with the demands of the use of large columns in industry.

2.1.5 Membrane separation

The property of membranes used in separation processes is their ability to control the permeation of different species. Most membranes can be divided to one of the two broad categories. In micro porous membranes, permeants are separated by pressure-driven flow through tiny pores. A separation is achieved between different permeants because one of the permeants is excluded (filtered) from some of the pores through which the smaller permeants move. In solution-diffusion membranes the membrane material is a dense polymer layer and contains no fixed pores. Permeants dissolve in the membrane material as in a liquid and then diffuse through the membrane down a concentration gradient. Separation of different permeants occurs because of differences in the solubility of the permeant in the membrane material and the rate at which the permeant diffuses through the membrane. The difference between the pore-flow and the solution-diffusion mechanisms lies in the relative size and lifetime of pores in the membrane. In dense polymeric solution-diffusion membranes, no permanent pores exist. However, tiny free volume elements, a few tenths of a nanometre in diameter, exist between the polymer chains from which the membrane is made. These free-volume elements are present as statistical fluctuations that appear and disappear on a timescale only slightly slower than the motion of molecules traversing the membrane. Permeating molecules diffuse from free-volume element to free-volume element at a rate determined by the thermal motion of the polymer chains from which the membrane is made. In contrast, in a pore-flow membrane the pores are fixed and do not fluctuate in position or size on the timescale of molecular motion. The larger the individual free-volume elements are, the more likely they are to be present long enough to produce pore-flow characteristics in the membrane. As a rule of thumb, the transition between permanent (pore-flow) and transient (solution-diffusion) pores appears to be in the range 0.5-1.0 nm diameter. This means that the processes of gas separation, reverse osmosis and pervaporation,

all of which involve separation of permeants with molecular weights of less than 200, use solution-diffusion membranes. On the other hand, microfiltration and ultra filtration, which involve separation of macromolecular or colloidal material, use finely micro porous pore-flow membranes [1].

2.2 Functional Polymers

Functional polymers include a variety of polymeric materials and a number of engineering plastics. These polymer systems often show more specific and better properties if processed as polymer aggregates. For example, organic polymers with polyconjugated double bonds consisting of special structures are known as synthetic metals, which show substantially high electron conductivity in a fiber or film form. On the other hand, ceramic materials with new properties, such as elasticity, have only recently prepared by organic synthetic techniques.

Recently, microporous polymeric materials as well as microcapsules have become of interest in a variety of industrial fields, not only in the general chemical industry, but also in the pharmaceutical, biomedical and electronics industries. Microporous membranes made of vinyl polymers are being applied as separators or filters to concentrate oxygen from air and to produce ultrahigh grades of water for the semiconductor industry. Other types of microporous vinyl polymers are used as highly hydrophilic materials in the fields of cosmetics and environmental hygiene.

The science and technology required for the preparation of microcapsules from different natural and synthetic polymeric materials has made rapid progress. They are used in various fields for their ability to solidify liquids; to isolate reactive compounds; to remove color, odor, and toxicity; as well as to regulate and control the release of included compounds. The immobilization of enzymes and the development of polymeric drugs are also playing an important role.

In addition, highly water-absorbing and oil-absorbing resins are of interest. These have developed rapidly in recent years by unique grafting and crosslinking of hydrophilic polymers. Transparent polymeric materials with optical functions are also noteworthy. Some are biocompatible, such as poly (2-hydroxethyl methacrylate), which serves as a material for soft contact lenses. Plastic optical fibers

are also widely used as substitutes for glass and quartz devices in various fields of technology, especially the biomedical and communication sciences.

The chemistry of so-called electronic functional polymers, in a narrow sense, has developed into a very exciting subject, particularly in the last 10 years. Some of the most attractive materials in this field are the photosensitive and photo responsive polymers. By using these phenomena, specifically designed polymers undergo reversible crosslinking reactions to become insoluble or soluble. A variety of both negative and positive types of photo resists is being produced. They are initially used in printing, paint, and color industries. The technology to exploit deep ultraviolet (UV) radiation resist with reversible functionality will be one of the most important developments in this industry in the near future. Other subjects of interest in this field, which are under development, are the electronic or X-Ray sensitive resists, as well as the design of more functional photo memory materials [33].

2.3 Polymer Beads by Suspension Polymerization

There are a lot of methods for the production of polymer particles by heterogeneous polymerization processes. These are emulsion, emulsifier-free emulsion, dispersion, precipitation and suspension polymerization. Suspension polymerization is particularly suited to the production of large polymer beads, typically in the range 5–1000 mm. The other processes referred to produce much smaller particles, and have been reviewed elsewhere [34-35].

Hoffman and Delbruch first developed suspension polymerization in 1909 [36]. Bauer and Lauth performed the first suspension polymerization based on acrylic monomers leading to the formation of beads in 1931 [37].

In suspension polymerization, the initiator is soluble in the monomer phase, which is dispersed by pulverized into the dispersion medium to form droplets (i.e. an emulsion is formed). The solubility of the dispersed monomer (droplet) phase and also the resultant polymer in the dispersion medium are usually low. The volume fraction of the monomer phase is usually within the range 0.1–0.5. Polymerisation reactions may be performed at lower monomer volume fractions, but are not usually economically viable. At higher volume fractions, the concentration of continuous phase may be insufficient to fill the space between droplets [38].

Polymerization proceeds in the droplet phase, and in most cases occurs by a free radical mechanism. Suspension polymerization usually requires the addition of small amounts of a stabilizer to hinder coalescence and break-up of droplets during polymerization. The size distribution of the initial emulsion droplets and, hence of the polymer beads that are formed, is dependent upon the balance between droplet break-up and droplet coalescence. The type in turn controls this and speed of agitator used, the volume fraction of the monomer phase, and the type and concentration of stabilizer used.

If the polymer is soluble in the monomer, a gel forms within the droplets at low conversion, leading to harder spheres at high conversion. If the polymer is insoluble in the monomer solution, precipitation will occur within the droplets, which will result in the formation of opaque, often irregularly shaped particles. If the polymer is partially soluble in the monomer mixture, the composition of the final product can be difficult to predict. Polymer beads find applications in a number of technologies, such as molding plastics. However, their largest application is in chromatographic separation media (e.g. as ion exchange resins and as supports for enzyme immobilization). Such applications frequently require large particle surface areas, which necessitates the formation of pores (of the required dimensions) in the bead structure. The polymer beads may be made porous by the inclusion of an inert diluents (or porogen) to the monomer phase, which may be extracted after polymerization [39].

2.3.1 Process conditions and droplet stability

In forming an emulsion by a comminution method, such as stirring, it has to be considered the final average droplet size. In the absence of recoalescence of droplets, this will be determined by the volume fraction of the oil phase (f), the mass (Ws) of stabiliser added (per unit volume of emulsion) and the properties of the stabilizer molecules, such as the molecular weight (Ms) and area subtended per surfactant molecule (A_s) at the oil: water interface.

$$A_s = \frac{1}{\Gamma_{max} \cdot N_A}$$

(2.2)

where Γ_{max} is the monolayer (plateau) volume of the adsorbed amount (mol area^{-1}) in the corresponding adsorption isotherm for that stabilizer at the oil:water interface (assuming Langmuirian type isotherm), and N_A is the Avagadro constant. It may be shown that the average particle diameter (d) is given by:

$$\bar{d} = \frac{6 \cdot \phi \cdot M_s \Gamma_{max}}{W_s}$$

(2.3)

if it is assumed all added stabilizer is adsorbed.

With regard to the total energy (work) input into the process, part of this energy is used to form the droplets ($\Delta W_1 = N \square \pi \square d^2 \square \gamma$ where N is the number of droplets formed, γ is the oil: water interfacial tension), but most (ΔW_1) is lost irreversibly as heat. It may be readily shown that

$$\Delta W_1 = \frac{6 V_o \cdot \gamma}{\bar{d}}$$

(2.4)

where V_o is the total volume of the oil (monomer) phase to be emulsified. Hence, for a given amount of oil, and a given ΔW_1 (difficult to control, but may be related to the stirring rate), d decreases as γ decreases, as found by Hopff [40]. For a given system, if the stirring rate (ΔW_1) is increased, d should decrease.

However in a stirred tank reactor, a balance between break-up and coalescence of the droplets determines the size distribution and mean size of the emulsion droplets during agitation, leading to a steady-state average droplet diameter greater than that predicted by Eq. (2.3). These two processes will continue to occur until a stage in the polymerization reaction at which the partially polymerized beads are sticky. At this point, satellite droplets (formed from droplet break-up) will attach to the surface of the polymer bead. In a product designed for chromatographic columns this will result in poor packing characteristics and brittle beads. Control of coalescence and break-up rates is therefore critical for production of polymer beads of uniform size. The rate of droplet coalescence is controlled by liquid drainage in the film between approaching droplets, and more significantly the rigidity of the two corresponding oil: water interfaces, since this controls the damping of thermally or mechanically induced oscillations in the film thickness.

It has been shown that in a batch reactor, coalescence and droplet break-up occur in different regions of the reactor [41–43]. Coalescence is found to occur predominantly in the region of circulating flow (where the shear stress is least), whereas droplet break-up is found to occur mainly in regions of high shear, such as in the vicinity of the agitator.

2.3.2 Stabilizers and control of stability

The majority of droplet stabilizers used in suspension polymerization are either water-soluble polymers or small, usually inorganic particles, which adsorb at the oil: water interface. Surfactants are sometimes added in low concentrations in particular to aid the initial dispersion process, but may have some stabilizing function as well.

2.3.3 Polymeric stabilizers

The well-known polymeric stabilizers used for oil-in-water suspension polymerization reactions are poly (vinyl alcohol)-co-(vinyl acetate) (formed from the partial hydrolysis (80–95%) of poly (vinyl acetate)), poly (vinyl pyrrolidone), salts of acrylic acid polymers, cellulose ethers and natural gums. Polymeric stabilizers used in inverse suspension polymerization reactions include block copolymers (e.g. poly (hydroxystearic acid)-co-(ethylene oxide) [44]. Surfactants used for oil-in-water suspensions include Spans [45] and the anionic emulsifier (sodium 12-butinoyloxy-9-octadecenate) [46].

The stabilizing properties of such polymers are influenced by various factors including molecular weight, copolymer composition and structure such as the blockiness and the presence and positioning of any branching [47]. For example, Goodall and Greenhill-Hooper used two partially hydrolyzed (88 and 98%) poly(vinyl acetate) samples to stabilize styrene: water emulsions. They found that the 88% hydrolyzed polymer adsorbed more strongly at the styrene: water interface than the 98% hydrolyzed sample. This resulted in a thicker layer of interfacial polymer and a more stable emulsion [48].

Since the stabilizer is adsorbed at the oil: water interface it will reduce the interfacial tension, which in itself would lead to smaller droplets on break-up. However, more significantly, the stabilizer forms an interfacial layer around the droplets, which reduces the rate of coalescence by a steric stabilization mechanism [49]. On the other

hand, the rate of droplet break-up is also reduced (in effect counteracting the effect of the reduced interfacial tension referred to above), since the much higher dilational modulus of the structured interfacial layer reduces the droplet elongation process involved in droplet break-up. Certain polymeric stabilizers (in particular modified cellulose ethers) also have the effect of reducing the rate of radical diffusion from the droplet phase into the continuous phase [50]. This will reduce the possibility of emulsion polymerization occurring in the continuous phase, which may result in the formation of small latex particles.

2.3.4 Polymerizations conditions and kinetics

Batch polymerizations are usually performed in a stirred tank type reactor. The stabilized monomer droplets may be considered as micro reactors, with the polymerization proceeding therein. This mini-bulk polymerization is usually initiated thermally and allowed to proceed to completion [51].

Suspension polymerization shows various advantages over actual bulk polymerization, including, ease of heat dissipation from the reaction and, hence, better temperature control and lower viscosity of the system throughout the reaction. Advantages compared with emulsion polymerization include lower levels impurities in the product and lower separation costs.

The monomer droplets are large enough to contain a large number of free radicals (may be as many as 10^8) [52] and this is why the polymerization in general proceeds with a similar mechanism to that of bulk polymerization, particularly when the polymer is soluble in the monomer.

Since polymerization occurs within the monomer droplets, this generally requires the use of an oil-soluble initiator, which is usually thermally activated (e.g. benzoyl peroxide or azobisisobutyronitrile (AIBN)), although suspension polymerization reactions have been initiated using ultrasound [53] or ultraviolet sources [54]. Other oil-soluble initiators which have been used for suspension polymerization reactions include: diethyl, dicetyl, and dimyristyl peroxydicarbonates peroxydicarbonates [55-56], and butylperoxyneodecanoate [56]. Mathur et al. have used water-soluble initiators, which are insoluble in oil, to initiate oil-in-water vinyl suspension polymerization reactions [57]. This requires the use of a phase transfer catalyst,

which transfers the radical precursor into the organic phase, where the generated free radicals initiate polymerization.

It has been shown that the concentration and type of (oil-soluble) initiator used in the suspension polymerization of a given monomer both have an effect, not only on the polymerization kinetics, but also on the average size and polydispersity of the beads that are formed [58-59]. Dowding et al. [59] produced porous suspension copolymers initiated using two different initiators (benzoyl peroxide and AIBN) and found that the initiator not only affected the final bead size, but also the average pore size. Average pore radii were found to be greater for benzoyl peroxide-initiated systems than for comparable systems initiated using AIBN. Typically, the concentrations of initiator used are 0.1–0.5 wt% (based on monomer). However, Mrazek et al. have reported that addition of part of the initiator during the reaction allows the amount of the initiator used to be reduced by as much as 15%, without any changes in the yield and the reaction time [60].

2.4 Controlled Polymerization Techniques

The term-controlled polymerization indicates control of a certain kinetic feature of a polymerization or structural aspect of the polymer molecules formed, or both. The ultimate goal is to obtain a high degree of control over compositional and structural variables that affect the physical properties of macromolecules, including molecular weight, molecular weight distribution (MWD), end functionality, tacticity, stereochemistry, block sequence, and block topology, where the parameters of molecular characterization are well represented by the ensemble average.

The experimental criteria for living polymerizations is the absence of chain transfer and termination can be obtained from both linear semi logarithmic kinetic plot (ln ($[M]_0/[M]$) vs. time) and linear dependence of number average molecular weight (Mn) vs. monomer conversion (Mn vs. conversion). There are no absolute living systems and the careful control of the experimental conditions (counter ion, temperature, and solvent) is necessary to obtain sufficient livingness to prepare well-defined polymers.

2.4.1 Anionic polymerization

Ziegler and Schlenk first developed the concept of anionic polymerization in early 1910. Their pioneering work on the polymerization of diene initiated with sodium metal set the stage for the use of alkali metal containing aromatic hydrocarbon complexes as initiators for various α-olefins. In 1939, Scott and coworkers used for the first time the alkali metal complexes of aromatic hydrocarbon as initiators for the polymerization of styrene and diene. However, in 1956, it was Michael Szwarc who demonstrated unambiguously the mechanism of anionic polymerization of styrene, which drew significant and unprecedented attention to the field of anionic polymerization of vinyl monomers [61-62]. Michael Szwarc used sodium naphthalenide as an initiator for the polymerization of styrene in tetrahydrofuran (THF). Upon contact with styrene, the green color of the radical anions immediately turned into red indicating formation of styryl anions. He suggested that the initiation occurs via electron transfer from the sodium naphthalenide radical anion to styrene monomer. The styryl radical anion forms upon addition of an electron from the sodium naphthalenide and dimerizes to form a dianion. After the incorporation of all the monomer, the red color of the reaction mixture persists, indicating that the chain ends remain intact and active for further propagation. This was demonstrated by the resumption of propagation with a fresh addition of another portion of styrene. After determining the relative viscosity of the first polymerized solution at its full conversion, another portion of styrene monomer was added and polymerization was continued. Thus, Szwarc characterized this behavior of the polymerization as living polymerization and called the polymers as living polymers [62]. Here, the term living refers to the ability of the chain ends of these polymers retaining. their reactivity for a sufficient time enabling continued propagation without termination and transfer reactions.

2.4.2 Cationic polymerization

Since the first reports of living cationic polymerization of vinyl ethers [63] and isobuthylene [64] in the 1980s, the scope of living cationic polymerization of vinyl monomers has been expanding rapidly in terms of monomers and initiating systems. Compared to anionic polymerization, living cationic polymerization can proceed under much less rigorous and much more flexible experimental conditions. The high vacuum technique is not indispensable, since alternative routes can consume

adventitious moisture without terminating the living chains. Nonetheless, rigorous purification of reagents is still required for the best control.

Initiation and propagation take place by electrophilic addition of the monomers to the active cationic sites. Therefore, the monomer must be nucleophilic and its substituents should be able to stabilize the resulting positive charge.

With a few exceptions [65-66], living cationic polymerization is initiated by the initiator/co initiator (Lewis acid) binary system. Selection of an initiating system for a given monomer is of crucial importance, as there are no universal initiators such as organolithiums in anionic polymerization. For example, while weak Lewis acids such as zinc halides may be necessary to effect living polymerization of the more reactive vinyl ethers, they are not effective for the living polymerization of the less reactive monomers, such as isobuthylene and Styrene.

2.4.3 Controlled radical polymerization (CRP)

All CRP systems have a dynamic equilibrium between propagating radicals and various dormant species [67-68]. There are two types of equilibria. Radicals may be reversibly trapped in a deactivation/activation process, according to Figure 2.4 or they can be involved in a degenerative exchange process (Figure 2.5).
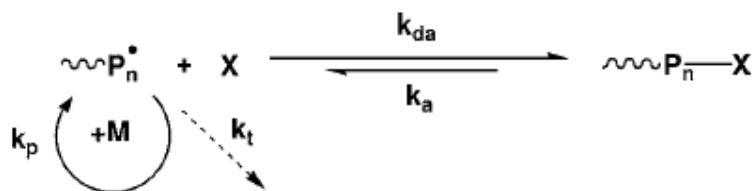
Figure 2.4: Controlled polymerization via deactivation/activation process.
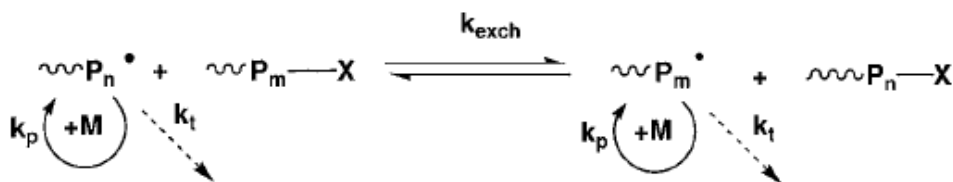
Figure 2.5: Controlled polymerization via degenerative exchange process.

The first one is more widely used and relies on the persistent radical effect (PRE) [69]. In systems obeying the PRE, newly generated radicals are rapidly trapped in a

deactivation process (with a rate constant of deactivation, k_{da}) by species X (which is typically a stable radical such as a nitroxide [70] or an organometallic species such as a cobalt porphyrine [71]). The dormant species are activated (with a rate constant k_a) either spontaneously/thermally, in the presence of light, or with an appropriate catalyst (as in ATRP) [72] to reform the growing centers. Radicals can propagate (k_p) but also terminate (k_t).

Good control over MW, polydispersity, and chain architecture in all CRP systems requires very fast exchange between active and dormant species.

Ideally, a growing radical should react with only a few monomer units before it is converted back into a dormant species. Consequently, it would remain active only for a few milliseconds.

2.4.3.1 Atom transfer radical polymerization (ATRP)

The most widely used CRP technique is ATRP [72-73]. This originates from the commercial availability of all necessary ATRP reagents, including transition metal compounds and ligands used as catalysts, as well as alkyl halide initiators, and also from the large range of monomers polymerizable by this technique under a wide range of conditions.

The basic working mechanism of ATRP involves homolytic cleavage of an alkyl halide bond R–X (or macromolecular Pn –X) by a transition metal complex Mt^n/L (such as $CuBr/bpy_2$) (bpy : bipyridine). This reaction generates reversibly (with the activation rate constant, k_a) the corresponding higher oxidation state metal halide complex $X–Mt^{n+1}/L$ (such as $CuBr_2/bpy_2$) and an alkyl radical R• (a representative example of this process is illustrated in Figure 2.6) [73]. R• can then propagate with a vinyl monomer (k_p), terminate by coupling and/or disproportionation (k_t), or can be reversibly deactivated by $X–Mt^{n+1}/L$ (k_{da}). Radical termination is diminished because of the PRE [69] that ultimately shifts the equilibrium toward the dormant species (activation rate constant $<<$ deactivation rate constant). The values of the rate constants in Figure 2.6 refer to styrene polymerization at 110 ^0C
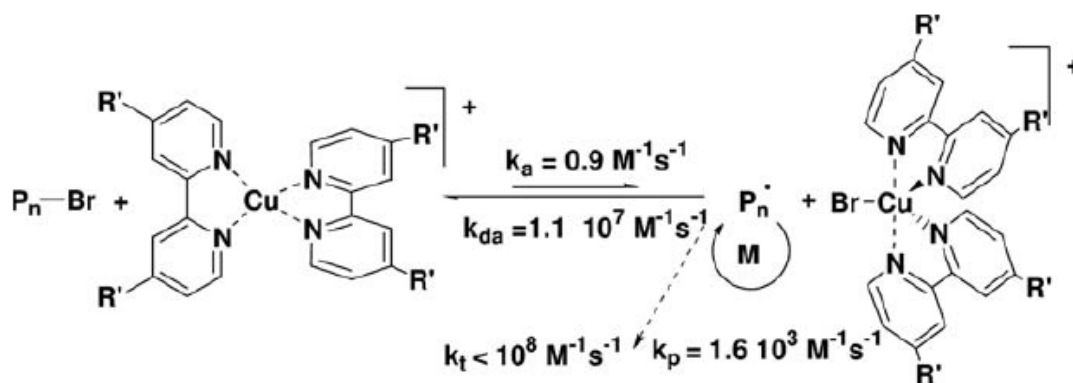
Figure 2.6: Polymerization of styrene by ATRP.

The synthesis of polymers with low polydispersities and predetermined MWs requires a sufficient concentration of deactivator. Polydispersities decrease with monomer conversion (p) and concentration of deactivator but increase with the k_p/k_{da} ratio.

2.4.3.2 Stable free radical polymerization (SFRP) : Aminoxyl-mediated polymerization (NMP) and organometallic-mediated radical polymerization (OMRP) systems

SFRP and, more specifically, nitroxide-mediated polymerization [70] (NMP) or organometallic-mediated radical polymerization (OMRP) [71] systems rely on the reversible homolytic cleavage of a relatively weak bond in a covalent species to generate a growing radical and a less reactive species (usually the persistent radical, but can be also species with an even number of electrons). This species should react reversibly only with growing radicals and should not react amongst themselves or with monomers to initiate the growth of new chains, and they should not participate in side reactions such as the abstraction of β-H atoms.

Nitroxides (aminoxyl radicals) were employed as stable free radicals in the polymerization of (meth)acrylates. The field of NMP became important after the paper by Georges who used TEMPO (2,2,6,6-tetramethyl-1-piperidynyl-N-oxy) as a mediator in styrene polymerization (Figure 2.7) [70]. TEMPO and substituted TEMPO derivatives form relatively strong covalent bonds in alkoxyamines that have very low equilibrium constants in NMP (ratio of rate constants of dissociation (activation) and coupling (deactivation), kd/kc = Keq = 2.0 10^{-11} M at 120 $^\circ$C for PS [68] and therefore require high polymerization temperatures.

Figure 2.7: Polymerization of styrene by TEMPO.

The OMRP of MA with Co porphyrines [71], one of the most successful CRP systems, leads to well-defined high MW polyacrylates and has been recently extended to PVAc [74]. However, similar compounds in polymerization of methacrylates act as very efficient catalytic chain TAs [75].

2.4.3.3 Degenerative transfer (DT) processes

Conventional free radical initiators are used in DT processes, and control is by the presence of Transfer agents- TAs- (RX) which exchange a group/atom X between all growing chains. This thermodynamically neutral (degenerative) transfer reaction should be fast in comparison to propagation (kexch > kp). At any instant, the concentration of dormant species Pn –X is much larger than that of the active species Pn*. Degree of polymerization is defined by the ratio of concentrations of consumed monomer to the sum of concentrations of the consumed TA and the decomposed initiator.

DT processes do not operate via the PRE. A steady state concentration of radicals is established via initiation and termination processes. In some cases, the exchange process may occur via some long-lived intermediates, which can either retard polymerization or participate in side reactions such as the trapping of growing radicals (Figure 2.8).

Figure 2.8: The mechanism of degenerative transfer (DT) processes.

2.4.3.4 Reversible addition-fragmentation transfer (RAFT)

RAFT polymerization is among the most successful DT processes [76-77]. While addition-fragmentation chemistry was originally applied to the polymerization of unsaturated methacrylate esters (prepared by catalytic chain transfer) [78], RAFT employs various dithioesters, dithiocarbamates, trithiocarbonates, and xanthates as TAs leading to polymers with low polydispersities and various controlled architectures (Figure 2.9) for a broad range of monomers [79-80]. The structure of a dithioester has a very strong effect on control. Both R and Z groups must be carefully selected to provide control. Generally, R* should be more stable than Pn*, to be formed and to efficiently initiate the polymerization. More precisely, the selection of the R group should also take into account stability of the dormant species and rate of addition of R* to monomer. The structure of group Z is equally important. Strongly stabilizing Z groups such as Ph are efficient for styrene and methacrylate but they retard polymerization of acrylates and inhibit polymerization of vinyl esters. On the other hand, very weakly stabilizing groups, such as $-NR_2$ in dithiocarbamates or $-OR$ in xanthates, are good for vinyl esters but less efficient for styrene.
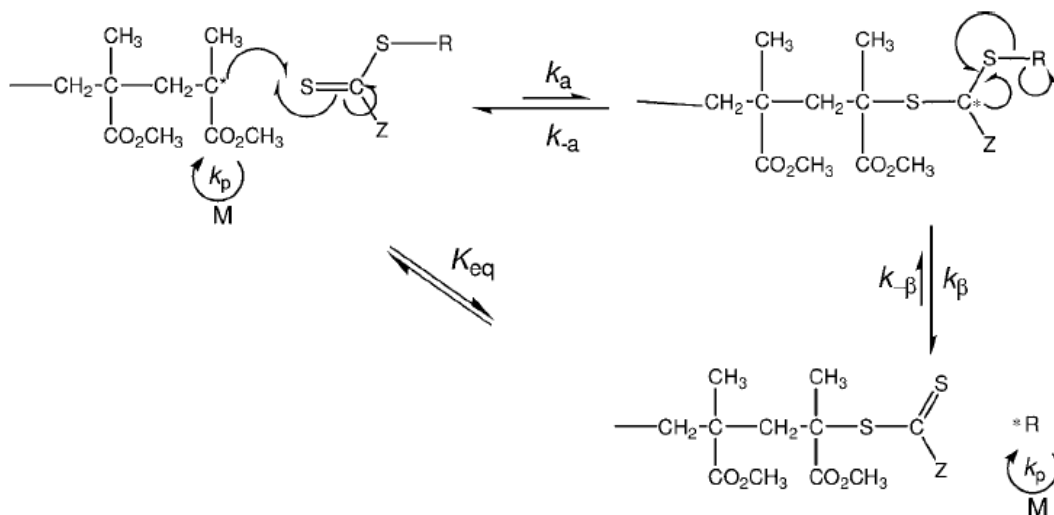
Figure 2.9: RAFT Mechanism of methyl methacrylate

2.5 Surface Modification of Polymer Beads Using ATRP.

Grafting of polymers on a solid surface plays an important role in many areas of science and technology, e.g., colloidal stabilization, adhesion, lubrication and rheology [81−83]. The conformation of those polymers in a solvent can dramatically

change with graft density; [84-85] at low graft densities, they will assume a "mushroom" conformation with the coil dimension similar to that of ungrafted chains. With increasing graft density, graft chains will be obliged to stretch away from the surface, forming the so-called "polymer brush". Polymer brushes may be categorized into two groups different in graft density. One is the "semi-dilute" brush, in which polymer chains overlap with each other but their volume fraction is still so low that the free energy of interaction can be approximated by a binary interaction, and the elastic free energy, by that of a Gaussian chain. Structure and properties of semi-dilute polymer brushes are relatively well understood both experimentally and theoretically. Theoretical analyses [86-87] predicted that the equilibrium thickness (L_e) of the semi-dilute polymer brush in good solvent varies like $L_e \propto N\sigma^{1/3}$ where N and σ are the degree of polymerization and the surface density of the graft chains, respectively. The most important feature of this expression is that L_e depends on N in a linear way, while the dimension of an isolated chain in good solvent is scaled as $N^{3/5}$. This means that the graft chains adopt a stretched conformation. Extensive efforts have been made to characterize the semi-dilute polymer brushes systematically prepared by the "grafting to" method using end-functionalized polymers or block copolymers with the terminal group or one of the blocks selectively adsorbed on the surface. For example, neutron reflectometry [88] and the interaction forces between polymer brush surfaces were directly measured by a surface force apparatus [89] and an atomic force microscope (AFM) [87] studied the brush height and the segment density profile in good solvent. These studies have supported the theoretical predictions mentioned above.

The other category is the "concentrated" brush or the high-density brush, for which the above-mentioned approximations are no longer valid and higher-order interactions should be taken into account. In this regime, therefore, graft chains are expected to exhibit different properties from those in the semi-dilute regime due to higher-order interactions between graft chains. Theoretical analyses taking account of these interactions predicted that the repulsive force will much more steeply increase with increasing graft density [90-91]. However, the structure and properties of high-density polymer brushes could not be well studied experimentally because of the difficulty of preparing well-defined high-density brushes. The above-mentioned grafting to method gives limited graft densities due to the concentration gradient

built up by the already grafted chains [92]. Namely, once the surface is significantly covered with polymers, they give a strong kinetic hindrance against the grafting of new chains. An alternative method to prepare polymer brushes is the "grafting-from" method, that is, the graft polymerization starting with initiating sites fixed on the surface. In this technique, the addition of monomer to growing chain ends or to primary radicals is not strongly hindered by the already grafted chains in a good solvent condition. Therefore, this technique is more promising to produce a polymer film with a larger thickness and a higher graft density than the grafting-to technique [93]. Earlier strategies were mostly based on conventional free radical polymerization (FRP), which successfully gave grafted films of increased density. However, no clear experimental evidence has been reported to confirm the achievement of structure and properties specific to high-density brushes, which suggests that the achieved graft density may still be in the semi-dilute regime. The generally poor control of chain length and chain-length distribution by conventional FRP poses complexities in defining the prepared brushes. In a polydisperse brush, longer chains will form the outer fringe of the swollen brush with a relatively low segmental density, which may mask the possibly unique properties of the higher density portion of the brush near the substrate surface.

Living polymerization techniques including anionic, cationic, ring-opening, ring-opening metathesis, and living radical polymerizations were successfully applied to surface-initiated graft polymerization to prepare a polymer brush with the basic brush parameters controlled [94]. Of these techniques, living radical polymerization (LRP) has been most widely used for its tolerance to impurities and versatility to various monomers. Surface initiated LRP has proved to provide a dramatic increase of graft density, giving well-defined high-density polymer brushes. Recent studies have revealed that such brushes have characteristic structure and properties quite different and unpredictable from those of the semi-dilute polymer brushes previously studied.

ATRP has been widely applied to surface-initiated graft polymerization on a variety of materials including flat substrates [95], fine particles [96], and porous materials [97].

Ejaz et al. first succeeded in synthesizing a dense brush of low-polydispersity poly (methyl methacrylate) (PMMA) by the surface-initiated ATRP with copper/ligand complexes. They deposited a commercially available silane-coupling agent, 2-(4-

chlorosulfonylphenyl) ethyltriethoxysilane (CTS), on a silicon wafer by the Langmuir–Blodgett technique to form a covalent bond by the coupling reaction with the silanol group on the silicon surface [95]. Figure 2.10 schematically illustrates the graft polymerization process: the activator such as a Cu(I) complex abstracts the halogen atom of the immobilized initiating dormant species, e.g., a chloride functional polymer supported reagent, or the grown dormant chain, giving a propagating radical, to which some monomer units are added until it is recapped to be a dormant chain. This cycle occurs repeatedly and randomly on the halogenated sites on the surface, thus allowing all graft chains to grow slowly and nearly simultaneously, when viewed in a longer time scale, hence in a controlled fashion.
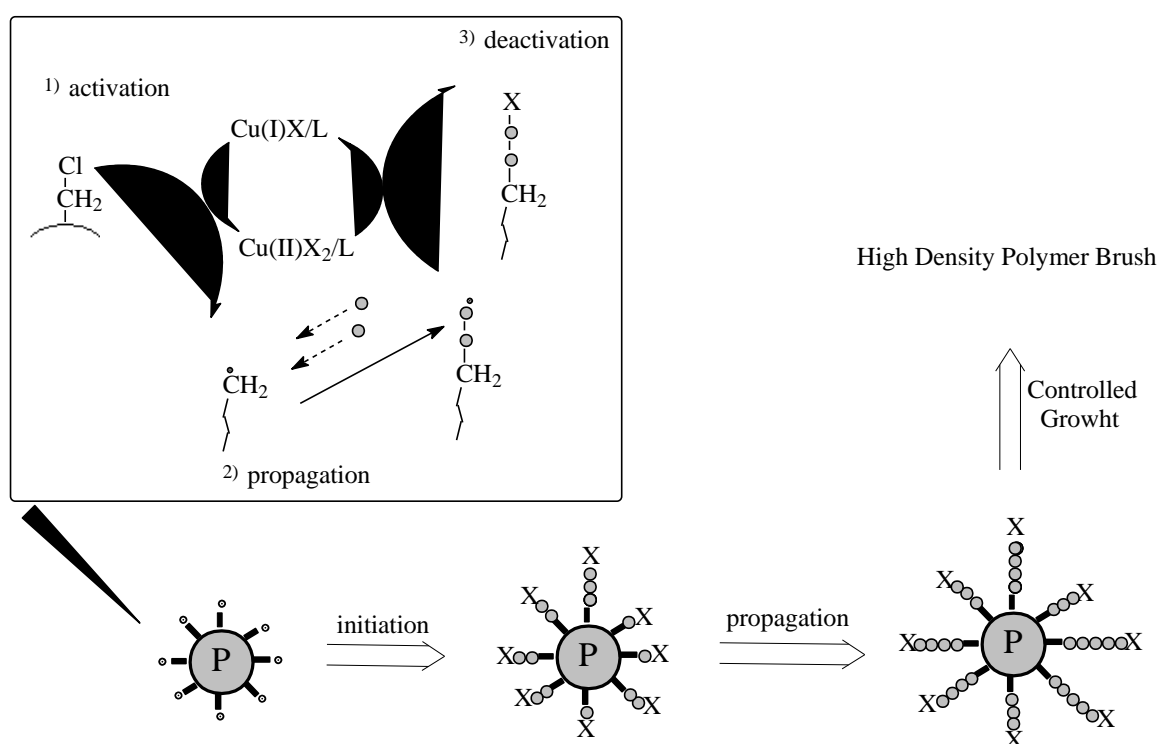
Figure 2.10: Schematic illustration of surface-initiated atom transfer radical polymerization on a polymer support.

2.6 Proteins

A protein is a biopolymer composed of basic building blocks called amino acids. Naturally, occurring proteins are made up to 20 different amino acids. Proteins are the most abundant biopolymers in living cells (constituting about 40 to 70 percent of dry cell weight) and have biological functions:

1) Structural components (e.g. collagen, keratin)

2) Catalysts (e.g. enzymes, catalytic antibodies)

3) Transport molecules (e.g. hemoglobin, serum albumin)

4) Protective molecules (e.g. antibodies)

A protein molecule can be a single poly (amino acid) chain or may comprise more than one poly (amino acid) chain, held together by covalent bonds or non-covalent interactions. A protein usually coils up and folds into a specific three-dimensional configuration, depending on the intrinsic properties of the protein as well as on the environment in which the protein exist. Structure of a protein can be defined at different level, these being,

a) Primary

b) Secondary

c) Tertiary

d) Quaternary

The primary structure of a protein is the sequence of amino acids present in the poly (amino acid) chains. The secondary structure describes the local structure of linear segments of the protein molecule. The three most common types of secondary structure are alpha helices, the beta sheets and the turns. The tertiary structure is the three-dimensional arrangement of all the atoms present in a single poly (amino acid) chain. The quaternary structure describes the arrangement of poly (amino acid) chains (subunits) in a particular protein.

Proteins are not entirely rigid molecules. In addition to these levels of structure, proteins may shift between several related structures while they perform their functions. In the context of these functional rearrangements, these tertiary or quaternary structures are usually referred to as conformations, and transitions between them are called conformational changes. The binding of a substrate molecule to an enzyme's active site, or the physical region of the protein that participates in chemical catalysis often induces such changes. In solution, proteins also undergo variation in structure through thermal vibration and the collision with other molecules.

2.6.1 Enzymes

The best-known role of proteins in the cell is as enzymes, which catalyze chemical reactions. Enzymes are usually highly specific and accelerate only one or a few chemical reactions. Enzymes carry out most of the reactions involved in metabolism, as well as manipulating DNA in processes such as DNA replication, DNA repair, and transcription. Some enzymes act on other proteins to add or remove chemical groups in a process known as post-translational modification. About 4000 reactions are known to be catalyzed by enzymes [98].

The rate acceleration conferred by enzymatic catalysis is often enormous as much as 10^{17} fold increase in rate over the uncatalyzed reaction in the case of orotate decarboxylase (78 million years without the enzyme, 18 milliseconds with the enzyme) [99].

The molecules bound and acted upon by enzymes are called substrates. Although enzymes can consist of hundreds of amino acids, it is usually only a small fraction of the residues that come in contact with the substrate, and an even smaller fraction — 3 to 4 residues on average — that are directly involved in catalysis. The region of the enzyme that binds the substrate and contains the catalytic residues are known as the active site.

2.7 Protein Isolation

2.7.1 The aim for isolating proteins

To gain perception: As working with living systems, it is necessary to isolate the component parts so that they may be studied, separately and in their interaction with other parts. The knowledge that is gained in this way may be put to practical use, for example, in the design of medicines, pesticides, or industrial processes.

To use in Medicine: Many proteins may be used as medicines to make up for losses or inadequate synthesis. Examples are hormones, such as insulin, which is used in the therapy of diabetes, and blood fractions, such as the so-called Factor VIII, which is used in the therapy of hemophilia. Other proteins may be used in medical diagnostics, an example being the enzymes glucose oxidase and peroxidase, which are used to measure glucose levels in biological fluids, such as blood and urine.

In every case, a pure protein is desirable as impurities may either be misleading, dangerous or unproductive, respectively. Protein isolation is, therefore, a very common, almost central, procedure in biochemistry.

2.7.2 Properties of proteins that affect the methods used in their study

Proteins have two properties, which determine the overall approach to protein isolation and make this different from the approach used to isolate small natural molecules.

- Proteins are labile. As molecules go, proteins are relatively large and delicate and their shape is easily changed, a process called denaturation, which leads to loss of their biological activity. This means that only mild procedures can be used and techniques such as boiling and distillation, which are commonly used in organic chemistry, are thus verboten.

- Proteins are similar to one another. All proteins are composed of essentially the same amino acids, differ only in the proportions, and sequence of their amino acids, and in the 3-D folding of the amino acid chains. Consequently, processes with a high discriminating potential are needed to separate proteins.

2.7.3 The General idea of protein isolation

In a protein isolation one have to attempt to purify a particular protein, from some biological (cellular) material, or from a bio product, since proteins are only synthesized by living systems. The aim is to separate the protein of interest from all non-protein material and all other proteins which occur in the same material. Removing the other proteins is the difficult part because all proteins are similar in their gross properties. In an ideal case, without any loss of the protein of interest, the total amount of protein would decrease while the activity (which defines the particular protein of interest) would remain the same (Fig. 2.11) [100].
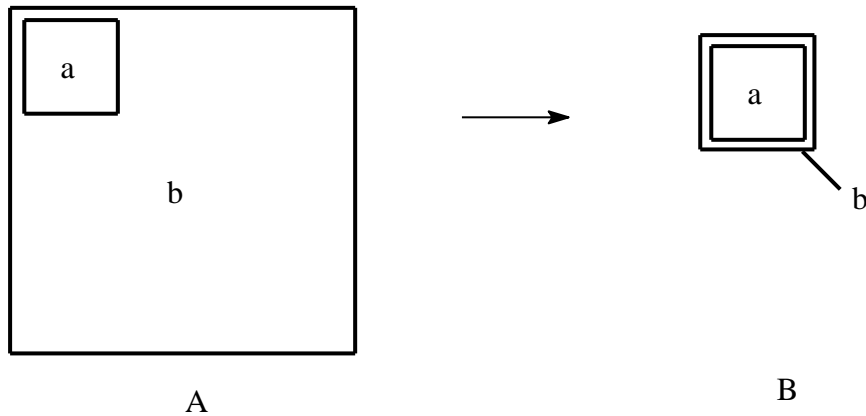
Figure 2.11: Schematic representation of a protein isolation.

At the beginning (Fig. 2.11 A) there is a small amount of the desired protein -a- and a large amount of total protein -b-. In the course of the isolation, -b- is reduced and consequently (Fig. 2.11 B) only -a- remains. Ideally, the amount of -a- remains unchanged but, in practice, this is seldom achieved and less than 100% recovery of purified protein is usually obtained.

As a general principle, one should aim to achieve the isolation of a protein;

- In as few steps as possible and,
- In as short a time as possible.

This decreases losses and the generation of isolation artifacts. In addition, to further study the protein, the isolation will have to be done many times over and the effort put into devising a quick, simple, isolation procedure will be repaid many times over. The overall approach to the isolation of a protein is shown in Fig. 2.12 [100].
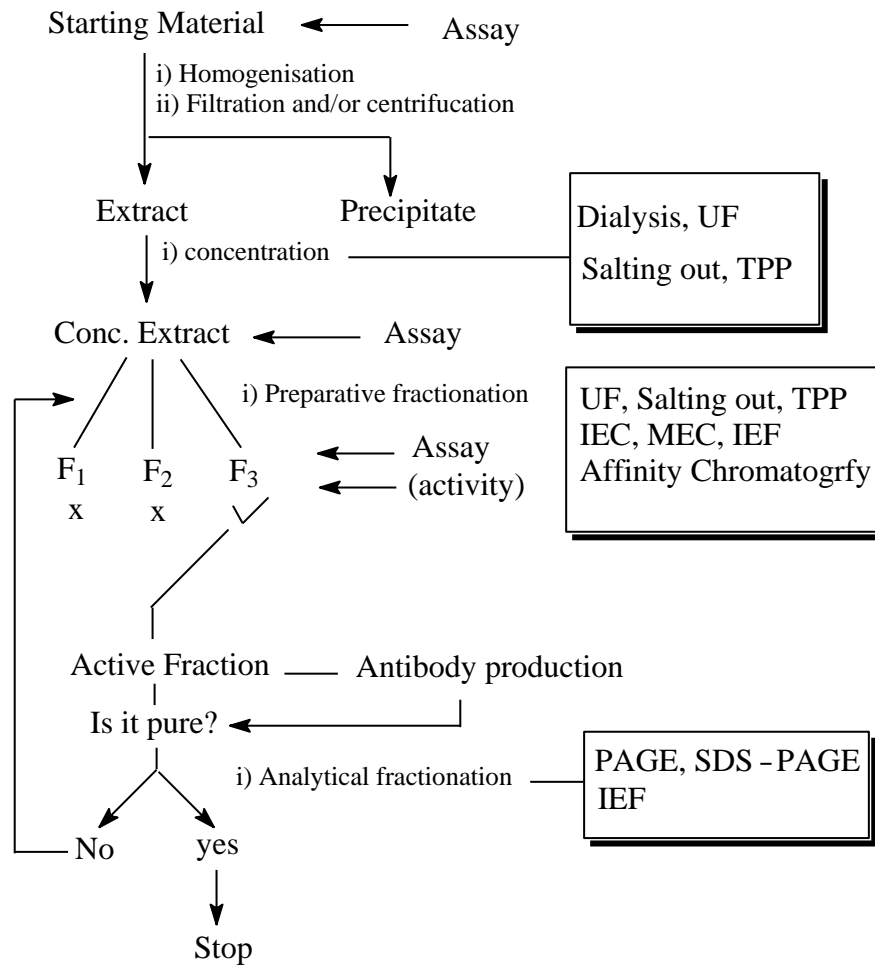
Figure 2.12: An overview of protein isolation.

To isolate a protein, one must start with some way of measuring the presence of the protein and of distinguishing it from all other proteins that might be present in the same material. This is achieved by a method, which measure the unique activity of the protein. With such an assay, likely materials can be analyzed in order to select one containing a large amount of the protein of interest, for use as the starting material.

Having selected a source material, it is necessary to extract the protein into a soluble form. This may be achieved by homogenizing the material in a buffer of low osmotic strength (the low osmotic pressure helps to lyses cells and organelles), and clarifying the extract by filtration and/or centrifugation steps.

The clarified extract is typically subjected to preparative fractionation. At this stage salting out usefully serves to separate protein from non-protein material. It is necessary to assay the fractions obtained, in order to select the fraction containing the

protein of interest. The selected fraction can then be subjected to further preparative fractionation, as required, until a pure fraction is obtained.

Experience has shown that there is an optimal sequence in which preparative methods may be applied. As a first approach it is best to apply salting out (or TPP) early in the procedure, followed by ion exchange or affinity chromatography. Salting out can, with advantage, be followed by hydrophobic interaction chromatography, because hydrophobic interactions are favored by high salt concentration. The precipitate obtained from TPP, however, is low in salt and so can be applied directly to an ion-exchange system, without prior desalting. Generally, molecular exclusion chromatography should be reserved for late in the isolation when only a few components remain, since it is not a highly discriminating technique. Affinity chromatography often achieves the desirable aims of a rapid isolation using a minimum number of steps and so it should always be explored and preferentially used where possible.

In this thesis a new a polymer supported material with hydrazine function was synthesized for using in preparative fractionation step of protein isolation. This hydrazine functional beads showed affinity toward invertase enzyme.

2.8 Chromatographic Purification Techniques in Protein Isolation

After concentration of the extract by one of the methods mentioned above, a chromatographic technique can be applied to the extract. Proteins are purified using chromatographic techniques (Fig. 2.13) [101] which separate according to differences in specific properties, as shown in Table 2.1.

Table 2.1: Chromatographic techniques used in protein purification.

Protein property	Technique
Charge	Ion Exchange (IEX)
Size	Gel Filtration interaction (HIC) (GF)
Hydrophobicity	Hydrophobic
Biorecognition	Affinity (AC)
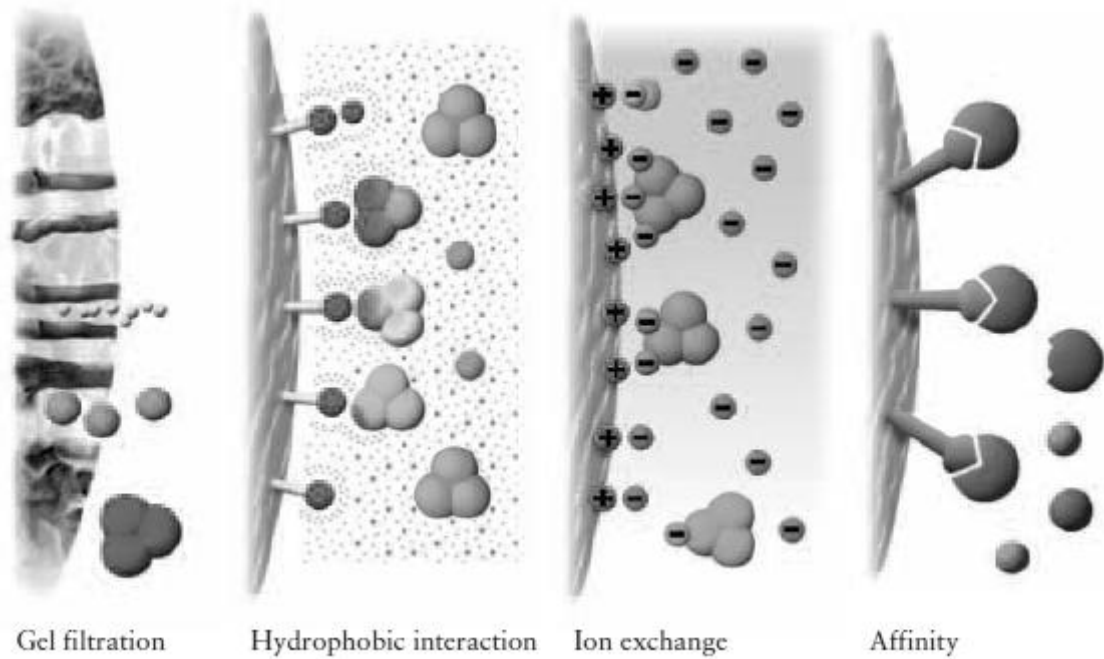
Figure 2.13: Separation techniques in chromatographic purification.

2.8.1 Ion exchange chromatography

Separation in ion exchange chromatography depends upon the reversible adsorption of charged solute molecules to immobilized ion exchange groups of opposite charge. Most ion exchange experiments are performed in five main stages (Fig 2.14) [102].
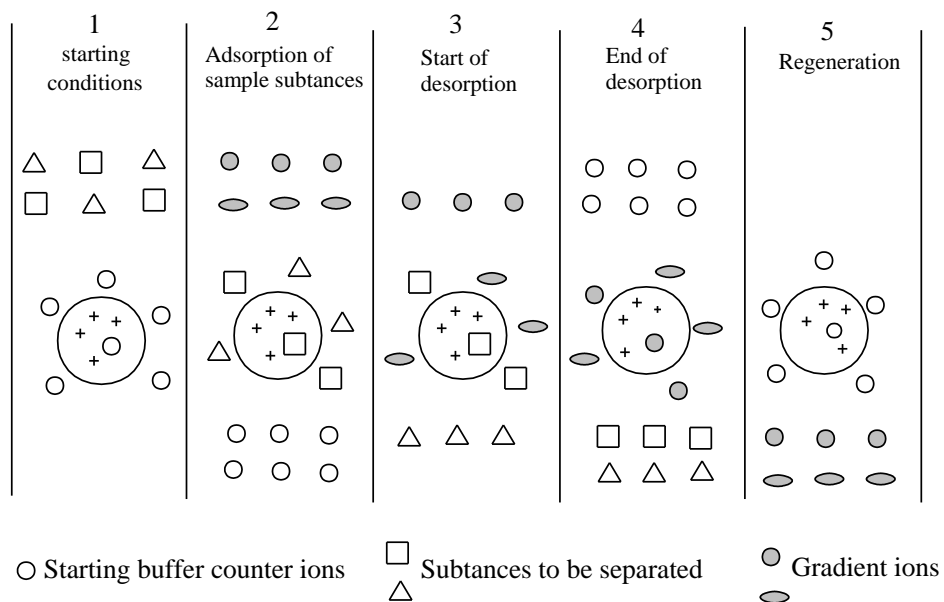
Figure 2.14: The principle of ion exchange chromatography (salt gradient elution).

The first stage is equilibration in which the ion exchanger is brought to a starting state, in terms of pH and ionic strength, which allows the binding of the desired solute molecules. The exchanger groups are associated at this time with exchangeable counter-ions (usually simple anions or cations, such as chloride or sodium).

The second stage is sample application and adsorption, in which solute molecules carrying the appropriate charge displace counter-ions and bind reversibly to the matrix. Unbound substances can be washed out from the exchanger bed using starting buffer.

In the third stage, substances are removed from the column by changing to elution conditions unfavorable for ionic bonding of the solute molecules. This normally involves increasing the ionic strength of the eluting buffer or changing its pH. In Fig. 2.14 desorption is achieved by the introduction of an increasing salt concentration gradient and solute molecules are released from the column in the order of their strengths of binding, the most weakly bound substances being eluted first.

The fourth and fifth stages are the removal from the column of substances not eluted under the previous experimental conditions and re-equilibration at the starting conditions for the next purification.

Separation is obtained since different substances have different degrees of interaction with the ion exchanger due to differences in their charges, charge densities and distribution of charge on their surfaces. These interactions can be controlled by varying conditions such as ionic strength and pH. The differences in charge properties of biological compounds are often considerable, and since ion exchange chromatography is capable of separating species with very minor differences in properties, for example two proteins differing by only one charged amino acid, it is a very powerful separation technique.

2.8.1.1 The matrix

An ion exchanger consists of an insoluble matrix to which charged groups have been covalently bound. The charged groups are associated with mobile counterions. These counter-ions can be reversibly exchanged with other ions of the same charge without altering the matrix. It is possible to have both positively and negatively charged exchangers (Fig. 2.15). Positively charged exchangers have negatively charged

counter-ions (anions) available for exchange and are called anion exchangers. Negatively charged exchangers have positively charged counter-ions (cations) and are termed cation exchangers.

Anion exchanger with
exchangeable counter ions

Cation exchanger with
exchangeable counter ions
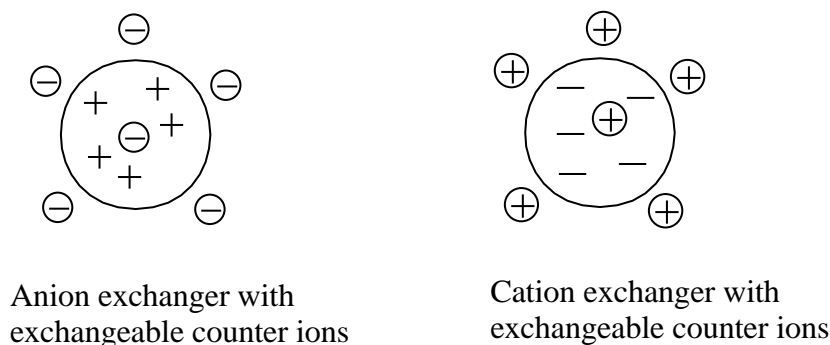
Figure 2.15: Ion exchanger types.

2.8.1.2 Charged groups

The presence of charged groups is a fundamental property of an ion exchanger. The type of group determines the type and strength of the ion exchanger; their total number and availability determines the capacity. There is a variety of groups which have been chosen for use in ion exchangers [103]; some of these are shown in Table 2.2.

Table 2.2: Functional groups used on ion exchangers.

Anion Exchangers	Functional Group
Diethylaminoethyl (DEAE)	$-O-CH_2-CH_2-N^+H(CH_2CH_3)_2$
Quaternary aminoethyl (QAE) CH$_3$	$-O-CH_2-CH_2-N^+(C_2H_5)_2-CH_2-CHOH-$
Cation exchangers	**Functional group**
Carboxymethyl (CM)	$-O-CH_2-COO^-$
Sulphopropyl (SP) CH$_2$SO$_3^-$	$-O-CH_2-CHOH-CH_2-O-CH_2-CH_2-$
Methyl sulphonate (S) CH$_2$SO$_3^-$	$-O-CH_2-CHOH-CH_2-O-CH_2-CHOH-$

Sulphonic and quaternary amino groups are used to form strong ion exchangers; the other groups form weak ion exchangers. The terms strong and weak refer to the extent of variation of ionization with pH and not the strength of binding. Strong ion

exchangers are completely ionized over a wide pH range whereas with weak ion exchangers, the degree of dissociation and thus exchange capacity varies much more markedly with pH.

2.8.2 Affinity chromatography

Affinity chromatography separates proteins on the basis of a reversible interaction between a protein and a specific ligand coupled to a chromatography matrix. The technique is ideal for a capture or intermediate step in a purification protocol and can be used whenever a suitable ligand is available for the protein of interest. With high selectivity, hence high resolution, and high capacity for the protein of interest, purification levels in the order of several thousand-fold with high recovery of active material are achievable. Target protein is collected in a purified, concentrated form.

Biological interactions between ligand and target molecule can be a result of electrostatic or hydrophobic interactions, van der Waals' forces and/or hydrogen bonding. To elute the target molecule from the affinity medium the interaction can be reversed, either specifically using a competitive ligand, or non-specifically, by changing the pH, ionic strength or polarity.

In a single step, affinity purification can offer immense timesaving over less selective multistep procedures. The concentrating effect enables large volumes to be processed. Target molecules can be purified from complex biological mixtures, native forms can be separated from denatured forms of the same substance and small amounts of biological material can be purified from high levels of contaminating substances.

For an even higher degree of purity, or when there is no suitable ligand for affinity purification, an efficient multi-step process must be developed using the purification strategy of Capture, Intermediate Purification and Polishing (CIPP). When applying this strategy affinity chromatography offers an ideal capture or intermediate step in any purification protocol and can be used whenever a suitable ligand is available for the protein of interest.

Successful affinity purification requires a biospecific ligand that can be covalently attached to a chromatography matrix. The coupled ligand must retain its specific binding affinity for the target molecules and, after washing away unbound material, the binding between the ligand and target molecule must be reversible to allow the

target molecules to be removed in an active form. Any component can be used as a ligand to purify its respective binding partner. Some typical biological interactions, frequently used in affinity chromatography, are listed below:

• Enzyme → substrate analogue, inhibitor, cofactor.

• Antibody → antigen, virus, cell.

• Lectin → polysaccharide, glycoprotein, cell surface receptor, cell.

• Nucleic acid → complementary base sequence, histones, nucleic acid polymerase, nucleic acid binding protein.

• Hormone, vitamin → receptor, carrier protein.

• Glutathione → glutathione-S-transferase or GST fusion proteins.

• Metal ions → Poly (His) fusion proteins, native proteins with histidine, cysteine and/or

Tryptophan residues on their surfaces.

Fig. 2.16 shows the stages in an affinity purification [101].

1. Affinity medium is equilibrated in binding buffer
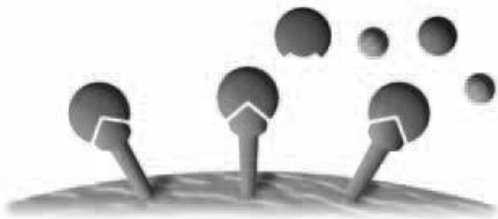
2. Sample is applied under conditions that favor specific binding of the target molecule to a binding subtances(ligand).

3.Target protein is recovered by changing conditions to favor elution of the bound molecules

4.Affinity medium is re-equilibrated with binding buffer

Figure 2.16: Affinity purification steps.

2.8.2.1 Affinity medium matrix

The list below highlights properties required for efficient chromatographic matrix :

- Extremely low non-specific adsorption, essential since the success of affinity chromatography relies on specific interactions.
- An open pore structure ensures high capacity binding even for large biomolecules, since the interior of the matrix is available for ligand attachment.
- Good flow properties for rapid separation.
- Stability under a range of experimental conditions such as high and low pH, detergents and dissociating agents.

In affinity chromatography, the particle size and porosity are designed to maximize the surface area available for coupling a ligand and binding the target molecule. A small mean particle size with high porosity increases the surface area. Increasing the degree of crosslinking of the matrix improves the chemical stability, in order to tolerate potentially harsh elution and wash conditions, and creates a rigid matrix that can withstand high flow rates. These high flow rates, although not always used during a separation, save considerable time during column equilibration and cleaning procedures.

2.8.2.2 The ligands of affinity medium

The ligand is the molecule that binds reversibly to a specific molecule or group of molecules, enabling purification by affinity chromatography.

The selection of the ligand for affinity chromatography is influenced by two factors: the ligand must exhibit specific and reversible binding affinity for the target substance(s) and it must have chemically modifiable groups that allow it to be attached to the matrix without destroying binding activity.

The dissociation constant (k_D) for the ligand - target complex should ideally be in the range 10^{-4} to 10^{-8} M in free solution.

Interactions involving dissociation constants greater than 10^{-4} M, for example the binding reaction between an enzyme and a weak inhibitor, are likely to be too weak for successful affinity chromatography. Conversely, if the dissociation constant is lower than approximately 10^{-8} M, for example the affinity between a hormone and

hormone receptor, elution of the bound substance without causing inactivation is likely to be difficult. If no information on the strength of the binding complex is available, a trial and error approach must be used [101].

2.8.3 Hydrophobic interaction (HI) chromatography

HI-chromatography [104] was discovered serendipitously when, in control experiments, ligands were omitted from the matrix/spacer arm combination. It was found that the resulting resins were nevertheless effective at separating proteins, due to hydrophobic interactions between the sample proteins and the aliphatic spacer arms. Following this discovery, HI-resins were purposefully designed to optimize the hydrophobic interaction. Hydrophobic bonds are increased in strength by an increase in buffer ionic strength. HI-chromatography therefore conveniently fits into an isolation scheme, immediately after a salting out step, as the high salt levels will promote binding to the HI-resin. Proteins can subsequently be eluted by decreasing the buffer ionic strength, either in a stepwise manner or in a gradient.

2.9 Protein Interactions with Solid Surfaces

Generally, the surfaces of materials of almost any type that come into contact with protein mixtures tend to become quickly occupied by proteins. Protein interactions with solid surfaces have been studied, and several reviews are available [105–109].

2.9.1 Interfaces

Interfaces and interactions that take place in interfacial regions can be complex. In fact, the interface has been described as a fourth state of matter [110]. The properties of atoms or atomic groups at a material surface are different from those of the bulk material. The first layer of atoms, in contact with the fluid phase, is particularly unique. Chemical composition, molecular orientation, and properties relevant to crystallinity differ at the surface. In addition, surfaces have different electrical and optical properties and can be characterized by atomic- or molecular-level textures and roughnesses. Surfaces have wettabilities or hydrophobic/hydrophilic balances related to the factors named above. Further, surfaces are generally energetically heterogeneous. For example, although a surface may be assigned a particular

wettability, it would most likely be the result of a distribution of surface regions of varying wettabilities.

In spite of this complexity, many researchers have met with success in describing some aspect of protein adsorption in terms of one or several surface properties. The effects of charge distribution, surface energy, and surface hydrophobicity have received much attention [105−109]. The extent of protein adsorption or biological adhesion in general could be determined purely by surface energetics, that is, the surface energies of the synthetic material, liquid medium, and adsorbates involved. Such an approach would imply that the free energy of adsorption is minimized at equilibrium. Adsorption would be favored if it caused the free energy function to decrease and would not be favored if it caused the function to increase. In the absence of electrostatic and specific receptor–ligand interactions, the change in free energy upon adsorption could be written

$$\Delta F_{ads} = \gamma_{AS} + \gamma_{AL} + \gamma_{SL} \tag{2.5}$$

where F_{ads} (J/m^2) is the free energy of adsorption per unit of surface area, and γ_{AS}, γ_{AL} and γ_{SL} (J/m^2) are the adsorbate-solid, adsorbate-liquid, and solid-liquid interfacial energies, respectively.

If all the required interfacial energies of equation (2.5) could be estimated, one could predict the relative extent of adsorption among different surfaces. This would lead to a distinction between two situations [111-112], depending on whether adsorbate surface energy is greater than or less than the surface energy of the suspending liquid. Concerning protein adsorption from aqueous media, equation (2.5) would predict increasing adsorption with decreasing surface energy. In other words, a given protein would be expected to adsorb with greater affinity to hydrophobic as opposed to hydrophilic surfaces.

2.9.2 Isoelectronic point, pI

The isoelectronic point or isoionic point is the pH at which the amino acid does not migrate in an electric field. This means it is the pH at which the amino acid is neutral. If the pH of the solution is greater than the pI, the net charge of the protein would be negative, whereas if the pH is less than the pI, the net charge of the protein would be positive. The pI is given by the average of the pK$_a$'s that involve the

zwitterion so that give the boundaries to its existence. There are three cases to consider:

1) Neutral side chains

These amino acids are characterized by two pK_a's : pK_a1 and pK_a2 for the carboxylic acid and the amine respectively. The isoelectronic point is the average of, these two pK_a's,

$$pI=1/2(pK_a1+pK_a2) \tag{2.6}$$

At very acidic pH (below pK_a1) the amino acid have an overall positive charge and at very basic pH (above pK_a2) the amino acid have an overall negative charge (Figure 2.17).
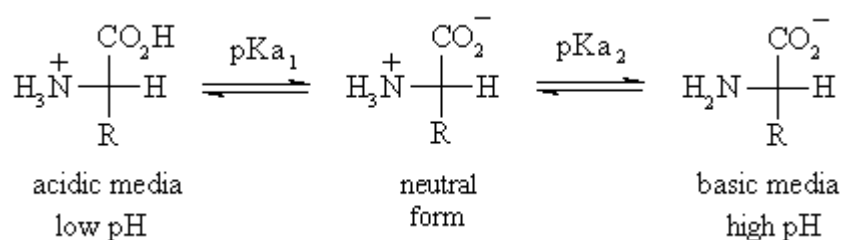
Figure 2.17: The overall charge of amino acids with neutral side chains.

The other two cases introduce other ionizable groups in the side chain "R" described by a third acid dissociation constant, pK_a3

2) Acidic side chains

The pI will be at a lower pH because the acidic side chain introduces an extra negative charge. So the neutral form exists under more acidic conditions when the extra negative charge has been neutralized. For example, for aspartic acid shown in Figure 2.18, the neutral form is dominant between pH 1.88 and 3.65, pI is halfway between these two values, so that pI = 1/2 (pK_a1 + pK_a3), so pI = 2.77.
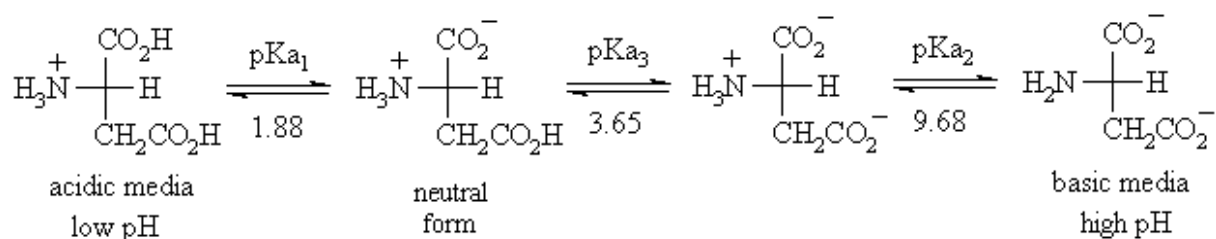
Figure 2.18: The overall charge of amino acids with acidic side chains.

3) Basic side chains

The pI will be at a higher pH because the basic side chain introduces an extra positive charge. So the neutral form exists under more basic conditions when the extra positive charge has been neutralized. For example, for histidine the neutral form is dominant between pH 6.00 and 9.17, pI is halfway between these two values, so that pI = 1/2 (pK$_a$2 + pK$_a$3), so pI = 7.59.

2.9.3 Proteins at interfaces

The net charge of a protein in solution is dependent on the difference between pH of the solution and the isoelectric point (pI) of the protein. The maximum adsorption occurs at the isoelectric point. As the out-of-balance charge of a protein increases, it will be in a more extended form than when the net charge is zero [113].

Norde and Lyklema [114] suggested that the degree to which pH affects the adsorption of a protein is determined by its conformational stability. They found that plateau values of adsorbed mass were independent of pH for structurally stable proteins, whereas those of less stable proteins varied considerably, apparently because less stable proteins were able to change structure with solution conditions. The effect of pH on protein adsorption and desorption can depend on solution history as well [115]. Kondo and Higashitani [116] studied the adsorption of model proteins with wide variation in molecular properties. They explained the pH dependence of adsorbed mass in terms of lateral interactions. In particular, they suggested that lateral interactions between large protein molecules are stronger than those between small molecules. Large proteins would thus be expected to show maximum adsorption around their pI's, whereas the effect of pH on smaller proteins would be less pronounced.

Ionic strength also affects protein adsorption. At low ionic strength, protein surface charge fully contributes to the total electrostatic interaction [113]. At high ionic strength, the surface charges of proteins are shielded, reducing electrostatic interactions between proteins, whether attractive or repulsive [115]. Luey et al. [117] showed that ionic strength effects on adsorbed mass are very much related to solid surface properties. They observed that increased ionic strength reduced the electrostatic repulsion between negatively charged β-lactoglobulin molecules and the

hydrophilic, negatively charged surface they studied. By contrast, increased ionic strength resulted in little change in adsorbed mass at hydrophobic surfaces.

2.9.4 Surface-induced conformational changes

It is well known that a given protein can exist in multiple adsorbed conformational states on a surface [118–120]. These states can be distinguished by differences in occupied area, binding strength, tendency to undergo exchange events with other proteins, and catalytic activity or function. All these features of adsorbed protein are interrelated and can be time-dependent. For example, decreases in surfactant-mediated elution of proteins from an adsorbed layer are observed as protein–surface contact time increases [121]. It has been observed that the extent of conformational change experienced by adsorbed fibrinogen increases with contact surface hydrophobicity [122]. This is consistent with findings of Elwing et al. [123], who used elipsometry to make inferences regarding conformational changes experienced by complement factor III, a plasma protein, on hydrophilic and hydrophobic silica surfaces. The results of Elwing et al. also showed that greater values of adsorbed mass were found on hydrophobic as opposed to hydrophilic surfaces. Protein molecules are assumed, in general, to change conformation to a greater extent on hydrophobic surfaces. This is due to the effect of hydrophobic interactions between the solid surface and hydrophobic regions in the protein molecule. In fact, surface-induced unfolding is often characterized as entropically driven, because the hydrophobic protein interior associates with hydrophobic regions of the surface during unfolding. These interactions can give the molecule an extended structure, covering a relatively large area of the surface. If the repulsive force normally acting between native protein molecules is decreased for such structurally altered molecules, one would expect to measure a greater adsorbed mass on hydrophobic as opposed to hydrophilic surfaces. On the other hand, adsorption of positively charged protein to hydrophilic (negatively charged) silica can result in greater conformational change than adsorption of the same protein to hydrophobic silica, even with a greater extent of adsorption being observed at the hydrophobic silica surface [124]. It is thus important to recognize that multiple factors affect the extents of protein adsorption and conformational change.

2.9.5 Steady-state adsorption behavior

Numerous protein adsorption isotherms have been constructed and compared based on temperature, pH, ionic strength, conformational stability of the protein in solution, and solid surface charge and hydrophobicity. The effects of protein conformational stability and solid surface properties are revealed with effects of pH and ionic strength.

The effect of pH and ionic strength on protein adsorption is dependent on which type of interactions predominate (e.g., electrostatic, hydrophobic, or van der Waals interactions). At a negatively charged surface, if electrostatic interactions predominate, adsorbed mass should be greater at pH values below the isoelectric point relative to pH values above it. Below the isoelectric point, the protein and surface would be of opposite charge, whereas both the protein and surface would be negatively charged at pH values greater than the isoelectric point. As ionic strength increases, the electrostatic interaction would be reduced because of shielding of the protein by counterions; consequently, increasing the ionic strength should decrease adsorbed mass at pH values less than the isoelectric point and increase the adsorbed mass at greater values of pH. The relationship between adsorbed mass and changes in pH and ionic strength becomes inextricably linked to protein conformational stability. In general, pH and ionic strength conditions that lead to a less stable conformation for the protein in solution will lead to an increased adsorbed mass, assuming that the protein molecule would be more stable on the solid surface [117].

2.9.6 Models for protein adsorption

The thermodynamic treatment of protein adsorption from solution could be directly analogous to that for adsorption of small nonpolar molecules from the vapor phase for which there are several well-developed surface equations of state. For such simple molecule adsorption, the adsorbent surface geometric and energetic irregularities along with specific sorbate–surface interactions are generally the chief complexities. For protein adsorption in practice, however, thermodynamic treatment of equilibria is severely limited by the additional complexities arising from specific solvent–protein interactions, protein conformational variations both in solution and on the adsorbent surface, and frequent multipoint attachment configurations.

The most models used for protein adsorption equilibria are simple empirical or semi theoretical models that are useful according to their goodness-of-fit to the experimental data. The semi theoretically based Langmuir adsorption isotherm given by :

$$q=q_mC/(K_D+C) \tag{2.7}$$

Where q is quantity adsorbed per unit of adsorbent, C is concentration of protein in solution, q_m is maximum quantity adsorbed at high C, and K_D is the disassociation or binding constant. Although the physical assumptions underlying the development of this model are not followed by protein adsorption via ion Exchange, the model nonetheless has provided a good fit if salt concentration-dependent parameters are used.

Another common adsorption model is the temkin isotherm model. The Temkin isotherm can be expressed by the following equation :

$$X=a+blnC \tag{2.8}$$

Where X is q is quantity adsorbed per unit of adsorbent, C is concentration of protein in solution, a and b are constants related to adsorption capacity and intensity of adsorption.

Numerous ion exchange protein adsorption studies have been performed with measures of adherence to the Langmuirian behavior.

The thermodynamic parameters such as change in standard free energy (ΔG^o), enthalpy (ΔH^o) and entropy (ΔS^o) can be determined by using the following equations:

$$lnK_c = \frac{\Delta S^0}{R} - \frac{\Delta H^o}{RT}$$
$$\Delta G_{ads} = \Delta H_{ads} - T\Delta S_{ads} \tag{2.9}$$

Where R (8.314 J/mol K) is the gas constant, T (K) the absolute temperature and K_c (L/g) is the standard thermodynamic equilibrium constant defined by q_e/C_e. By plotting, a graph of ln K_c versus 1/T the values, ΔH° and ΔS° can be estimated from the slopes and intercepts.

2.9.7 Kinetics modeling

Adsorption is time-dependent process and it is very important to know the rate of adsorption for design and evaluate the adsorbent for the adsorption of proteins. In many cases, the kinetics of adsorption based on the overall adsorption rate by the adsorbents is described by the first order Lagergren model and pseudo second-order. The first-order rate expression of Lagergren is given as:

$$\frac{dq}{dt} = k_1 (q_e - q_t) \tag{2.10}$$

Where q_e and q_t are the amount of dye adsorbed on adsorbent at equilibrium and time t, respectively (mg/g), and k_1 is the rate constant of first order adsorption (min^{-1}). Integrating equation (7) for the boundary conditions t = 0 to t = t is the following:

$$log(q_{eq} - q_t) = log\ q_{eq} - (k_1 \cdot t) / 2.303 \tag{2.11}$$

The plot of log $(q_e - q_t)$ versus t will give a straight line and the value of k1 can be obtained from the slope of the graph. The second-order kinetic model is expressed as:

$$\frac{dq}{dt} = k_1 (q_e - q_t)^2 \tag{2.12}$$

Where, k_2 is the pseudo-second-order rate constant of adsorption (g mg^{-1}min^{-1}). The linearized integrated form of (9) is given as:

$$1/q_t = 1 / k_2 q_{eq} t + 1 / q_{eq} \tag{2.13}$$

If the pseudo second-order kinetics is applicable to the system, then the plot of t / q_t versus t will give a linear relationship with 1 / q_e and 1 / $k_2 q_e^2$ as a slope and intercept, respectively.

The values of q_e and k_2 can be determined from the slope and intercept and there is no need to know any parameters beforehand. The pseudo second-order kinetics model has been successfully applied to several biosorption systems as reported by McKay and Ho [125].

3. EXPERIMENTAL PART I

3.1 Materials and Instruments

3.1.1 Materials

Invertase (-fructofuranosidase, EC 3.2.1.26, Grade VII from baker's yeast) (Sigma–Aldrich), glucose oxidase (GOD, EC 1.1.3.4. Type II from *Aspergillus niger*) (Sigma–Aldrich), peroxidase (POD, EC 1.11.1.7, Type II from horseradish) (Sigma–Aldrich), bovine serum albumin (BSA) (Sigma–Aldrich), *o*-dianisidine dihydrochloride (Sigma–Aldrich), sucrose (Sigma–Aldrich), glucose (Sigma–Aldrich), ethyleneglycol dimethacrylate (EGDMA) (Fluka), glycidyl methacrylate (GMA) (Fluka), α'- α'- azobisisobutyronitrile (AIBN) (Fluka), bipyridine (Fluka), hydrazine (Fluka), 2-methyl pyrrolidone (NMP) (Fluka), 4-vinylbenzyl chloride (Fluka), polyvinyl alcohol (fully hydrolyzed very low molecular weight, MW 7000–10,000) (Sigma–Aldrich), CuBr (Fluka), Tris-HCl (tris(hydroxymethyl)aminomethane-HCl) (Sigma–Aldrich), Chlorosulfonic acid (Sigma–Aldrich), styrene (Fluka), divinylbenzene (DVB) (Sigma–Aldrich), Aminomethanesulphonic acid (Fluka), Ethyl acrylate (Fluka), Methylene Blue, Crystal violet (Merck), Acetaldehyde (Fluka), Benzaldehyde (Fluka) salicyl aldehyde (Fluka), Hydrazine (Fluka),

3.1.2 Instruments

JEOL (JSM 5600) scanning electron microscope, UV-Vis Spectrophotometer (Perkin-Elmer Lamda 25), Dionex HPLC system. FT-IR (Nicolet 380), Sonicator Model Misonix S-4000, Illinois, USA)

3.2 Preparation of Polymeric Sorbents

Polymeric methacrylate, acrylate and sulfonamide based sorbents were prepared and modified with hydrazine, amine, carboxylic acid and sulfonic acid groups to adsorb different bioactive molecules, dyes and aldehydes.

3.3 Preparation of PVBC (polyvinyl chloride) Microspheres

Crosslinked PVBC microspheres were prepared by suspension polymerization according to the literature [126]. VBC (5.0 mL, 31.9 mmol), EGDMA (1.5 mL, 7.8 mmol), and AIBN (0.12 g, 0.71 mmol) were dissolved in toluene (7.2 mL). The resulting solution was dispersed in an aqueous medium, prepared by dissolution of PVA (0.25 g) in water (80 mL). The polymerization was carried out in a magnetically stirred glass flask (100 mL) at 78 °C for 8 h. After polymerization, the PVBC microspheres were washed exhaustively with water and ethanol respectively, to remove the diluents and unreacted monomers. They were subsequently dried in vacuum at 50 °C. The microspheres were sieved and a proper size fraction (75-150 μm diameters) was isolated.

3.4 Grafting of Poly (glycidyl methacrylate) (PGMA) onto PVBC by Surface Initiated Atom Transfer Radical Polymerization (SI-ATRP)

Graft polymerization of glycidyl methacrylate (GMA) was achieved through PVBC initiation sites on the beaded polymer.

PVBC microspheres was accomplished in a magnetically stirred glass flask (100 mL) by immersing the microspheres (5 g) into a reaction mixture containing 20 mL (0.15 mol) of GMA, 0.432 g (3 mmol) of CuBr, 0.936 g (6 mmol) of bipyridine, and 10 mL Dioxane. The suspension was purged with nitrogen for approximately 10 min to remove the dissolved oxygen. The flask was then sealed. Polymerization was carried out at 65 °C for 18h.

At the end of the reaction period, the reaction content was poured into 250 ml acetone to remove homopolymer and the grafted resin was added to 10% of EDTA solution to remove copper salt contaminants. The mixture was filtered and was washed with excess of water (500 ml) and alcohol (100 ml) respectively. Vacuum dried sample weighed 20 g.

In addition, grafting kinetics of PGMA onto resin was investigated at different reaction times and conversion time plot was obtained.

3.4.1 Epoxy content of the poly(GMA) grafted resin

The amount of available functional epoxy group content of the resin was determined by pyridine-HCl method according to the literature [127].

0.2 g of the graft resin was left in contact with 10 mL of pyridine-HCl solution and refluxed for 1 hour. After filtration, 2 mL of filtrate was taken and epoxy content of the solution was determined by titration with 0.055 M NaOH solution in the presence of phenol-phatalein color indicator. Epoxy content of the resin was found as 7.1 mmol / g resin.

3.4.2 Modification of the poly(GMA) grafted resin with hydrazine (resin 1) and ammonia

The beads about (10 g) were transferred into a reaction flask containing hydrazine (50 mL) and 2-methyl pyrrolidone (30 mL) at 0 °C and the mixture was shaken at 150 rpm at room temperature for 24 h and the reaction mixture was heated at 90 °C for 5 h. After cooling, the hydrazine modified beads were transferred into purified water (500mL) and stirred magnetically for 2 h. The beads were then filtered and were washed sequentially with purified water (1.0 L) and methanol (25 mL). The hydrazine functionalized poly (VBC-g-GMA) beads were dried under vacuum at 25°C for 24 h.

Poly (VBC-g-GMA) beads (10 g) were also aminated with 0.5M ammonia at pH 10.0, and at 65 °C in a reactor. The reaction was carried out for 5 h. After the reaction, the aminated beads were washed with excess of distilled water.

3.4.3 Determination of hydrazine content of the resin 1

Resin 1 (about 0.1 g) was transferred in a mixture of HCl (0.6 M, 50 mL) and KI (0.1M, 5 mL), and stirred continuously at room temperature for 24 h. The consumed iodine was determined by titration with 0.1M sodium thiosulfate solution. The hydrazine content of the polymer beads was found as 6.4 $mmol.g^{-1}$.

3.4.4 Sorption of the invertase enzyme of the resin 1

Sorption experiments of resin 1 were performed depending on pH, ionic strength and temperature.

3.4.4.1 Preparation of the buffer solutions

Buffer solution were prepared from acetic acid (50 mM) and sodium acetate (50 mM) for pH 4-5, sodium hydrogen phosphate (50 mM) and potassium dihydrogen phosphate (50 mM) for pH 6 and (tris(hydroxymethyl) aminomethane-HCl (50 mM) for pH 7.0–8.0, respectively.

3.4.4.2 Purification of invertase from crude yeast extract

Saccharomyces cerevisiae cells were cultured and were maintained on the medium containing sucrose (30.0 g/L); peptone (5.0 g/L) and yeast extract 3.0 g/L at pH 6.0. The culture was maintained on agar slants at 30 ^{0}C for 18 h by periodic transfer and was used for inoculation of S. cerevisiae cells to liquid medium (10 mL). The same medium (100 mL) was used as invertase production medium. The medium was incubated at 30 ^{0}C and 200 rpm for 24 h. At the end of incubation period, yeast biomass was harvested by centrifugation at 5.000 rpm, 4 ^{0}C for 10 min. The biomass was washed twice and suspended in Tris–HCl buffer (20 mM, pH 7.5). The yeast cells suspension was sonicated four times for 30 s using a sonicator. The homogenate was centrifuged at 4^{0}C and at 15.000 rpm for 10 min and the supernatant obtained was used as the source of invertase.

The purification of invertase was carried out as described above except that crude yeast extract solution was used as an adsorption medium instead of pure invertase solution. The elution of proteins from affinity beads was determined by measuring the initial and final concentrations of protein within the adsorption medium using Coomassie Brilliant Blue as the method described by Bradford [128]. A calibration curve constructed with invertase solution of known concentration (0.05–0.50 mg/mL) was used in the calculation of protein in the solutions.

The activity of invertase was determined by measuring the amount of glucose liberated from the invertase-catalysed hydrolysis of sucrose per unit time as described in literature [129]. A Dionex HPLC system (Dionex Co., Germering, Germany) was used for the determination of the purity of the purified invertase samples. The HPLC system consisted of a quaternary pump with an on-line vacuum degasser (Model P580 A), an auto sampler, a column oven (Model STH 585) and an UV–vis diode array detector (Model 340 S). Chromatographic separation of proteins was achieved on a Supelco, Discovery, BIO Wide Pore C5 HPLC column (150mm×4.6mmi.d.;5µm) protected by a guard column (Supelco C5; 20mm, 4.6 i.d.). All sample solutions used in chromatographic studied was pre-filtered through a syringe membrane filter (0.2µm, Millipore) to remove particles and large aggregates. HPLC mobile phases A and B were prepared by adding trifluoroacetic acid (TFA; 0.1%, v/v) to MilliQwater and 75% acetonitrile and 25% MilliQwater, vice-versa respectively. The mobile phases were filtered prior to use. The chromatographic

separation was performed using a gradient at 1.0mL/min flow rate (0–25 min, phase B from 0% to 100%) and the sample injection volume of the auto sampler was 20μL. The UV–vis detector was set at 220 nm and the temperature was maintained at 25 °C.

3.4.4.3 Effect of pH, temperature and ionic strength on invertase adsorption

Adsorption of invertase on both hydrazine and amino groups functionalized beads was studied at various pHs (50mM, pH 3.5, 4, 5.0, 6, 6.5, 7 and 8). The effects of temperature and ionic strength on invertase adsorption were carried out at pH 4.0 for both affinity beads at four different temperatures (i.e., 5, 15, 25 and 35 ^{0}C) and at different NaCl concentrations (between 0.2 and 1.0 M), respectively. All experiments were conducted in duplicates with 50 mg affinity beads and initial concentration of invertase was 0.5 mg/mL in each set experiments.

3.4.4.4 Effect of initial concentration of invertase on adsorption capacities

To determine the adsorption capacities of both affinity beads, the initial concentration of invertase was changed between 0.125 and 2.0 mg/mL in acetate buffer (5.0 mL, pH 4.0). A calibration curve was prepared using invertase as a standard (0.1–2.0 mg/mL). The amount of invertase adsorbed onto affinity beads was determined by subtracting the absorbance at 280 nm after adsorption from the value before adsorptions using UV–vis spectrophotometer.

3.4.4.5 Dynamic binding capacity experiments

The continuous system was made from Pyrex glass (length 6.0 cm, diameter 1.8 cm, total volume 15.3 mL). A 10 g of dry hydrazine functionalized poly (VBC-g-GMA) beads was soaked in de-ionized water for 24 h and then packed in a column (the bed volume, 13.3 mL). The column was equilibrated with acetate buffer (50 mM, pH 4.0). Invertase solution (2.0 mg/mL) was prepared in acetate buffer (50 mM, pH 4.0), and introduced into the column by means of peristaltic pump at a constant flow rate. When the adsorptive sides of the hydrazine functionalized beads in the column were saturated, the column was washed with 50 mL of the same buffer solution to remove non-specifically adsorbed protein. Dynamic binding capacity (DBC)was calculated from breakthrough curves at 5% breakthrough point using the method of Griffith et

al. [40]. At 5% breakthrough, the total amount of protein in the system (including column and dead space) is calculated from equation giving as;

$$Q_{5\%} = A\,u\,C_o \int \left(1 - \frac{C}{C_o}\right) dt \tag{3.3}$$

where $Q_{5\%}$ is the total amount of invertase adsorbed at 5% breakthrough point (mg), u is superficial velocity of liquid phase (cm/h), t is the time of adsorption (h), A is the cross-sectional area of column (cm^2) C_o and C are the concentrations of invertase in feeding solution and in effluent at the moment of t, respectively (mg/mL). The protein contained in the dead space is calculated by

$$Q_d = V_d\,C_0 \tag{3.4}$$

where V_d is the dead volume (mL) and Q_d is the amount of protein in dead volume (mg).So, the DBC at 5% breakthrough is estimated as follows.

$$DBC = \frac{(Q_{5\%} - Q_d)}{m} \tag{3.5}$$

Where, m is the mass of adsorbent (g) in the sedimented bed volume.

3.4.4.6 Adsorption isotherms and thermodynamic parameters

The adsorption isotherm was obtained from batch experiment at different temperatures. Three theoretical isotherm models, Langmuir and Scatchard's equation [130,131], Freundlich [132] and Dubinin–Radushkevich [133] were used to analyze the experimental data. One of the most widely used isotherm equations for modeling adsorption data is the Langmuir equation, which for dilute solutions may be represented as:

$$q_e = q_m\,bC_e\,/\,1 + bC_e \tag{3.6}$$

In order to confirm the Langmuir isotherm mechanism, the experimental data was analyzed according to the Scatchard's plot [131].

$$\frac{q_e}{C_e} = q_m b - q_e b \tag{3.7}$$

In Eqs. (3.6) and (3.7), C_e is the equilibrium concentration of protein in solution (mg/L), q_e is the equilibrium amount of protein adsorbed on the affinity beads at time t (mg/g). q_m is the maximum adsorption capacity of the affinity beads (mg/g) and b (i.e., the adversely of dissociation constant of the ligand/surface interaction, K_d, or equal to association constant, K_a, ($b = K_a = (1/K_d)$) is the energy of adsorption

dissociation constant. K_d has dimension of concentration, and the protein binding is stronger when it is smaller. The Freundlich expression is an empirical equation based on adsorption on a heterogeneous surface. The Freundlich equation is commonly presented as:

$$q_e \; K_F \, (C_e)^{1/n} \tag{3.8}$$

where K_F and n are the Freundlich constants characteristic of the system. K_F and n are indicator of the adsorption capacity and adsorption intensity, respectively. The slope and the intercept of the linear Freundlich equation are equal to $1/n$ and $\ln K_F$, respectively. The Dubinin–Radushkevich (D–R) isotherm is also widely used in adsorption studies because it does not assume a homogeneous surface or constant adsorption potential [133]. The D–R equation is given by the following relationship:

$$\ln q_e = \ln q_m - K\varepsilon^2 \tag{3.9}$$

where q_e is the amount of the invertase adsorbed at the equilibrium, K is the constant related to the mean free energy of sorption, q_m is the theoretical saturation capacity, and ε is the Polanyi potential, equal to $RT \ln (1 + (1/C_e))$. The values of q_m and K can be obtained by plotting $\ln q_e$ versus ε^2. The constant (K) is related to the mean free energy of adsorption per mole of the adsorbate as it is transferred to the surface of the solid from infinite distance in the solution, and the mean free energy (E) can be computed using the following relationship [133]. The Dubinin–Radushkevich (D–R) constant can give the valuable information regarding the mean energy of adsorption by the following equation:

$$E = (2K)^{-1/2} \tag{3.10}$$

3.4.4.7 Kinetic studies

In order to analyze the adsorption kinetics of invertase, the pseudo first-order and the pseudo second-order kinetics models were applied to the experimental data. The first-order rate equation of Lagergren is one of the most widely used for the adsorption of solute from a liquid solution. It may be rearranged to obtain a linear form and represented as follows:

$$\log (q_{eq} - q_t) = \log q_{eq} - (k_1 \cdot t) / 2.303 \tag{3.11}$$

The second-order equation based on adsorption equilibrium capacity may be expressed in the form:

$1/q_t = 1/k_2q_{eq}t + 1/q_{eq}$ **(3.12)**

where k_1 and k_2 are the rate constant of the first and second order adsorption (min^{-1}) (gmg^{-1} min^{-1}), respectively and q_{eq} and q_t denote the amounts of adsorbed invertase at equilibrium and at time t (mg/g), respectively.

3.4.4.8 Activity assays of free and immobilized invertase

The activities of both free and immobilized enzyme were determined as described literature [129]. The activity-pH profiles of the free and immobilized invertase were studied in acetate buffer (50 mM) in the pH range 4.0–5.5 and in phosphate buffer (50 mM) in the range pH 6.0–8.5. The effect of temperature on the free and immobilized invertase was studied in acetate (50 mM, pH 5.5), and phosphate buffer (50 mM, pH 6.0), respectively.

The results of dependence of invertase activity on pH, temperature, and storage stability are presented in a normalized form with the highest value of each set being assigned the value of 100% activity. K_m and V_{max} values of the free enzyme were determined by measuring initial rates of the reaction with sucrose (30–300 mM) in acetate buffer (50 mM, pH 5.5) at 35^{0}C. K_m and V_{max} were calculated from the initial rate of the kinetic data. The activities of the free and the immobilized invertase were expressed in μmol glucose/min/mg of enzyme. Sucrose hydrolysis performance of the free and immobilized enzyme preparations was determined by measuring the glucose content of the medium according to a method described in literature [134] using an UV/Vis spectrophotometer at 525 nm.

3.4.5.9 Reusability and storage stability of enzymes

To determine the reusability of the hydrazine functionalized beads for adsorption and cleaning of invertase was repeated six times by using the same affinity beads. Enzyme desorption were performed in a NaOH solution (1.0 M). The enzyme adsorbed beads were placed in the cleaning medium while stirring at 100 rpm at 25^{0}C for 2 h. The beads were removed from cleaning medium washed several times with acetate buffer (50 mM, pH 5.5) and were then reused in subsequence enzyme immobilization. The storage stability of invertase was studied in wet states. The enzyme immobilized affinity beads were stored in phosphate buffer (50 mM) at 4°C. The activity of the immobilized invertase was determined as described above for a

storage period of up to 2 months. The residual activity was defined as the fraction of total activity recovered after immobilization of invertase on the affinity beads compared with the same quantity of free enzyme.

3.5 Preparation of Crosslinked Poly (styrene-divinyl benzene) Beads

Beads were prepared by the suspension polymerization of a mixtured styrene (54 mL, 0.48 mol) and DVB (55 % grade, 10 ml, 0.038 mol) in toluene (60 mL), using gum-Arabic as stabilizer, according to literature [135]. The beads were sieved and the 420-590 μm size fractions were used for further reactions.

3.5.1 Chlorosulfonation of the resin

The beaded polymer was chlorosulfonated using chlorosulfonic acid as described in the literature [135]. The degree of chlorosulfonation was determined by analysis of the liberation of chloride ions. For these purpose, a polymer (0.2 g.) sample was added to 10% NaOH (20 ml) and boiled for 4 h. After filtration and neutralization with HNO_3 (5 M), the chlorine content was determined by the mercuric-thiocyanate [135].

3.5.2 Preparation of aminosulphonic based resin (Resin 2)

Chlorosulfonated resin 2 (10 g) was added portion wise to a stirred of aminomethanesulphonic acid 6 g (0.049 mol) and 7 mL triethylamine (acid scavenger) in 30 mL 1-methyl-2-pyrrolidone (NMP) 30 mL at 0 °C. The mixture was shaken with a continuous shaker for at room temperature for 12 hours. The reaction content was poured into water (500 mL), filtered and washed with excess water and acetone respectively. The resin dried under vacuum at room temperature for 24 h. The yield was 12.5 g.

3.5.3 Determination of sulphonamide content of the resin 2

For determination of the sulphonamide content, 0,2g. polymer sample was left in contact with 20 ml 0.5 M NaOH for 24 h. After filtration, 1 ml of the filtrate was taken and the base content of the solution was determined by titration with 0.1 M HCl solution in the presence of phenol–phatalein color indicator. A total sulphonamide content of the polymer was calculated as 3.1 mmol g^{-1} resin.

3.6 Interaction of Trypsin with Resin 2

3.6.1 Effect of pH , temperature and ionic strength on trypsin adsorption

The trypsin adsorption experiments were carried out batch wise by using 50 mg beads and 5 ml of trypsin (0.3mg/mL) at different pH medium and ionic strentgh. The pH values were varied between 4.0 and 8.0. Invertase adsorption of the resin 2 was studied at pH 4 and at 5, 15, 30 and 37 ^{0}C. In addition, these experiments were investigated at different NaCl concentrations (between 0.2 and 1.0M) at room temperature. In a typical adsorption experiment was conducted with solution and initial concentration of trypsin was in each set experiments. Trypsin adsorption by the beads was determined by measuring the initial and final concentration of trypsin by using UV-Vis spectrophotometer.

3.6.2 Effect of initial concentration of trypsin on adsorption capacities

To determine the adsorption capacity of the resin 2, the initial concentration of trypsin was changed between 0.1 and 1.5 mg/mL at pH 4.0. A calibration curve was prepared using invertase as a standard (0.1–2.0 mg/mL). The amount of trypsin adsorbed onto the beads was determined by subtracting the absorbance at 280 nm after adsorption from the value before adsorptions using UV–vis spectrophotometer.

3.6.3 Desorption of trypsin

The desorption of adsorbed trypsin from the resin was studied in a batch system. The trypsin adsorbed on the beads were placed within desorption medium containing 1.0 M KSCN at pH 8.0, and the amount of released trypsin was determined for 3 h. In order to show the reusability of the resin, adsorption–desorption cycle of trypsin was repeated 4 times.

3.6.4 Adsorption isotherms

The adsorption isotherm was obtained from batch experiment at different temperatures. Two theoretical isotherm models, Langmuir [130] and Freundlich [132] were used to analyze the experimental data.

In order to confirm the Langmuir isotherm mechanism, the experimental data was analyzed according to the Scatchard's plot.

3.6.5 Trypsin Sorption Kinetics of the Resin 2

For this purpose, 50 mg of resin 2 interacted with 5 mL of buffer solution (pH =4). Then the mixture was filtered, 5 mL of 0.3 mg /mL trypsin was added to the resin. The mixtures were stirred magnetic stirring bar and aliquots of the solution were taken at appropriate time intervals for analysis of the residual protein contents analysed by using UV.Vis spectrophotometer. The measurements were carried out at 280 nm.

In order to analyze the adsorption kinetic results of trypsin, the pseudo first-order and the pseudo second-order kinetic model which was described by Ho [125].

4. EXPERIMENTAL PART II

Synthesized polymeric sorbents were used in environmental applications: removal of aldehydes by using hydrazine functional sorbent (resin1) and basic dyes removal by acid containing sorbents (resin 2 and resin 3).

4.1 Aldehyde Adsorption Experiments of Resin 1

Invertase enzyme has aldehyde group. Therefore, the resin can be used to remove aldehydes from organic solutions. The maximum loading capacity of the resin 1 and aldehyde desorption conditions of the resin 1 were investigated.

4.1.1 Aldehyde loading capacities of the resin 1

Acetaldehyde, benzaldehyde, and salicylaldehyde were used in the sorption experiments. To estimate the maximum aldehyde binding capacities of the resin 1, 0.5 g of resin 1 was interacted with 15 mmol of aldehyde in 20 mL of methanol for 24 h at room temperature. This amount was chosen in order to have a 7.5–8.7-fold excess of the theoretical capacities. At the end of this period, the resin was removed by filtration and a sample of each filtrate (1 mL) was diluted with methanol up to appropriate concentrations (10^{-5} M). Quantitative determinations of aldehydes were carried out colorimetrically according to the procedure based on 2,4-dinitrophenylhydrazone formation yielding an absorption maximum around 480 nm [127].

The amounts of sorbed aldehydes were calculated by subtracting the final aldehyde contents (nonsorbed amounts) from the initial contents of the interacted solutions.

4.1.2 Aldehyde desorption from loaded resin 1

In order to investigate the desorption capacity of resin 1, aldehyde-loaded sample (0.2 g) were treated with 5 M HCl solutions of carbonyl-free methanol/water (1 : 1) mixtures. After filtration of solutions, desorbed aldehyde was calculated according to the procedure explained above.

4.2 Extraction of Basic Dyes

The synthesized other polymeric sorbents were used in basic dye removal from aqueous solutions.

Dye capacities of the resin were determined by mixing a weighed amount of polymer sample (0.2 g) with 20 mL aqueous dye solution (1 g dye/100 mL water). In these experiments, the dyes Methylene blue and Crystal violet were used as basic dyes. The mixture was stirred for 24 h and then was filtered. The dye concentrations were determined colorimetrically at different wavelengths and the dye loading capacities were calculated from the initial and final dye contents of the solution. 1 mL of the filtrate was used for determination of the residual dye.

4.2.1 Dye sorption kinetics of the resin 2

Batch kinetic experiment was studied by using highly diluted dye solution (1.3×10^{-3} g dye /L water). For this purpose, resin (0.2 g.) was wetted with distilled water (1.5 mL) and added to a solution of dye (90 mL). The mixtures were stirred with a magnetic stirring bar and aliquots of the solution (5 mL) were taken at appropriate time intervals for the analysis of the residual dye contents by the method as described above.

4.2.2 Regeneration of the basic dye loaded resin

The dye loaded samples (0.1 g) were interacted with 10 mL of H_2SO_4 (5 M) and stirred at room temperature for 24 h. After cooling, the mixtures were filtered, and 2 mL of the filtrate was removed for colorimetric analysis of the dyes. Regeneration capacity of the resin was found as 0.38 g / g resin for methylene blue.

4.3 Poly (ethyl acrylate) Grafting onto PVBC Microspheres

Graft polymerization of ethyl acrylate was achieved through chlorine initiation sites on the crosslinked Polyvinyl benzyl chloride.   A typical procedure is as follows:

0.053 g, (3.68 mmol) of CuBr, 0.172 g (1.09 mmol) of bipyridine and 2 mL of ethyl acrylate were put in a polymerization tube under nitrogen atmosphere.   Polymer sample (0.1 g) was added to the flask and the mixture was heated to 90 °C for 20 h. At the end of the reaction period, the reaction content was poured into 100 mL acetone to remove homopolymer and the grafted resin was added to 10% of EDTA

solution to remove copper salt. The mixture was filtered and was washed with excess of water and alcohol, respectively. Vacuum dried sample weighed 0.468 g.

Also, grafting kinetics of Poly (ethyl acrylate) from resin was investigated at different reaction times and conversion time plot was obtained.

4.3.1 Hydrolysis of the poly (ethyl acrylate) graft PVBC microspheres (Resin 3)

5 g of the poly (ethyl acrylate) grafted resin was interacted with 50 mL of 10 % NaOH for 24 h and 50 mL of 1 M H_2SO_4 for 8 h respectively. Hydrolyzed resin was filtered and was washed with excess of water and acetone respectively. The resin was dried under vacuum.

The resin was characterized by using titrimetric method and FT-IR spectrophotometric method.

4.3.2 Determination of carboxylic acid content of the resin 3

For the determination of the carboxylic acid content, 0.3 g of the resin was left in contact with 10 mL of NaOH (0.2 M) for 1 day. After filtration, 2 mL of the filtrate was taken and acid content of the solution was determined by filtration with 0.1 M HCl in the presence of phenol-phatalein color indicator. A total carboxylic acid content was found 3.56 mmol.g^{-1} resin.

4.3.3 Basic dyes removal studies

Dye adsorption capacities of the resin 3 were determined by mixing a 0.2 of resin sample with 20 mL aqueous basic dye solutions. In these experiments, the dyes Methylene Blue and Crystal violet were used (stock dye solution 1.0 g dye/100 mL water). The mixture was stirred for 24 h at room temperature and then was filtered. Methylene Blue and Crystal violet concentrations were determined spectrophotometericaly at 664 and 590 nm, respectively, and the dye loading capacities of the resin were calculated from the initial and final dye contents of the solutions.

4.3.4 Basic dyes sorption kinetics of the resin 3

Resin 3 is able to remove the basic dyes completely even from highly diluted aqueous dye solutions, which are industrially highly important. Here batch kinetic sorption experiments were performed with dilute dye solutions between (2.5x10^{-3} and

1.3x10^{-3} g/L) to investigate the efficiency of the resin in the presence of trace quantities of dyes.

For this purpose resin 3 (0.2 g.) was wetted with distilled water (1.5 mL) and was added to a solution of dyes (100 ml of 0.1 g. dyes in 90 mL water). The mixtures were stirred magnetic stirring bar and aliquots of the solution (5 mL) were taken at appropriate time intervals for analysis of the residual dye contents by the method as described above.

4.3.5 Regeneration of the Basic dye loaded resin 3

For the regeneration of the dye loaded resin 3, H$_2$SO$_4$ (5.0 M) solution was used as a regeneration agent according to the literature. When dye adsorbed resin were contacted with 5 M H$_2$SO$_4$ for 24 h, all the adsorbed Methylene Blue and Crystal Violet were desorbed from the resin 3.

5. RESULTS AND DISCUSSION I

In this part, separation results of biomolecules by polymeric sorbents were given.

5.1. Synthesis and Characterization of Hydrazine Modified Resin

The Resin 1 was prepared starting from copolymerization VBC-EGDMA by using suspension polymerization method. The surface morphology of the beads was exemplified by scanning electron microscopy (SEM) micrographs in Figure 5.1.
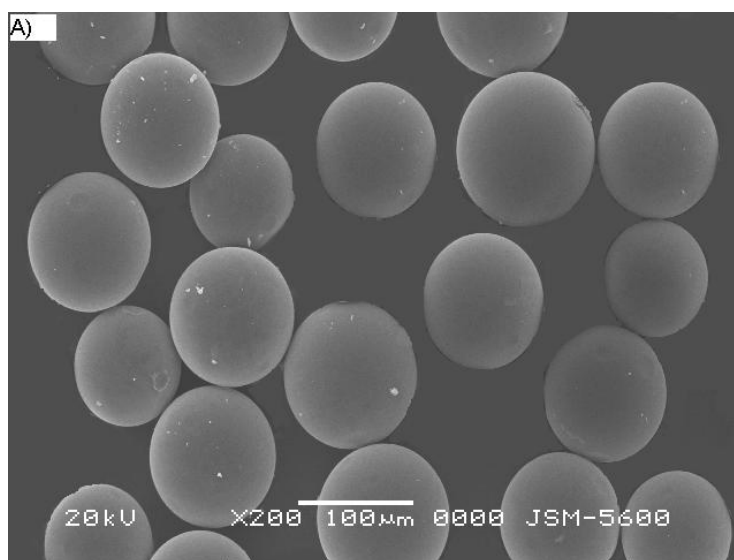
Figure 5.1: SEM micrograph the PVBC beads at 200× magnification.

The PVBC/EGDMA beads have spherical form with a smooth surface. Fibrous polymer grafted beads can be suitable matrices due to their intrinsically high specific surfaces, providing the quantity and accessibility of the interaction sites for high immobilization capacity.

The PGMA was grafted from the PVBC beads by using ATRP method (Figure 5.2). The surface halogen atoms (i.e., Cl) of the p(VBC) beads were successfully used as the initiating groups for atom transfer radical polymerization. Bipyridine and CuBr were used for SI-ATRP of glycidylmethacrylate.
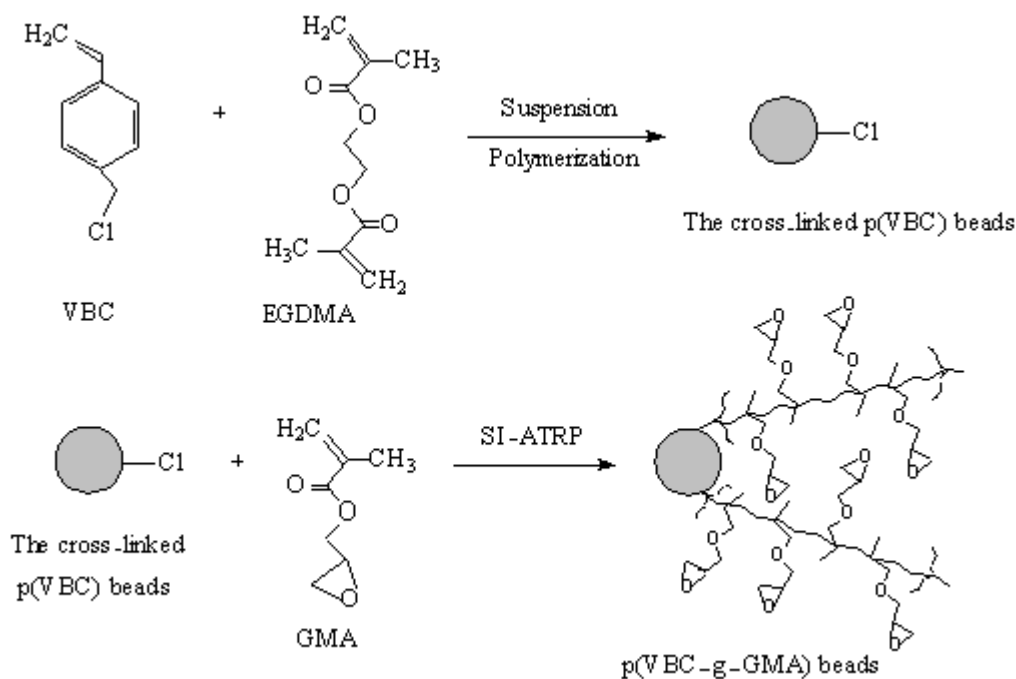
Figure 5.2: Preparation of PGMA grafted from PVBC.

The SI-ATRP reactions were carried out at different time intervals for determination of the mass increase. The grafting percentage (GP) was determined by calculating the percentage increase in weight using following equation:

$$GP = \left[\frac{(m_{gf} - m_0)}{m_0} \right] 100\%$$

(5.1)

Where, m_0 and m_{gf} are the weights of the beads before and after grafting, respectively. The grafting percentage – time plot is presented in Figure 5.4.

As seen in this figure, an increase in the grafting time from 3 to 18 h leads to increase more than 250% in grafting percentage. There was not found homopolymer in the polymerizing mixture by precipitation in ethanol.

The PVBC resin was modified with excess of hydrazine to obtain hydrazine modified Resin 1 (Figure 5.3).
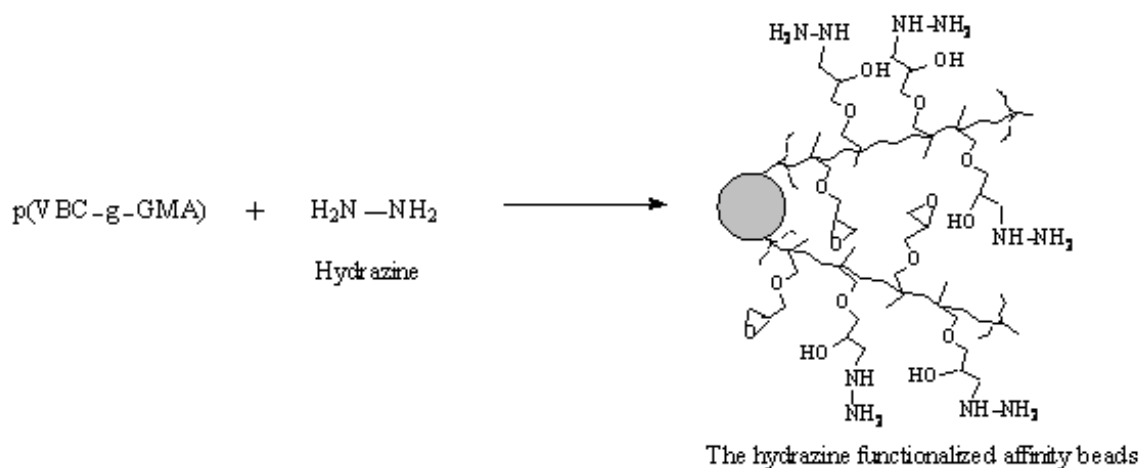
Figure 5.3: Modification of p (VBC-g-GMA) resin with hydrazine.

The equilibrium-swelling ratios of the PVBC, p (VBC-g-GMA) and hydrazine functionalized beads were determined as 1.12, 1.36 and 1.43, weight basis, respectively. The hydrazine functionalization of PGMA brushes causes an increase inswelling ratio due to introduction of hydrazine groups. Specific surface area of the PVBC, p (VBC-g-GMA) and hydrazine functionalized beads was found to be 4.1, 5.3 and 6.3m^2/g, respectively.
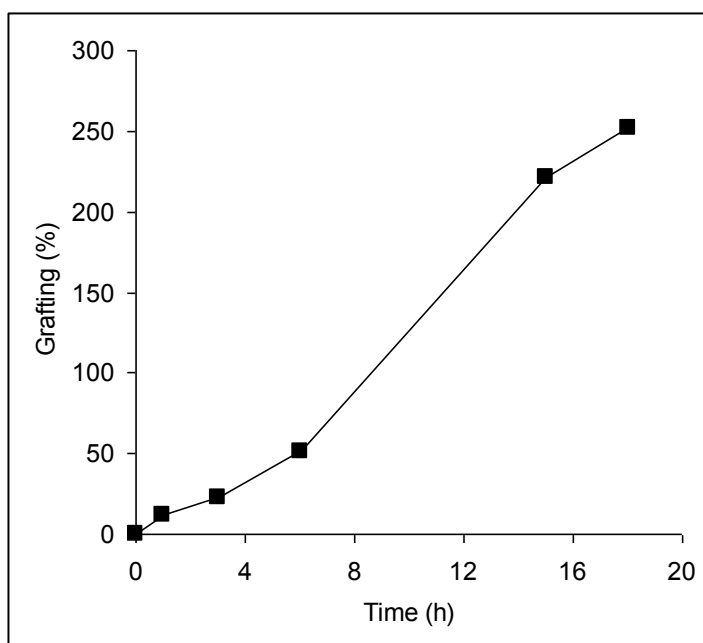
Figure 5.4: Grafting efficiency of p(GMA) from the p(VBC/ EGDMA) beads versus time plot.

The resin was characterized determination of the epoxy content. The maximum epoxy group content of the beads was determined as 7.1 mmol/g. The amount of

hydrazine and/or amino group contents of the beads were found to be 6.4 and 6.7 mmol/g beads, respectively, by using the difference between initial and final iodine concentration in the solution.

FTIR spectra of the PVBC, p (VBC-g-GMA) and hydrazine functionalized beads were presented in Figure 5.5. The peak at 2951 cm^{-1} is the characteristic adsorption peak of the aromatic ring of the PVBC beads (Fig.5.5 A). The FTIR spectra of the grafted p(VBC-g-GMA) beads have symmetric and asymmetric vibrations of the epoxy rings are observed at 1253 and 904 cm^{-1}, respectively (Figure 5.5 B). The FTIR spectra of hydrazine functionalized beads had absorption bands different from that of the poly (VBC-g-GMA) beads (Figure 5.5 B) at 3243 and 1653cm^{-1} corresponds to the $-NH_2$ stretching vibration and N–H deformation, respectively. These are due to the incorporation of the hydrazine groups on the grafted polymer structure (Figure 5.5 C).
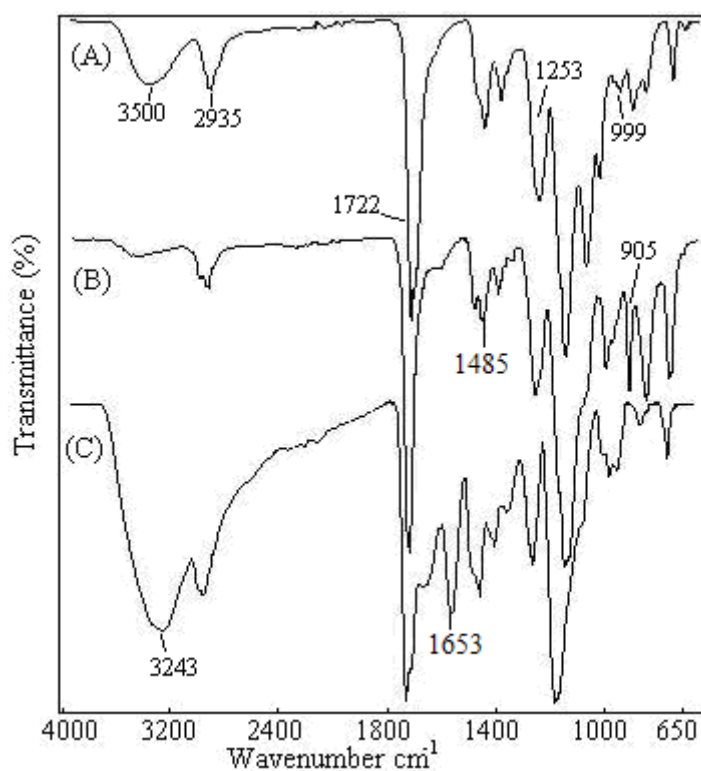
Figure 5.5: The FTIR spectra: (A) PVBC, (B) p(VBC-g-GMA) and (C) poly(VBC-g-GMA)-hydrazine beads.

5.2 Invertase Adsorption of Resin 1

The invertase sorption experiments were examined in different solid/liquid ratio, different pH and ionic strength.

5.2.1 Purification of invertase from crude yeast extract

Purification of invertase from crude yeast extract was studied in a batch system. The purity and the amount of adsorbed invertase on the hydrazine-functionalized beads were determined by HPLC using the eluent obtained from protein-adsorbed beads. The chromatogram of the standard invertase sample with a retention time 17.3 min was presented in Figure 5.6. The initial and remaining concentrations of invertase in the samples were calculated by integration of the peak areas.
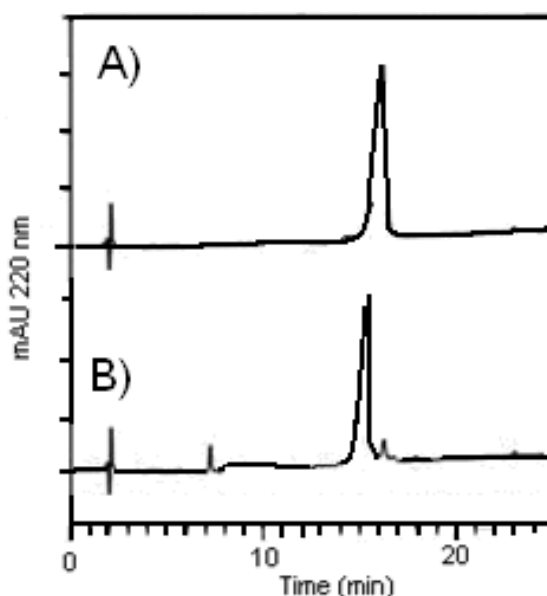
Figure 5.6: HPLC chromatogram for hydrazine functionalized beads showing: (A) commercial invertase, (B) purified invertase with the hydrazine functionalized beads.

The purity of eluted invertase was determined by HPLC as 92% with a recovery of 67%. Thus, hydrazine functionalized beads provided an efficient single step purification protocol to purify invertase from crude yeast extract, showing a high binding capacity and a high selectivity for invertase.

5.2.2 Solid/liquid ratio

The effect of the solid/liquid ratio on the adsorption efficiency of the hydrazine-functionalized beads was studied by varying the amount of beads from 25 to 125 mg in the adsorption medium (5.0 mL), while keeping other parameters (pH, agitation speed, initial concentration of invertase, contact time and volume of the adsorption medium) constant and the results are presented in Fig 5.7. As seen in this figure, it can be observed that adsorption efficiency of the beads improved with increasing dose while in constant protein solution (5 mL). This is expected due to the fact that the higher dose of beads in the solution, the greater availability of interaction sites for the invertase molecules. At 0.5 mg/L initial concentration of invertase, the percent maximum invertase adsorption efficiency was about 70% at the solid/liquid ratio of 10 mg/mL for affinity beads. In other words, the percent adsorption efficiency was about 70% in use at 5.0mL adsorption solution with 50 mg affinity beads. The equilibrium amount of protein adsorbed on the affinity beads (q) from adsorption medium was decreased with increasing adsorbent dosage in the 5.0 mL adsorption medium. This result was anticipated because for a fixed initial solute concentration, increasing adsorbent doses provides greater surface area (or adsorption sites), whereas the adsorbed invertase molecules quantity (q) per unit weight of the beads decreased by increasing the affinity beads quantity. In the remaining invertase adsorption experiments, a 50 mg of affinity beads were used in 5.0 mL adsorption medium.
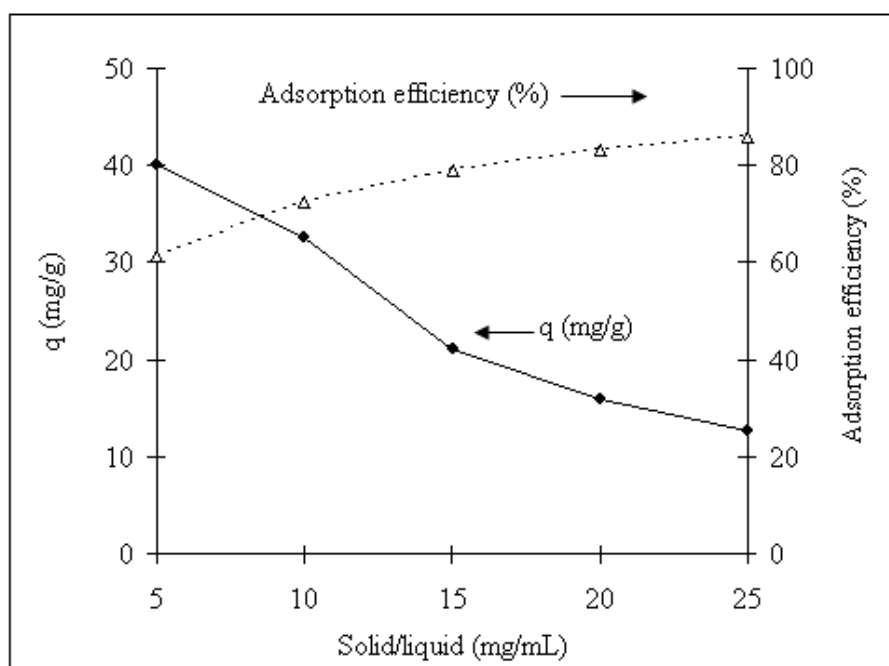
Figure 5.7: Effect of adsorbent dosage on the adsorption of invertase on the hydrazine functionalized beads. Experimental conditions; initial concentration of invertase 0.5 mg/mL; pH: 4.0; temperature: 25 ^{0}C.

5.2.3 Effect of pH on invertase adsorption capacity

The pH value of the solution affects both external charge distribution of invertase molecules and the functional groups of the affinity beads. In order to investigate the effects of pH on the invertase adsorption efficiency and capacity of both affinity beads, the medium pH was changed between pH 3.5 and 8.0. As seen in Figure 5.8, the maximum invertase adsorption capacity for hydrazine and amino groups functionalized beads were observed at around pH 4.0 and 5.5, respectively. The isoelectronic (pI) value of invertase is 3.2. The invertase molecules have net negative charges when medium pH is higher than 3.2 [136]. On the other hand, the pKa value of the hydrazine and amino groups is around 8.1 and 7.4, respectively. Thus, both functional groups have net positive charge at below their pKa values. At around pH 4.0 and 5.5, the electrostatic interaction between invertase molecules and both affinity beads should be predominant. Increasing the pH thereafter caused a decrease in adsorption capacity. Specific interactions between invertase molecules and hydrazine and/or amino functionalized affinity beads at pH 4.0 and 5.5, respectively, may result from both the ionization states of functional groups on affinity beads (i.e. primary, secondary amino and hydroxyl groups on the polymer chains) and the

73

amino acid side chains and carbohydrate moieties of the invertase molecules. Proteins that change conformation as a function of their environment (pH, salt, temperature etc.), such as invertase, it has a molecular mass of 123 kDa, and it could change conformational structure upon binding on a functional surface. Thus, invertase molecules would expand and contact according to the variation of the ionizable groups on its surfaces. At pH 4.0 and 5.5, the resulting invertase adsorption may be also due to suitable conformation of invertase molecules on both hydrazine and amino functionalized fibrous beads surface, respectively. As medium pH rises, the hydrazine and/or amino functionalized grafted polymer chains are closely packed, limiting the interaction of invertase with functional groups, thus, a decrease in adsorption capacity will be observed for both affinity beads. In addition, at pHs above the pKa value of invertase, the carboxylic groups are ionized and interact with functional groups of both the affinity beads. On the other hand, in the basic pH region, the functional groups of the grafted polymer chains were deprotonated and the amounts of adsorbed invertase for both functionalized beads were consequently decreased.
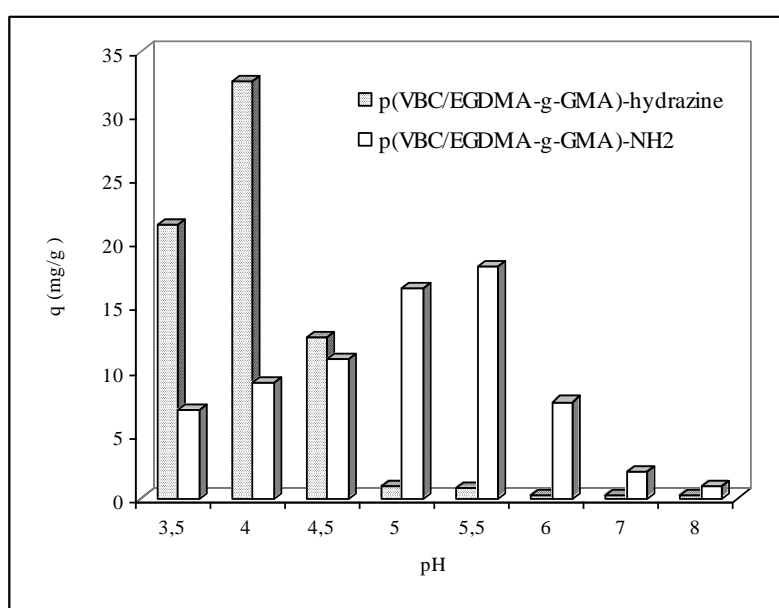
Figure 5.8: Effects of pH on invertase adsorption on the hydrazine and amino group functionalized beads. Experimental conditions; initial concentration of invertase 0.5 mg/mL; contact time: 2 h; temperature: 25 °C.

5.2.4 Effect of ionic strength on adsorption capacity

The enthalpy of adsorption would be affected not only by the pH value on the electron donating capability, but also by the salt concentration on the electrostatic interaction between invertase and the functional groups of both affinity beads. As seen in Figure 5.0, the adsorption capacity of the hydrazine functionalized beads was not significantly changed for invertase with increasing NaCl concentration from zero to 1.0M as the ionic strength increases. A similar observation was reported previously by Johansson et al. [137]. They studied the interaction of several multi-modal ligands with negatively charged biomolecules [137]. Different type multimodal ligands were immobilized on Sepharose 6 support and the adsorption properties of the negatively charged protein BSA was under different NaCl concentrations. They reported that the non-aromatic multi-modal anion-exchange ligands based on primary or secondary amines (or both) are optimal for the capture of proteins at high salt conditions. They also suggested that these new multi-modal anion-exchange ligands could be designed to take advantage not only of electrostatic but also of hydrogen bond interactions. In our case, the immobilized hydrazine ligand has a primary and a secondary amino group. In addition, during the epoxy ring opening reaction a hydroxyl group was formed in the proximity of the hydrazine ligand. Thus, the relative position of the hydroxyl groups on the hydrazine modified polymer chains could also provide an additional hydrogen bonding sites for the target biomolecules. Thus, a created specific binding side could also improve the adsorption capacity of invertase. On the other hand, the adsorption capacity of the amino group modified beads was reduced for invertase about 2.69 folds with increasing salt concentration (Fig.5.9).
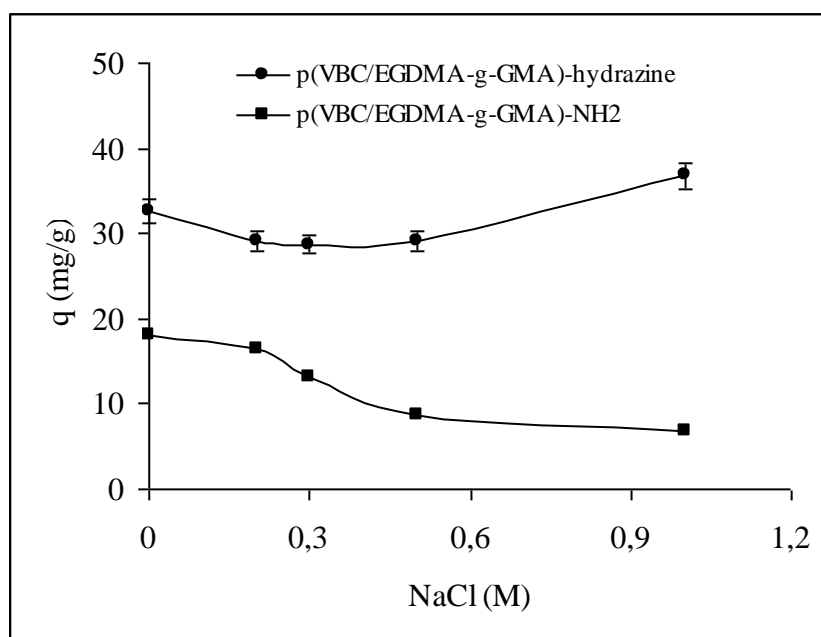
Figure 5.9: Effects of ionic strength on invertase adsorption on the hydrazine and amino group functionalized beads.

5.2.5 Effect of initial concentration of invertase

The adsorption capacity of invertase for hydrazine and amine groups functionalized beads were determined by changing the initial concentration of invertase between 0.1 and 2.0 mg/mL (Figure 5.10). An increase the invertase concentration in adsorption medium led to a linear increase in the amount of adsorbed invertase onto both affinity beads up to 2.0mg/mL invertase in the adsorption medium. It should be noted that there was a high amount of invertase adsorption on the hydrazine functionalized beads was observed (86.7 mg/g) compared to amine groups functionalized counterpart (30.4 mg/g). The hydrazine functionalized affinity beads significantly increased the invertase adsorption capacity about 2.84 fold compared to amino groups containing beads. From these equilibrium adsorptions, it can be concluded that the invertase was specifically adsorbed by the hydrazine functionalized beads compared to amino group functionalized one.
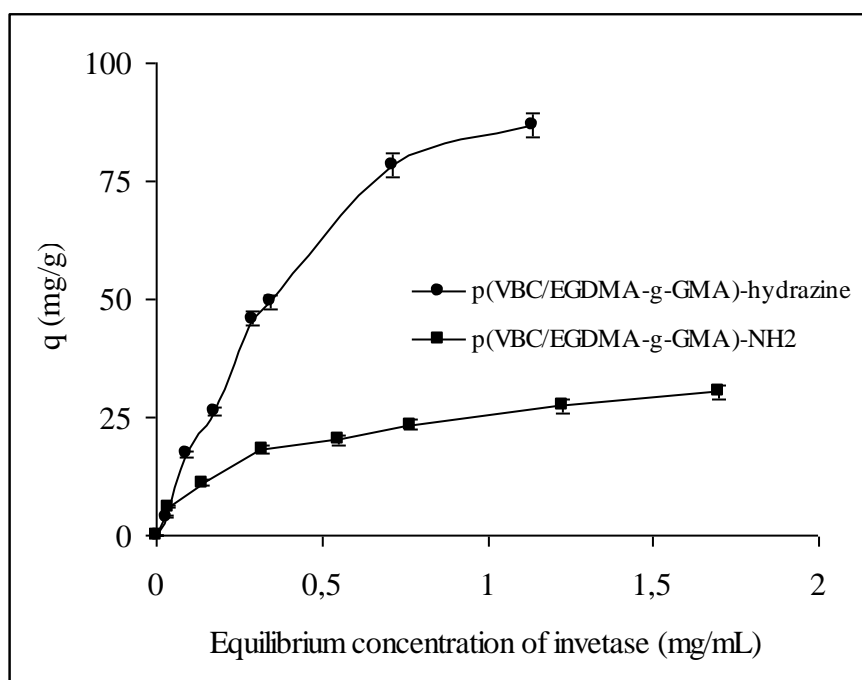
Figure 5.10: Effects of initial concentration of invertase on the adsorption capacity of the hydrazine and amino group functionalized beads.

5.2.6 Evaluation of adsorption isotherms

Three theoretical isotherm models viz. Langmuir and Scatchard equation's, Freundlich and Dubinin–Radushkevich (D–R) models) were used to analyse the experimental data. The Langmuir model is based on the assumption of surface homogeneity such as equally available adsorption sites, monolayer surface coverage, and no interaction between adsorbed species. Both the corresponding semi-reciprocal plots (C_{eq}/q_{eq} versus C_{eq}) and Scatchard plots (q_{eq}/C_{eq} versus q_{eq}) of the experimental data gave a non-linear plot for the affinity beads. In other words, a non-linear Scatchard plot indicates the adsorption heterogeneity [138-139]. Since the Langmuir model is formulated for homogenous adsorption. The adsorption of invertase onto the affinity beads cannot be described in terms of this model. When the Scatchard plots showed a deviation from linearity, the experimental datawere analyzed in terms of the Freundlich and D–R models. These isotherm models are usually adopted for heterogeneous adsorption. The linear plots of ln q versus ln C showed that the Freundlich isotherm can be representative for the invertase adsorption. The magnitude of K_F and n values of Freundlich model showed easy uptake of invertase from aqueous medium with a high adsorption capacity of the affinity beads at high temperatures. Values of $n>1$ for affinity beads indicates positive cooperativity in

binding and a heterogeneous nature of adsorption (Table 5.1). On the other hand, as seen in Table 5.1, the *n* values of the hydrazine-functionalized fibrous polymer were $n < 1$ at 5 and 15 °C and increased with the increasing of the temperatures. This could be resulted from the increase fibrous chains mobility at high temperatures. At low temperatures, the grafted fibrous polymer chains can be a compact form and results a negative cooperativity in binding of invertase. Thus, the experimental results showed that the fibrous polymer with functional hydrazine groups is an effective adsorbent for invertase at high temperature from aqueous medium.

The adsorption behavior might be predicted the physical adsorption in the range of 1–8 kJ/mol of the mean adsorption energies (*E*), and the chemical adsorption in more than 8 kJ/mol of the mean adsorption energies (*E*) [141]. D–R isotherms and parameters invertase was presented in Figure 5.11 and Table 5.1, respectively. *E* values were calculated as 3.02 kJ/mol for invertase, and found to be in the range of a typical free energy attributed to physical adsorption. At different temperature, the mean adsorption energy (*E*) of invertase from 2.32 to 5.72 kJ/mol reflected that the adsorptions were predominant on physical adsorption process. So, the D–R isotherm model best described the experimental data compared to other applied isotherm models.
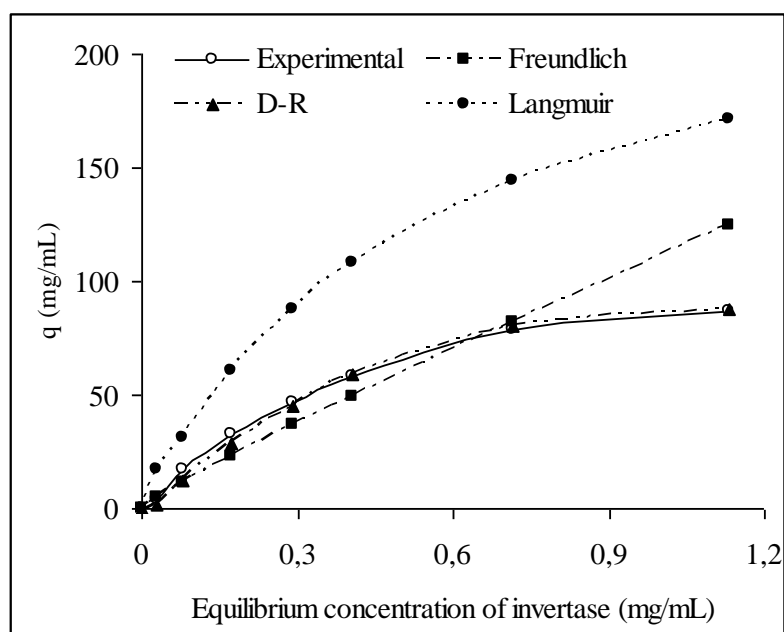
Figure 5.11: Experimental and model isotherm plots for the adsorption of invertase on the affinity beads.

Table 5.1: The D–R and Freundlich isotherm constants and correlation coefficients of isotherm models for the adsorption of invertase on hydrazine-functionalized beads.

Temperature (K)	Dubinin–Radushkevich (D–R) models constant						Freundlich model constant	
	q_{exp} (mg/g)	q_m (mg/g)	$Kx10^5$ (mol^2/kj^2)	E(kj/mol)	R^2	n	K_F	R^2
279	54.68	59.15	9.3	2.32	0.989	0.8	51.94	0.970
289	72.86	85.88	7.7	2.55	0.989	0.9	83.93	0.944
298	86.70	87.67	5.5	3.02	0.969	1.11	111.05	0.924
308	102.10	103.54	1.5	5.72	0.950	2.13	114.16	0.957

5.2.7 Kinetic studies

In Figure 5.12, the invertase adsorption rate is high at the beginning of adsorption and saturation levels were completely reached at about 120 min for invertase. After this equilibrium period, the amount of adsorbed protein molecules on the beads did not significantly change with time. A rapid removal of the invertase by the hydrazine-functionalized beads is desirable providing for a short solution adsorbent contact time in the actual process. This result is important, as equilibrium time is one of the important parameters for an economical protein and/or enzyme separation and purification system. In order to analyze the adsorption kinetics of invertase, the first-order and the second-order kinetics models were applied to the experimental data. The second-order equation fitted well with the experimental data (Figure 5.10). The comparison of experimental adsorption capacities and the theoretical values estimated from the first-order equation are presented in Table 5.2. The theoretical q values for the affinity beads were very close to the experimental q values in the case of the second-order kinetics. The second-order kinetics best described the data. In addition, Arrhenius plots in the temperature range from 5 to 35°C obtained from $1/T$ versus lnk_2 (k_2; second-order rate constant) appear linear; activation energies were found to be 11.04 kJ/mol for the hydrazine-functionalized beads. The lower activation energy calculated for the hydrazine ligand indicates that the adsorption of

invertase is a favorable process. This result also supports that the second-order kinetic model well fit the experimental data.

Table 5.2: The pseudo first and pseudo second-order kinetics constants for adsorption of invertase on the hydrazine-functionalized beads.

Temperature	q_{exp}(mg/g)	Pseudo First order			PseudoSecond order		
		q_{eq} (mg/g)	$k_1 \times 10^2$ (min^{-1})	R^2	q_{eq} (mg/g)	$k_1 \times 1o^2$ (g.min^{-1} .mg^{-1})	R^2
279	54.68	215.28	8.29	0.931	58.8	9.76	0.990
289	72.86	577.13	10.82	0.952	76.9	11.02	0.994
298	86.73	107.66	6.21	0.960	90.9	13.88	0.996
308	102.14	251.02	8.17	0.952	108.6	14.84	0.997
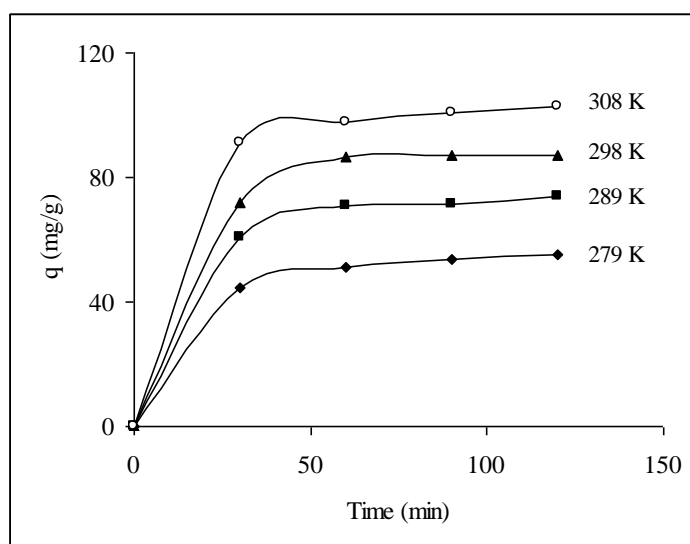
Figure 5.12: Second-order kinetics plots for invertase adsorption on the affinity beads. Experimental conditions; initial concentration of invertase 0.5 mg/mL; pH: 4.0; temperature: 25 °C; 50 mg of affinity beads was used in 5.0 mL adsorption medium.

5.2.8 Breakthrough capacity of invertase

Breakthrough curves of invertase in column are shown in Figure 5.13. The sharp breakthrough curve implies efficient adsorption performance and higher availability of column. The dynamic adsorption capacity of adsorbent in column was 68.2 mg/g, which was lower than batch adsorption capacity (86.7 mg/g). Complete saturation of the bed occurred after 70 bed volumes for low flow rate. The adsorption capacity decreased from 68.2 mg/g to 57.5 mg/g polymer with the increase of the flow rate from 0.08 to 0.17 mL/min (Figure 5.11). An increase in the flow rate reduces the

protein solution volume treated efficiently until breakthrough point and therefore decreases the service time of column. This is due to decrease in contact time between the invertase and the hydrazine functionalized beads at higher flow rates. When the flow rate decreases the contact time in the column is longer. Thus, invertase molecules have more time to diffuse the layers of the affinity beads and a better adsorption capacity is obtained.
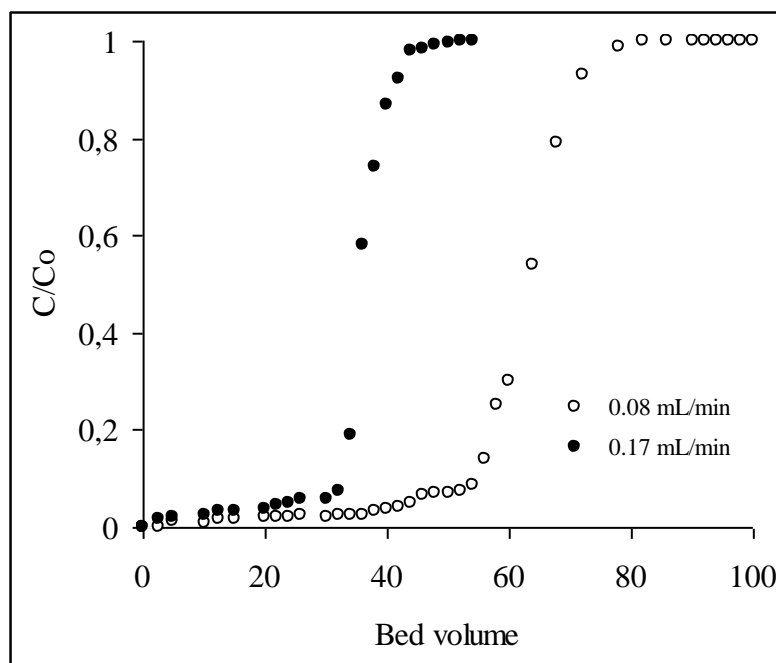
Figure 5.13: Breakthrough curves of invertase for hydrazine functionalized beads: initial concentration of invertase: 2.0 $mgmL^{-1}$; temperature: 25 °C ; pH 4.0

5.2.9 The effect of pH and temperature on the free and immobilized enzyme activity

The effect of pH on the activity of the free and immobilized invertase for hydrolysis of sucrose to glucose and fructose was examined in the pH range 4.0–8.5 at 35°C. As seen from Figure 5.14, the hydrolysis reaction has maximum activity for free and immobilized enzymes at pH 5.0 and at pH 6.0, respectively. This shift may depend on the immobilization method as well as the basic character of the support material. The pH profiles of the immobilized invertase display strongly improved stability of the optimum pH value, in comparison to that of the free form, which means that the immobilization method preserved the enzyme activity. Effect of temperature on the relative activity of free and immobilized invertase for affinity beads is shown in Figure 5.15. The immobilized enzyme showed an optimum reaction temperature

between 45 and 55°C, whereas free enzyme had an optimum temperature about 45°C. As was evident from the data, the immobilized enzyme possessed a better heat-resistance than that of the free enzyme. The immobilization of invertase on the fibrous polymer via electrostatic interaction might also reduce the conformational flexibility and may result in higher activation energy for the molecule to reorganize the proper conformation for the binding to substrate sucrose [140–143].
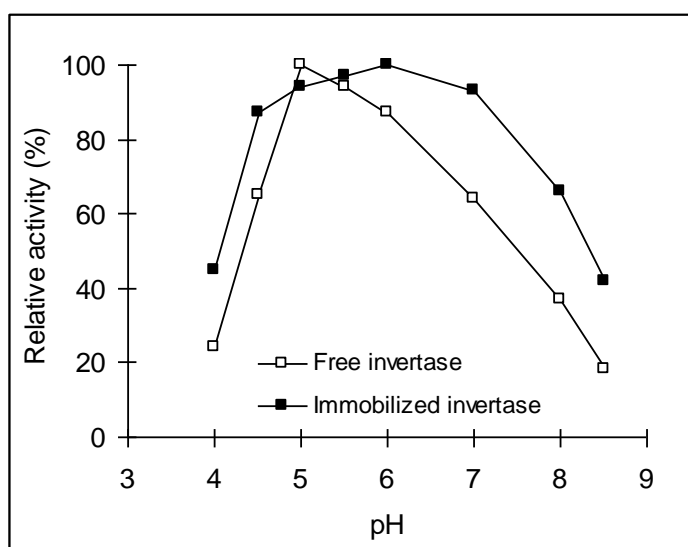
Figure 5.14: Effect of pH on the free and immobilized invertase activity: the relative activities at the optimum pH were taken as 100% for free and immobilized invertase. Experimental conditions; pH: 4.0–8.5; Temperature: 35°C.
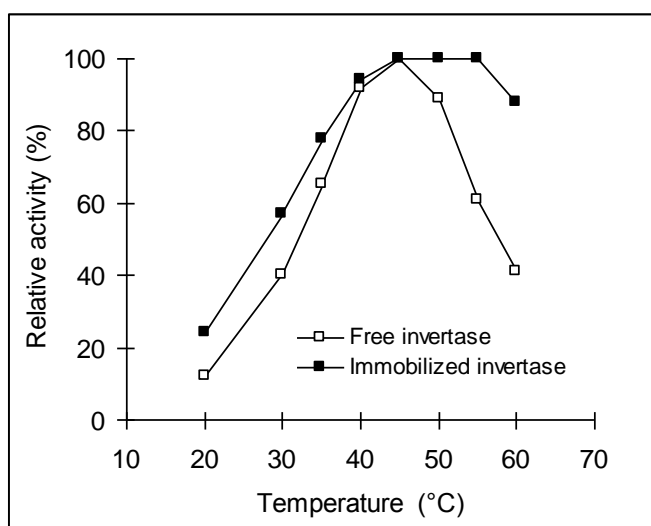
Figure 5.15: Effect of temperature on the free and immobilized invertase activity; the relative activities at optimum temperature were taken as 100% for free and immobilized invertase. Experimental conditions; pH: 5.5; Temperature: 35°C.

5.2.10 Storage stability of the invertase preparations

The free and the immobilized invertase preparations were stored at 4°C in the wet states. The activity loss of the immobilized invertase was about 27% in the 2 month storage period. The free enzyme lost all its activity within 5 week. Thus, the immobilized invertase exhibits higher storage stability than that of the free form (Figure 5.16). The higher stability of the immobilized invertase could be attributed to the prevention of denaturation as a result of multipoint interaction of invertase molecules on the hydrazine functionalized polymer chains. On the basis of this observation, PGMA grafted and hydrazine functionalized beads should provide a stabilization effect, minimizing possible distortion effects imposed from aqueous medium on the conformational structure of the immobilized enzyme. The generated multipoint ionic interactions between enzyme and hydrazine functional groups should also convey a higher conformational stability to the immobilized enzyme. Thus, the affinity beads and the immobilization method provide higher shelf life when compared with that of its free enzyme [144–148] .
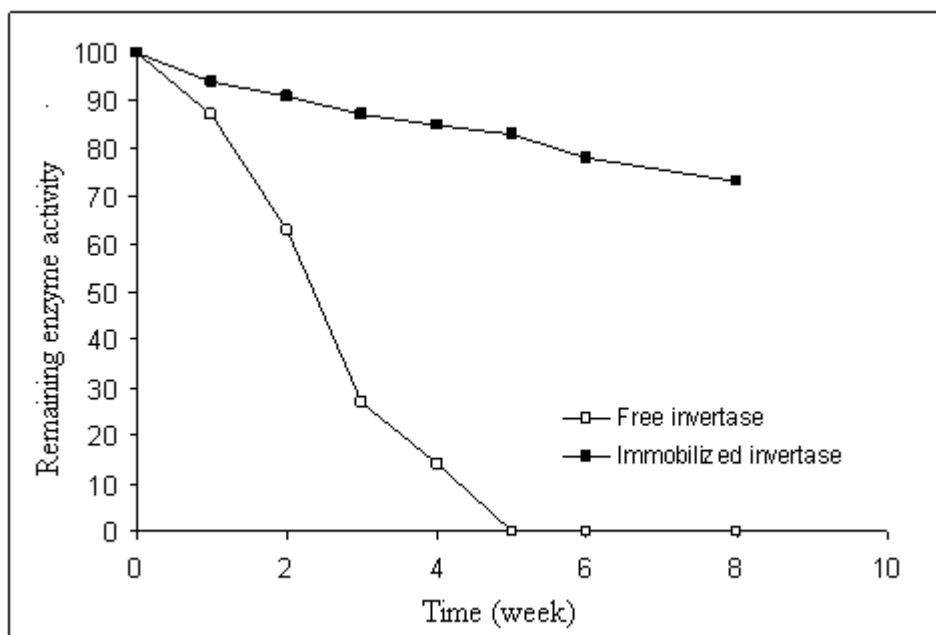
Figure 5.16: Storage stabilities of the free and immobilized invertase. Storage conditions: pH: 6.0, Temperature: 35°C.

5.2.11 Regeneration of the beads for reuse in enzyme immobilization

The cleaning of adsorbed invertase after inactivation from the affinity beads was achieved under alkaline condition. The invertase adsorbed on the hydrazine

functionalized p(VBC/EGDMA-g-GMA) beads was placed within the cleaning medium containing 1.0M NaOH. The adsorption–desorption cycle of invertase was repeated six times by using the same affinity beads. The immobilization capacity of the affinity beads did not change significantly after six times use in the repeated use of the support after regeneration of the affinity beads in 1.0M NaOH for 2 h. The sixth adsorption–desorption cycle of invertase, the amount of immobilized enzyme (83.5 mg/g beads) was about 3.6% lower than that of the first use (86.7 mg protein/g beads). This indicates that the prepared hydrazine functionalized beads were of high stability in repeated utilization.

5.3 Preparation and Characterization of the Resin 2

Sulfonic acid containing resin was prepared reaction with crosslinked chlorosulfonated polystyrene resin and aminomethane sulfonic acid (Figure 5.17).
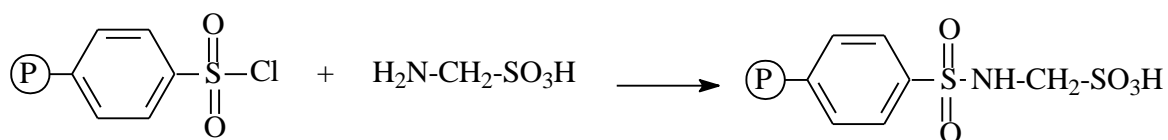
Figure 5.17: Preparation of the Resin 2.

The resin 2 was characterized by FT-IR spectroscopy (Figure 5.18). In the sulfonamide resin, S=O stretching vibration occurs at 1323 cm^{-1} and 1122 cm^{-1}. The S=O stretching vibrations in sulfonic acid group are observed at 1409 cm^{-1} and 1033 cm^{-1}.
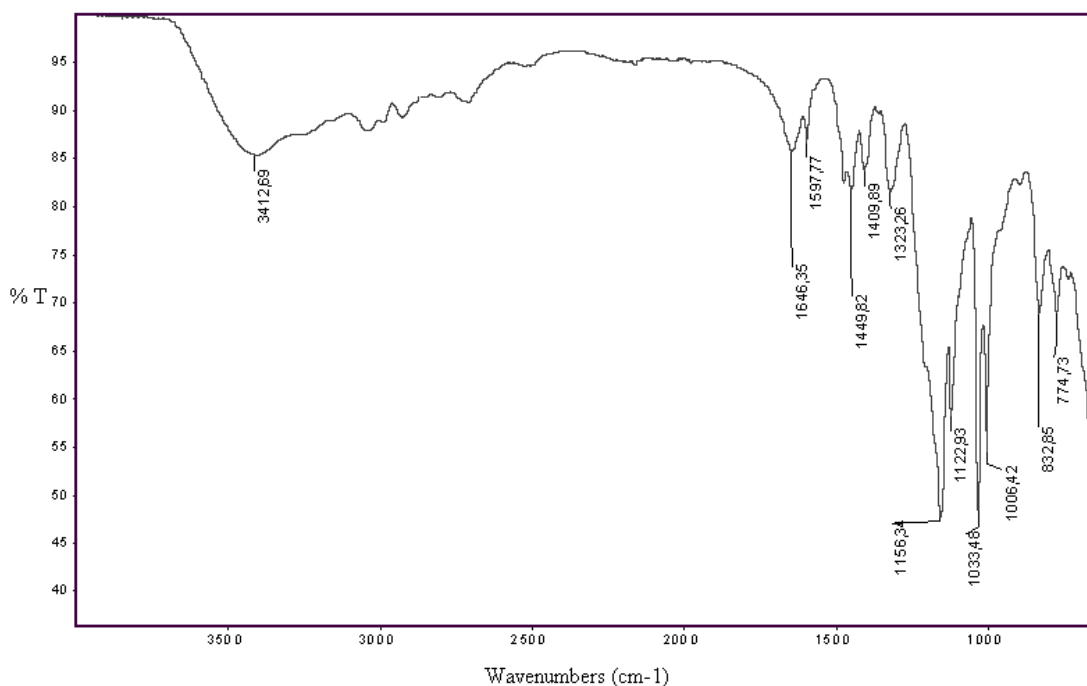
Figure 5.18: FT-IR spectrum of the Resin 2.

5.3.1 Effect of pH on trypsin adsorption capacity

Adsorption experiments were investigated at pH 4.0–8.0 (Figure 5.19). As seen in the Figure 5.20, the electrostatic interaction between trypsin and the resin was the strongest at around pH 4 and gave the highest adsorption capacity. The isoelectronic (pI) value of trypsin is 10.5. The trypsin molecules would be cationic at pH values below 10.5. The trypsin molecules have net positive charges when medium pH is less than 10.5. On the other hand, the sulfonic acid group of the beads has pKa =1.6 value. Therefore functional group has net negative charges when medium pH is higher than 1.6. At around pH 4.0, the electrostatic interaction between the protein ''trypsin'' and ion-exchange adsorbent should be predominant. Increasing the pH thereafter caused a decrease in adsorption. Proteins that change conformation as a function of their environment (pH, salt, temperature, etc.), such as trypsin, which has a molecular mass of 24 kDa, could change conformation upon binding functional surface. Thus, trypsin molecules would expand and contact according to the variation of the ionizable groups on the surfaces. At pH 4.0, the resulting trypsin adsorption may also be due to suitable conformation of trypsin molecules on the polymer surface. At pHs above the pKa value of 1.6, the sulfonic groups are ionized and interact with basic protein trypsin. On the other hand, in the basic pH region, the

85

amino groups of the trypsin were deprotonated and the amount of adsorbed trypsin was consequently decreased.
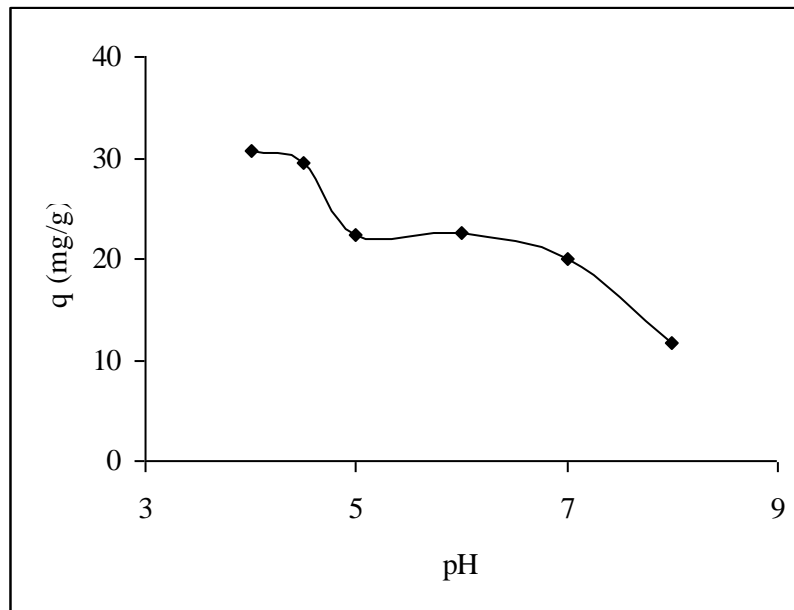
Figure 5.19: Effects of pH on the trypsin adsorption capacity of the Resin 2.

5.3.2 Effect of ionic strenght on trypsin adsorption capacity

The ionic strenght effects on adsorption capacity of Resin 2 were studied by using NaCl solution. The adsorption capacity of the Resin 2 was decreased for trypsin from 35,49 mg/g to 23,78 mg/g with increasing NaCl concentration from zero to 1.0M (Figure 5.20). The decrease in trypsin adsorption capacity of the beads with increasing ionic strength should be resulted from decrease in the electrostatic interactions between trypsin and ion-exchange beads. This behavior may be explained by the formation of more compact structures of the trypsin molecules at high-ionic strengths because of the conformational changes.
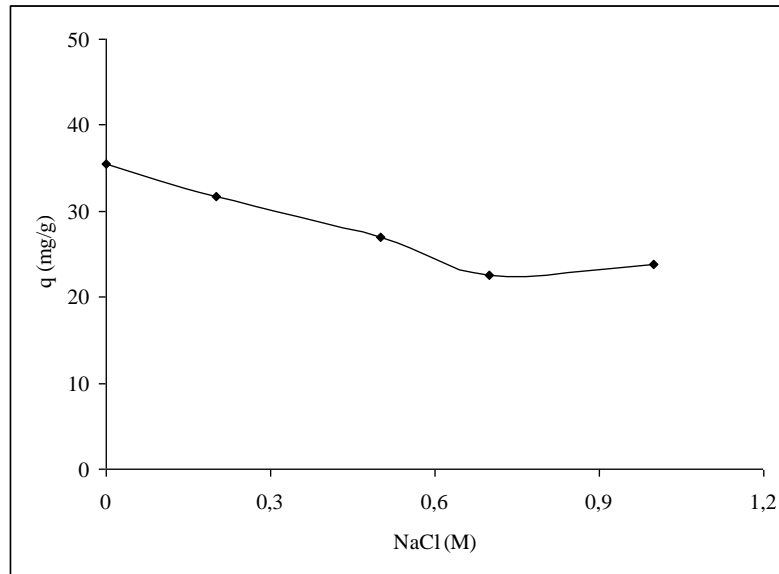
Figure 5.20: Effects of ionic strenght on the trypsin adsorption capacity of the Resin2.

5.3.3 Effect of initial concentration of invertase

Figure 5.21 shows the effects of the initial concentration of trysin on the resin capacity for four different temperatures (5, 15, 30, 37 ^{0}C). As seen in this figure, with increasing trypsin concentration in the solution, the adsorbed amount of trypsin per unit mass of polymer beads increases and then approaches saturation.
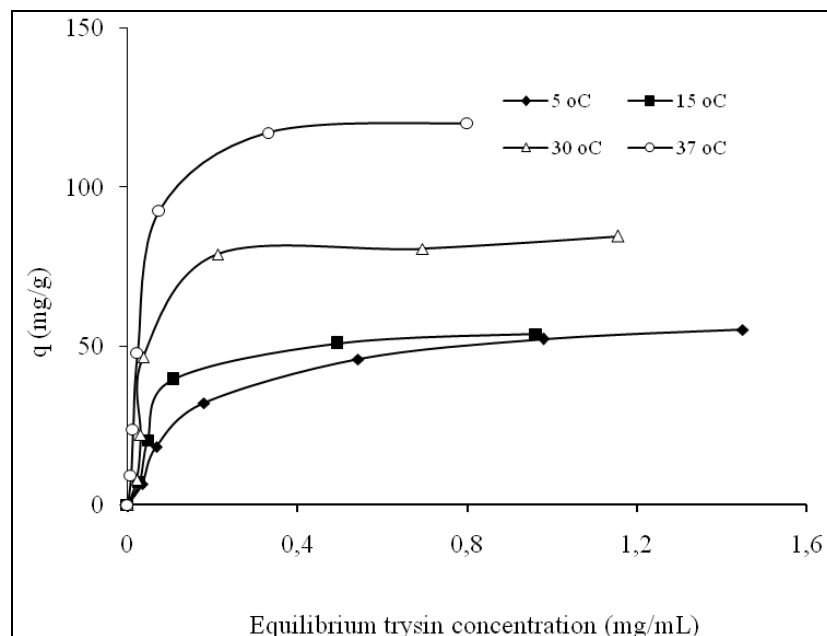
Figure 5.21: Effects of initial concentration on the trypsin adsorption capacity of the Resin 2.

5.3.4 Evaluation of adsorption isotherms

Two theoretical isotherm models (Langmuir and Freundlich) were used to analyze the experimental data. The corresponding semi-reciprocal plot (C_{eq}/q_{eq} versus C_{eq}) of the experimental data gave a linear plot (Figure 5.22) with a correlation factor of 0.976 for the affinity beads at 30^0C. The non-linear plot of ln q versus ln C (correlation factor = 0.67) at 30^0C showed that adsorption of invertase onto the affinity beads cannot be described in terms of the Freundlich isotherm. Langmuir and Freundlich isotherm constants and correlation coefficients of isotherm models for the adsorption of trypsin were given in Table 5.3.
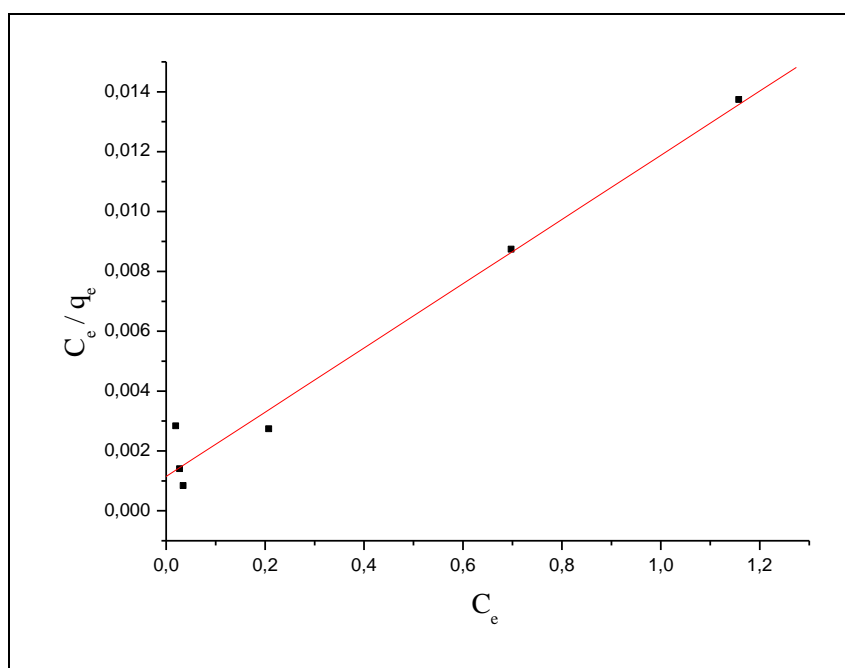
Figure 5.22: Langmiur isotherm plot of trypsin adsorption onto resin 2.

Table 5.3: Langmuir and Freundlich isotherm constants and correlation coefficients of isotherm models for the adsorption of trypsin on Resin 2.

Temperature (K)	Langmuir models constant				Freundlich constant		model
	q_{exp} (mg/g)	q_m (mg/g)	K (ml/mg)	R^2	n	K_F	R^2
278	55	63.7	4.62	0.992	1.93	55.7	0.86
288	72.86	53	8.32	0.98	2.04	83.93	0.98
303	86.70	84	14.78	0.976	2.17	111.05	0.67
310	119.92	129.87	18	0.992	2.05	114.16	0.79

5.3.5 Kinetic studies

In order to analyze the adsorption kinetics of trypsin, the pseudo first-order and the pseudo second-order kinetics models were applied to the experimental data. First order and Second order kinetic parameters for the adsorption trypsin were given in Table 5.4.

Table 5.4: First order and Second order kinetic parameters for the adsorption trypsin.

Kinetic Model	k	R^2
Pseudo First order	0.019 min^{-1}	0.984
Pseudo Second order	8.1x10^{-4} g.min^{-1}.mg^{-1}	0.976

5.3.6 Regeneration of the beads for reuse in trypsin immobilization

The adsorption–desorption cycle of invertase was repeated four times by using the same beads. The immobilization capacity of the beads did not change significantly after four times use in the repeated use of the support after regeneration of the affinity beads in 1.0 M KSCN at pH 8.0 for 3 h.

6. RESULTS and DISCUSSION II

Environmental application results of the synthesized sorbents were given in this part. Invertase enzyme has aldehyde group. Hydrazine group can sorb aldehyde groups selectively from the organic mixture by hydrazone formation. It is very important to separate organic contaminants from the solvents. Therefore, the resin1 was used to separate aldehydes.

6.1 Aldehyde Sorption Capacity of The Resin 1

Based on the reversible aldehyde-binding ability of hydrazine, aldehyde sorption of the polymer can be represented as shown in Figure 6.1.

$$\text{\Large www} NH\text{-}NH_2 \;+\; RCHO \quad \underset{HCl}{\overset{-H_2O}{\rightleftharpoons}} \quad \text{www} NH\text{-}N{=}CH\text{-}R$$
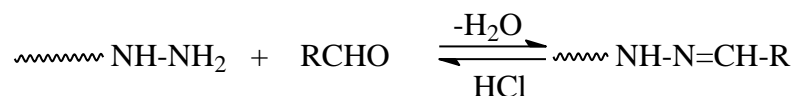
Figure 6.1: Aldehyde binding mechanism of the Resin 1.

The aldehyde sorption must proceed via hydrazone formation. To break up the hydrazone moiety, concentrated HCl solution is used and the aldehyde sorbed is released from the polymer. This fact is the key point of the reversible aldehyde binding, which allows recovery of the sorbed aldehyde. After separation of the stripped aldehyde the hydrazine groups in the polymer are in hydrazinium hydrochloride salt form. These are readily converted into free hydrazine form by a simple base treatment (1 M NaOH), and the crosslinked polymer becomes regenerated. In order to show practical efficiency of the resinous product, the resin samples were contacted separately with two-fold excess of aldehydes for 24 h at room temperature. The loading capacities in these conditions were found by determination of the residual aldehyde concentrations of the solutions (Table 6.1). The aldehyde determination was carried out colorimatically by using 2,4-dinitrophenyl hydrazine method.

Table 6.1: The aldehyde sorption capacity of the resin 1 in methanol.

Aldehyde	Capacity (mmol / g. resin)	Regeneration(mmol / g. resin)
Salicyl aldehyde	0.205	0.200
Acetaldehyde	1.756	1.746
Benzaldehyde	0.448	0.417

Having a low molecular weight, acetaldehyde is expected to show higher binding ability. Most probably the acidic character of the phenolic OH group in salicylaldehyde is responsible for its high uptake, due to the basicity of the resin itself.

6.1.1 Recovery of the sorbed aldydes and regeneration of the Resin1

Desorption experiments were performed by using 5 M HCl and results were given in Table 6.1. The benzaldehyde loaded resin was desorbed about 93% in the first experiment. The second desorption, the resin was regenerated 100%.

6.2 Extraction of Basic Dyes

Dye sorption was similar to protein sorption. Acidic function containing sorbents can interact basic proteins and basic dyes. Therefore, dye contaminants are very serious problem for environment and human health.

We used our resins for removal of basic dyes. Also, dye sorbed resins will used to separation of biomolecules.

6.2.1 Dye sorption characteristics of Resin 2

Dye extraction experiments were carried out simply by contacting wetted bead samples with aqueous dye solutions at room temperature. Capacities were assigned by colorimetrical analysis of residual dye contents. Dye sorptions capacities are given in Table 6.2.

Table 6.2: Sorption capacities of the Resin 2.

Dye	Dye concentration (g dye / 100 mL)	Capacity (g dye/ g resin)
Methylene Blue	0.40	0.38
	0.50	0.40
	0.75	0.39
	1.00	0.39
Crystal violet	0.40	0.39
	0.50	0.42
	0.75	0.44
	1.00	0.40

These experiments were studied different dye concentrations and the loading experiments indicate no significant capacity change is observed at different initial dye concentrations.

The resin shows reasonably high dye sorptions. It is important to note that the resin can be used in a wide pH range (Table 6.3).

At low pH, the sulfonic acid groups on the surface of resin that are responsible for binding with basic dye are predominantly protonated ($-SO_3H$), hence incapable of binding basic dye. As pH increased, sorption became favorable due to the deprotonation of the acid groups ($-SO_3H$), resulting in sorption sites that were available for binding with basic dye. With increasing pH, the number of positively charged sites decreased and the number of negatively charged sites increased. This phenomenon favors the sorption of positively charged dye due to electrostatic attraction.

Table 6.3: Maximum dye sorption capacity of the resin 2 depending on pH.

Dye	pH	Capacity (g dye / g resin)
Methylene Blue	2	0.16
	4	0.26
	8	0.37
Crystal violet	2	-
	4	0.30
	8	0.40

6.2.2 Dye sorption kinetics of the Resin 2

This material is able to remove the basic dyes completely even from highly diluted aqueous dye solutions, which are industrially highly important. Here batch kinetic sorption experiments were performed with very dilute dye solutions (1.3×10^{-3} g L^{-1}) to investigate the efficiency of the resin in the presence of trace quantities of dyes, The (concentration – time) plot (Figure 6.2) shows that within about 40 minutes contact time, the dye concentration falls to zero.
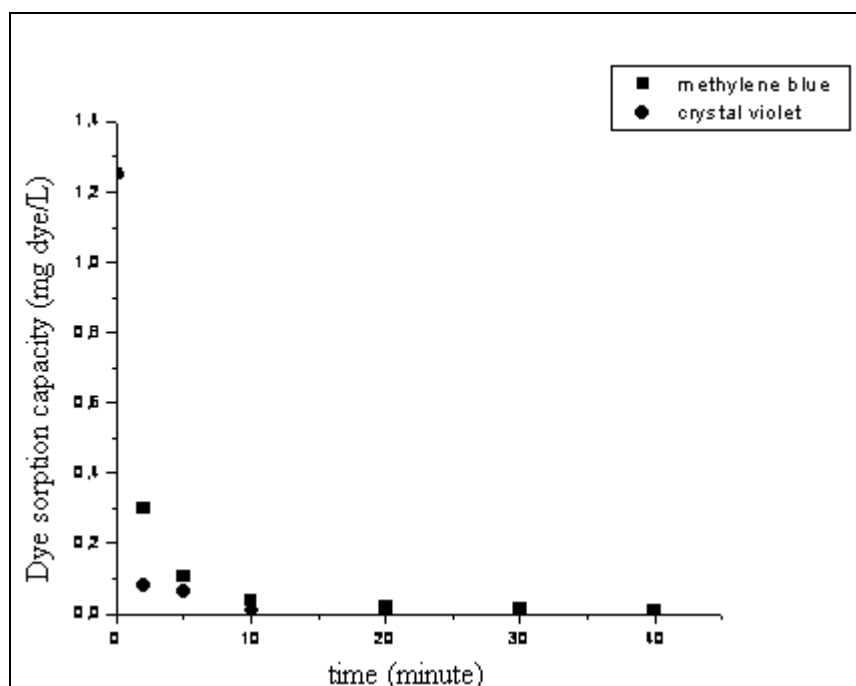
Figure 6.2: Dye sorption kinetics of the Resin 2.

The kinetic data was treated with the Ho's pseudo-second-order rate equation [125]. The pseudo-second-order model plots of methylene blue and crystal violet sorption are shown in Figure 6.3. The high values of correlation coefficients showed that the data fitted well to the pseudo-second-order rate kinetic model (Table 6.4).
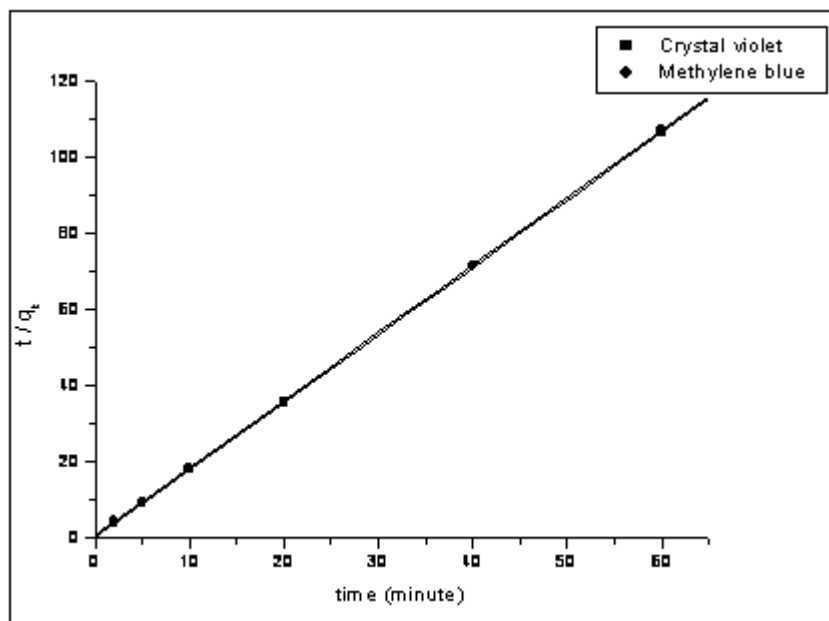
Figure 6.3: The pseudo-second-order model plots of methylene blue and crystal violet sorbed by the Resin 2

Table 6.4: Pseudo-second order kinetic parameters for the adsorption of methylene blue and crystal violet.

Dye	k_2 ($g.min^{-1}.mg^{-1}$)	R^2
Methylene blue	3.84	0.9999
Crystal violet	9.94	1

6.2.3 Regeneration of the Resin 2

Alkaline regeneration works well for strong and weak basic sorbents and acid regeneration works for most dyes.

For the regeneration of dyes from loaded resin, 5 M H_2SO_4 was used. When loaded samples were contacted with 5 M H_2SO_4 for 24 h, the amount of recovered dyes is around 0.38 g dye / g polymer for methylene blue and 0.39 about 93% of the capacity of fresh polymer.

Additionally, the resin does not hydrolyze in acid and base solutions, due to the high stability of the sulfonamide linkage to acid and base hydrolysis. This property is very important for the regeneration.

6.3 Preparation and Characterization of the Resin 3

In this study, core-shell types of polymers with poly(ethylacrylate) shells were obtained by SI-ATRP method. Graft polymerization of ethylacrylate can be obtained from the chloromethyl initiator groups on the p(VBC) beads (Figure 6.4). In the polymerizations [CuBr/[L] ratio was chosen as 1/2.

$$P-\langle\text{aryl}\rangle-CH_2-Cl \xrightarrow[\text{Ethylacrylate}]{\text{CuBr, Bipyridine}} P-\langle\text{aryl}\rangle-CH_2-(CH_2-CH)_n-$$

with pendant $C=O$ and OC_2H_5 groups; then by hydrolysis to $P-\langle\text{aryl}\rangle-CH_2-(CH_2-CH)_n-$ with pendant $C=O$ and OH groups.
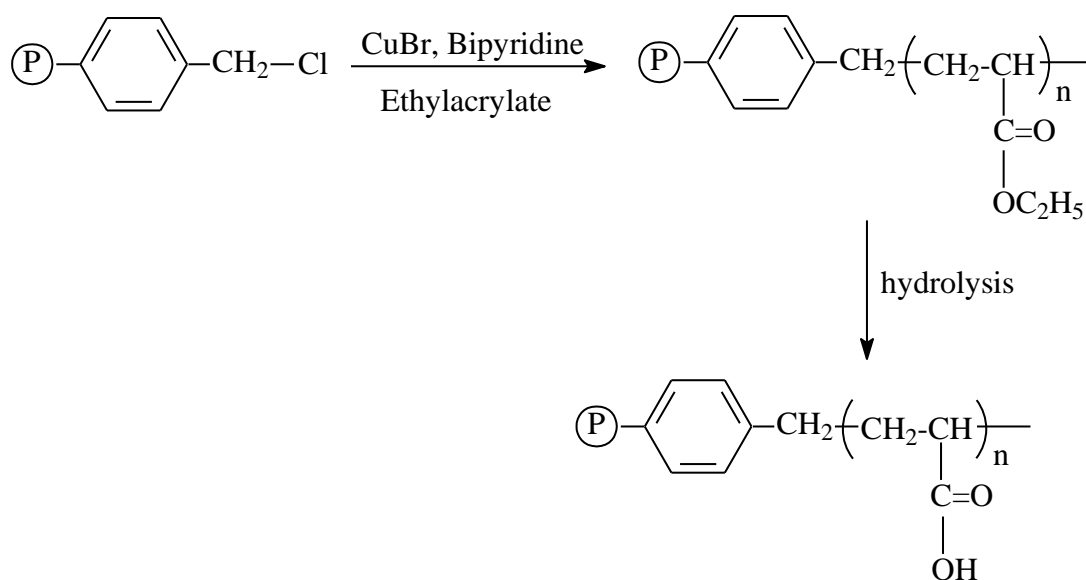
Figure 6.4: Preparation of Resin 3.

The grafting degree reaches to 368.2% (assigned by mass increase) in 20 h. The grafting degree-time plot was given in Fig.6.5.
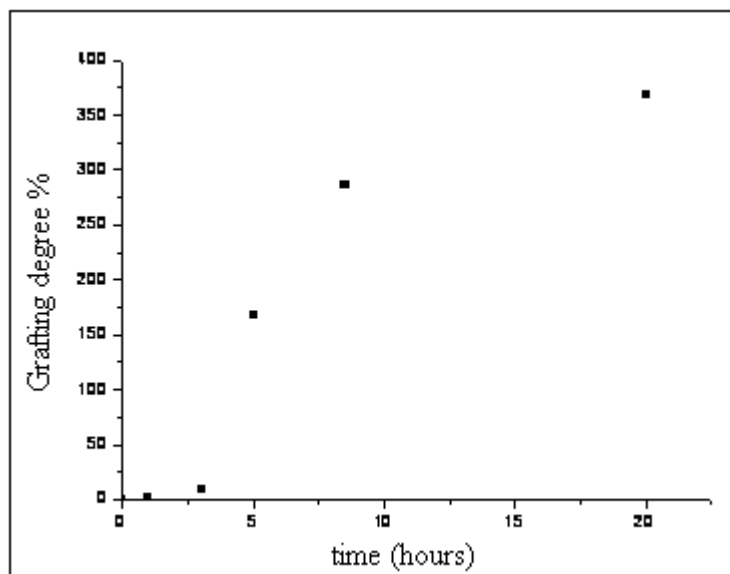
Figure 6.5: Conversion-time plot of the Resin 3.

FT-IR spectra of the grafted beads represent strong C–O stretching vibrations band at 1721 cm^{-1}, which indicate incorporation of the poly(ethylacrylate) on the p(VBC) resin structure (Figure 6.6a). Poly (acrylic acid) function on the beads surface was obtained after alkali hydrolysis of poly (ethylacrylate) core-shell structure of the resin. Carboxylic acid content was determined by using titrimetric method and was found to be 3.56 mmol/g resin. The hydrolyzed resin was also characterized by FT-IR spectroscopy (Figure 6.6b). In the hydrolyzed resin, C=O stretching vibration bands are observed at both 3356 cm^{-1} and 1600 cm^{-1}.
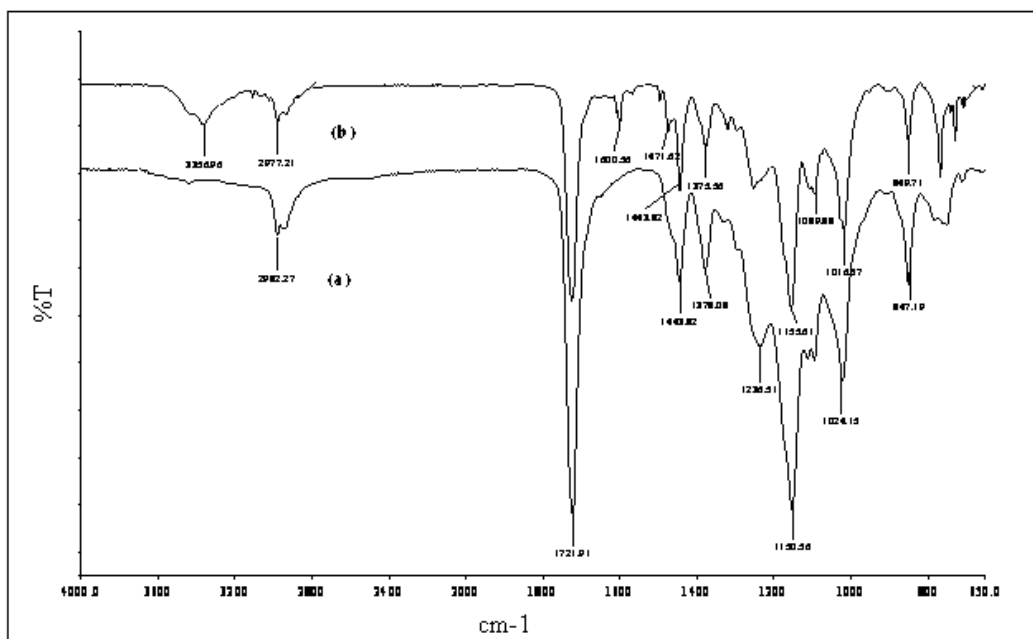
Figure 6.6: FT-IR spectra of Resin 3.

6.4 Dyes Removal Studies

The basic dyes removal experiments from aqueous solution were carried out simply by contacting swelled resin samples with aqueous dye solutions at room temperature. The adsorption capacities of the resin were determined using colorimetrical analysis. The adsorption capacities of the resin for Methylene Blue and Crystal Violet were 300 and 250 mg dye/g resin, respectively. It is important to note that the resin can be used over a wide pH range (Table 6.5), with significant differences in the adsorption capacity for both dyes.

At low pH, the carboxyl groups on the surface of resin that are responsible for binding with basic dye are predominantly protonated (-COOH), hence incapable of binding basic dye. As pH increased, sorption became favorable due to the deprotonation of the carboxyl groups (-COO$^-$), resulting in sorption sites that were available for binding with basic dye. With increasing pH, the number of positively charged sites decreased and the number of negatively charged sites increased. This phenomenon favors the sorption of positively charged dye due to electrostatic attraction. This property is important for industrial applications.

Table 6.5 pH depending on dye sorption of the resin 3

Dye	pH	Capacity (mg dye / g resin)
Methylene Blue	4.0	210
	6.0	250
	7.0	300
	8.0	200
Crystal violet	4.0	-
	6.0	190
	7.0	250
	8.0	200

6.4.1 Dye adsorption kinetics of the resin 3

This material is able to remove the anionic dyes completely even from highly diluted aqueous dye solutions, which are highly important. We performed batch kinetic sorption experiments with highly diluted dye solutions between (2.5×10^{-3} and 1.3×10^{-3} g / L) to investigate the efficiency of the resin in the presence of low dye concentrations. The concentration– time plot (Fiure 6.7) shows that within about 60 minutes contact time, the dye concentration of crystal violet falls to zero.
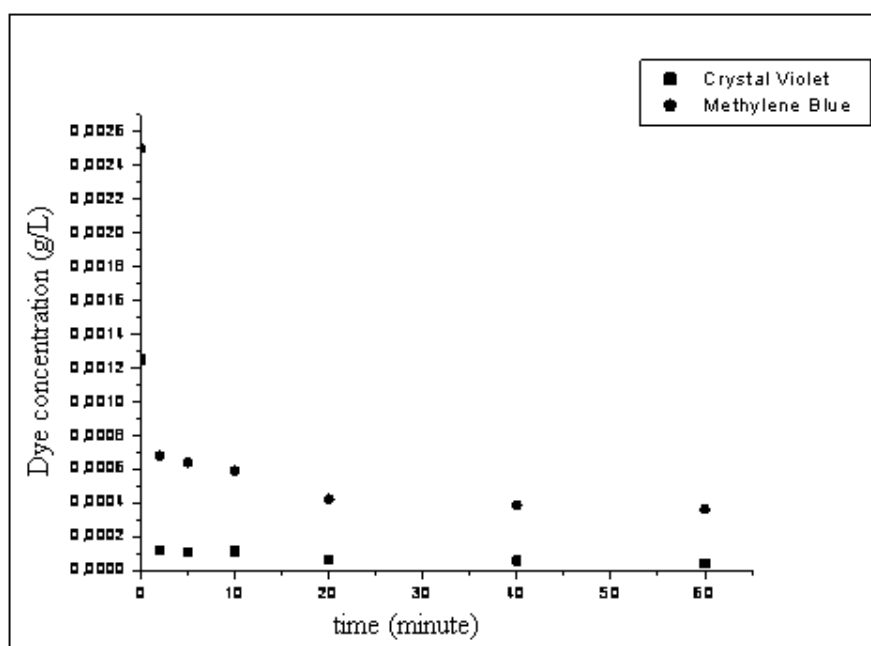
Figure 6.7: Methylene blue and crystal violet adsorption kinetics of the Resin 3

The sorption kinetics is an important aspect of pollutants removal process control. The linear form of the equation that describes the adsorption kinetics corresponding to the pseudo second-order model [125] is as follows:

$$t/q_t = 1/k_2 q_e^2 + 1/q_e t \qquad \qquad (6.1)$$

The rate parameters k_2 and qe can be directly obtained from the intercept and slope of the plot of t/q_t versus t (Fig.6.8). If the pseudo-second order kinetics is applicable, the plot gives a linear relationship, which allows computation of k_2.
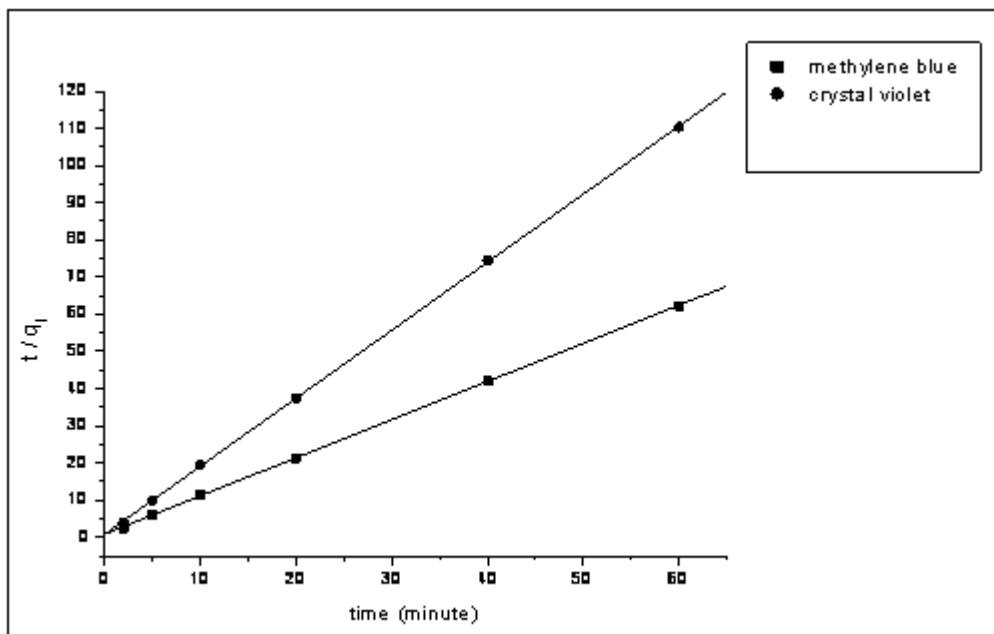
Figure 6.8: The pseudo-second-order model plots of Methylene Blue and Crystal Violet adsorbed by the resin

Table 6.6: Pseudo-second order kinetic constants for basic dyes sorption onto the Resin 3.

Dye	k_2 ($g.min^{-1}.mg^{-1}$)	R^2
Methylene blue	1.24	0.9999
Crystal violet	4.60	0.9996

The kinetic values were obtained by linear regression are reported in Table 6.6 The high values of correlation coefficients showed that the data fitted well to the pseudo-second-order rate kinetic model.

6.4.2 Regeneration of the Resin 3

For the regeneration of dyes from loaded resin, 5 M H_2SO_4 was used. When the dye adsorbed samples were contacted with 5 M H_2SO_4 for 24 h, the amount of recovered dyes is around 0.25 g dye / g polymer for Methylene Blue and 0.21 g dye / g polymer for crystal violet. These values are about 83 % of the capacity of fresh polymer. Regeneration experiments were repeated twice. Colorless beads were obtained after the regeneration process.

7. CONCLUSION

In this thesis, hydrazine, amine, carboxylic acid and methanesulfonic acid containing resins were prepared and characterized.

Hydrazine, amine, carboxylic acid containing resins were synthesized starting from crosslinked polyvinyl benzyl chloride. Poly (glycidyl methacrylate) and poly (ethyl acrylate) were grafted onto the PVBC by using ATRP method. Grafted resins were modified hydrazine, amine and carboxylic acid groups by using ring opening and ester hydrolysis respectively.

Hydrazine group can sorb aldehyde to form hydrazone. This mechanism was used in sorption of enzymes. The resin 1 was interacted different enzymes but invertase enzyme can be sorb selectively pH between 4 and 5.5 respectively. Hydrazine function resin sorpion capacity of the invertase was found higher than according to the amine function resin.

Sorption experiments were investigated depending on pH, ionic strength and temperatue. The adsorption isotherms and kinetic characteristics of the resins were studied. In addition, thermodynamic parameters of the resin were found.

Poly (ethyl acrylate) was grafted onto PVBC by ATRP and was hydrolyzed ester group to obtain poly (acrylic acid) group (Resin 3). Resin 3 was used to remove basic dyes. Dye sorption properties depending on pH, dye sorption kinetics and desorption of the dye loaded resin was investigated.

Methanesulfonic acid function was obtained starting from reaction with crosslinked chlorosulfonated poly (styrene) and methane sulfonic acid (Resin2). Resin 2 has sulfonamide group. Sulfonamides do not hydrolyze in acidic and basic media easily. This property is very important for regeneration process. Resin 2 was used sorption of Trypsin protein and sorption of the protein was studied in different pH, ionic strength and temperature. Sorption kinetics, and desorption conditions were also investigated. The resin was also used to remove basic dyes from water.

REFERENCES

[1] **Cooke M., Poole C. F., Wilson I. D., and Adlard E. D.** (Eds.), 2000: *'Encyclopedia of Separation Science'*,Academic Press.

[2] **Kiralp, S., Topcu, A., Bayramoğlu, G., M. Yakup Arıca, and Toppare, L.,**2008: Alcohol determination via covalent enzyme immobilization on magnetic beads, *Sensors and Actuators B: Chemical*, **128,** 2, 521-528,

[3] **Goddard J. M., and Hotchkiss J. H.,** 2007: Polymer surface modification for the attachment of bioactive compounds, *Prog Polym Sci*, **32**, 698–725.

[4] **Grazu V., Abian O., Mateo C., Batista-Viera F., Fernandez-Lafuente R., Guisan J. M.,** 2005: Stabilization of enzymes by multipoint immobilization of thiolated proteins on new epoxy-thiol supports, *Biotechnol Bioeng*, **90,** 597–605.

[5] **Bayramoglu, G., Arıca, M. Y.,** 2009: Preparation and characterization of comb type polymer coated poly(HEMA/EGDMA) microspheres containing surface-anchored sulfonic acid: Application in γ-globulin separation, *Reactive and Functional Polymers*, **69**, 189-196,

[6] **Bayramoglu, G., Yavuz, E., Senkal, B. F., and Arıca, M. Y.,** 2009: Glycidyl methacrylate grafted on p(VBC) beads by SI-ATRP technique: Modified with hydrazine as a salt resistance ligand for adsorption of invertase, *Colloids and Surfaces A: Physicochemical and Engineering Aspects,* **345**, 127-134,

[7] **Xu F. J., Li Y. L., Kang E. T., and Neoh K. G.,**.2005: Heparin-coupled poly(poly(ethylene glycol) monomethacrylate)–Si(1 1 1) hybrids and their blood compatible surfaces, *Biomacromolecules,* **6**, 1759–68.

[8] **DeFife M. K., Shive S. M., Hagen K.M., Clapper D.L., and Anderson J.M.**, 1999: Effects of photochemically immobilized polymer coatings on protein adsorption, cell adhesion, and the foreign body reaction to silicone rubber, *J Biomed Mater Res*, **44**, 298–307.

[9] **Dong R., Krishnan S., Baird B. A., Lindau M., and Ober C. K.**, 2007: Patterned biofunctional poly(acrylic acid) brushes on silicon surfaces. *Biomacromolecules*, **8,** 3082–92.

[10] **Hasegawa T., Matsuura K., Ariga K., and Kobayashi K.**, 2003: Multilayer adsorption and molecular organisation of rigid cylindrical glycoconjugate poly(phenylisocyanate) on hydrophilic surfaces, *Macromolecules,* **33,** 2772–5.

[11] **Miyata T., Jikihara A., and Nakamae K.,** 1996: Preparation of poly(2-glucosyloxyethyl methacrylate)–concanavalin A complex hydrogel and its glucose-sensitivity, *Macromol Chem Phys*, **197**, 1135–46.

[12] **Okada M.,** 2001: Molecular design and syntheses of glycopolymers. *Prog Polym Sci*, **26**, 67–104.

[13] **Huang J., Li X., Zheng Y.,Zhang Y., Zhao R., Gao X., Yan H**., 2008: Immobilization of Penicillin G Acylase on Poly[(glycidyl methacrylate)-*co*-(glycerol monomethacrylate)]-Grafted Magnetic Microspheres, *Macromolecular Bioscience,* **8,** 508-515.

[14] **Kurosawa S., Aizawa H., Talib Z. A., Atthoff B., and Hilborn J.**, 2004: Synthesis of tethered-polymer brush by atom transfer radical polymerization from a plasma-polymerized-film-coated quartz crystal microbalance and its application for immunosensors, *Biosens Bioelectron*, **20,** 1165–76.

[15] **Lei Z., and Bi S.**, 2007: Preparation and properties of immobilized pectinase onto the amphiphilic PS-b-PAA diblock copolymers, *J Biotechnol*, **128,** 112–9.

[16] **Cullen S. P., Liu X., MandelI C., Himpsel F.J., and Gopalan P.,** 2008: Polymeric brushes as functional templates for immobilizing ribonuclease A: study of binding kinetics and activity, *Langmuir,* **24,** 913–20.

[17] **Xu F. J., Cai Q. J., Li Y. L., Kang E. T., and Neoh K.G.**, 2005: Covalent immobilization of glucose oxidase on well-defined poly(glycidyl methacrylate)–Si(1 1 1) hybrids from surface-initiated atom-transfer radical polymerization, *Biomacromolecules,* **6,** 1012–20.

[18] **Kawakita H., Masunaga H., Nomura K., Uezu K., Akiba I., Tsuneda S.**, 2007: Adsorption of bovine serum albumin to a polymer brush prepared by atom-transfer radical polymerization in a porous inorganic membrane, *J Porous Mater,* **14**, 387–91.

[19] **Huang J., Han B., Yue W., and Yan H., 2007:** Magnetic polymer microspheres with polymer brushes and the immobilization of protein on the brushes. *J Mater Chem,* **17,** 3812–8.

[20] **Bayramoğlu, G., Ekici, G., Beşirli, N., Arica, M. Y.,** 2007: Preparation of ion-exchange beads based on poly(methacrylic acid) brush grafted chitosan beads: Isolation of lysozyme from egg white in batch system, *Colloids and Surfaces A: Physicochemical and Engineering Aspects*, **310**, 68-77.

[21] **Ying L., Yin C., Zhou R. X., Leong K. W., Mao H. Q., Kang E. T, et al.**, 2003: Immobilization of galactose ligands on acrylic acid graft-copolymerized poly(ethylene terephthalate) film and its application to hepatocyte culture. *Biomacromolecules,* **4,** 157–65.

[22] **Yin C., Ying L., Zhang P. C., Zhou R. X., Kang E. T., Leong K. W., et al.**, 2003: High density of immobilized galactose ligand enhances hepatocyte attachment and function. *J Biomed Mater Res A*, **67A,** 1093–104.

[23] **Dumont J., Fortier G.**, 1996: Behavior of glucose oxidase immobilized in various electropolymerized thin films, *Biotechnol Bioeng*, **49**, 544–52.

[24] **Cen L., Neoh K. G., and Kang E. T.,** 2003: Surface functionalization of polypyrrole film with glucose oxidase and viologen, *Biosens Bioelectron*, **18,** 363–74.

[25] **Bayramoğlu, and, G., Arıca, M. Y.,** 2008: Preparation of poly(glycidylmethacrylate–methylmethacrylate) magnetic beads: Application in lipase immobilization, *Journal of Molecular Catalysis B: Enzymatic*, **55,** Pages 76-83

[26] **Arica M. Y., Bayramoglu G., Bicak N**., 2004: Characterisation of tyrosinase immobilised onto spacer-arm attached glycidyl methacrylatebased reactive microbeads, *Process Biochem*, **39**, 2007–17.

[27] **Bayramoğlu, G., Loğoğlu, E., and Arica, M. Y.,** 2007: Cytochrome c adsorption on glutamic acid ligand immobilized magnetic poly(methylmethacrylate-co-glycidylmethacrylate) beads, *Colloids and Surfaces A: Physicochemical and Engineering Aspects,* **297**, 55-62,

[28] **Yu W. H., Kang E. T, and Neoh K. G**., 2004: Controlled grafting of well-defined epoxide polymers on hydrogen-terminated silicon substrates by surface-initiated ATRP at ambient temperature, *Langmuir*, **20,** 8294.

[29] **Edmondson S., and Huck W. T. S.**., 2004: Controlled growthand subsequent chemical modification of poly(glycidyl methacrylate) brushes on silicon wafers. *J Mater Chem,* **14,** 730–4.

[30] **Iwata R., Satoh R., Iwasaki Y., and Akiyoshi K**., 2008: Covalent immobilizationm of antibody fragments on well-defined polymer brushes via sitedirected method, *Colloids Surf B: Biointerfaces*, **62,** 288–98.

[31] **Bayramoğlu G., and Arıca M.Y.,** 2009: Immobilization of laccase onto poly(glycidylmethacrylate) brush grafted poly(hydroxyethylmethacrylate) films: Enzymatic oxidation of phenolic compounds, *Materials Science and Engineering: C,* **29**, 1990-1997,

[32] **Sun C, Zhou F, Shi L, Yu B, Gao P, Zhang J, et al.,** 2006: Tribological properties of chemically bonded polyimide films on silicon with polyglycidyl methacrylate brush as adhesive layer. *Appl Surf Sci*, **253,** 1729–35.

[33] **Takemoto K., Ottenbrite R.M., Kamachi M.** (Eds.), 1997: *Functional Monomers and Polymers*, CRC Press

[34] **Gilbert R. G.,** 1995: Emulsion *Polymerization: A Mechanistic Approach*, Academic, London,

[35] **Lovell P.A., and El-Aasser M. S.,** 1997: *Emulsion Polymerization and Emulsion Polymers*, Wiley, Chichester,.

[36] **Hoffman F., and Delbruch K.,** Patent, 1909: No. 250 690, Farbenfabriken Bayer, Germany.

[37] **Bauer W., and Lauth H.,** Patent (Ger.) 1931: No. 656,134, Rohm and Haas, Darmstadt,

[38] **Munzer M., Trommsdorff E., Schildknecht C. E., Skeist I.** (Eds.), 1977: *Polymerization Processes*, Wiley, New York, , p. 106.

[39] **Seidl** J., **Malinsky J., Dusek K., and Heitz W.,** 1967: *Adv. Polym. Sci.* **5** 113.

[40] **Hopff H., and Lutz E.,** 1958: *Kunstst. Plast.* **5** 341.

[41] **Y. Mlynek, W. Resnick**, 1976*: AIChE J., ***22,** 289.

[42] **B. Weinstein,** 1973: *AIChE J.* **19,** 304.

[43] **C.A. Coulaloglou, L.L. Tavlarides**, 1976: *AIChE J.* **22**, 289.

[44] **J. Hernandez-Barajas, D.J. Hunkeler**, 1995: *Polym. Adv. Technol., ***6,** 509.

[45] **G.J. Wang, M. Li, X.F. Chen,** 1997: *J. Appl. Polym. Sci.* **65** 789.

[46] **X.L. Xu, Z.C. Zhang, B. Fei, X.W. Ge, M.W. Zhang**, 1998: *Acta Polym. Sin.* 134.

[47] **Mendizabal E., Castellanosortega J. R., and Puig J.E.,** 1992: A method for selecting a polyvinyl alcohol as stabilizer in suspension polymerization. *Colloids Surf.* **63,** 209-217.

[48] **Goodall A. R., and Greenhill-Hooper M. J.,** 1990: *Makromol. Chem. Macromol. Symp*., **35,** 499.

[49] **Dawkins J.V., in: Geoffrey A., Bevington J. C., (Eds.),** 1989: Comprehensive Polymer Science. The Synthesis, Characterization and Applications of Polymers, **vol. 4,** Pergamon, Oxford,.

[50] **S.M. Ahmed,** 1984: J. Dispers. Sci. Technol., **5,** 421.

[51] **Grulke E. A., in: Mark H. F., Bikales N. M., Overberger C. G., Menges G., Kroschwitz J. I., (Eds.),** 1989: Encyclopedia of Polymer Science and Engineering, **vol. 16**, Wiley, New York, p. 443.

[52] **Kalfas G., and Ray W. H.**, 1993: Modeling and experimental studies of aqueous suspension polymerization processes. 1. Modeling and simulations, *Ind. Eng. Chem. Res*., **32,** 1822-1830.

[53] **Blondeau D., Bigan M., and Despres P.**, 1995: Ultrasound suspension polymerization method for preparation of 2-hydroxyethylmethacrylate macroporous copolymers, *React. Funct. Polym*., **27,** 163-173.

[54] **Saito R., Ni X., Ichimura A., and Ishizu K.**, 1998: Synthesis of core–shell type microsphere with reactive seed microspheres, *J. Appl. Polym. Sci.* **69**, 211-216.

[55] **Arslanalp C., Erbay E., Bilgic T., and Savasci O. T.,** 1991: Agitation scale-up model for the suspension polymerization of vinyl chloride, *Angewandle Makromol. Chem.,* **211**, 35-51.

[56] **Rogestedt M., Jonsson T., Hjertberg T.,** 1993: Effect of polymerization initiator on early colour of poly(vinyl chloride). *J. Appl. Polym. Sci*., **49,** 1055-1063.

[57] **Mathur R., Mathur S., Kanoongo N., Narang C. K., and Mathur N. K.,** 1992: Use of phase transfer catalysts to aid initiation in suspension vinyl polymerization, *Polymer,* **33,** 217-218.

[58] **Uyama H., Kato H., and Kobayashi S.**, 1994: Dispersion polymerization of N-vinylformamide in polar media. Preparation of monodisperse hydrophilic polymer particles. *Polym. J., 26,* 858-863.

[59] **Dowding P.J., Goodwin J.W., and Vincent B.**, 1998: The characterization of porous styrene–glycidyl methacrylate copolymer beads prepared by suspension polymerization, *Colloids Surf. A Physicochem. Eng. Asp.* **145,** 263-270.

[60] **Mrazek Z., Lukas R., and Sevcik S.,** 1991: On gradual dosage of the initiator in the suspension polymerization of vinyl chloride**.** *Polym. Eng. Sci.*, **31,** 313-320.

[61] **Szwarc, M., Levy,M. Milkovich, R.**, 1956: Polymerization initiated by electron transfer to monomer. A new method of formation of block polymers. *J. Am. Chem. Soc.*, **78,** 2656-2657.

[62] **Szwarc, M.**, 1956: 'Living' Polymers. *Nature (London)*, **178,** 1168-1169.

[63] **Miyamoto, M., Sawamoto, M. And Higashimura, T.**, 1984: Living polymerization of isobutyl vinyl ether with hydrogen iodide/iodine initiating system. *Macromolecules*, **17**, 26-268.

[64] **Faust, R. and Kennedy, J. P.**, 1986: *Polym. Bull.*, **15,** 317

[65] **Cho, C. G., Feit, B. A. and Webster, O. W.,** 1990: Cationic polymerization of isobutyl vinyl ether: livingness enhancement by dialkyl sulphides, *Macromolecules*, **23,** 1918-1923.

[66] **Lin, C.-H. and Matyjaszewski, K.**, 1990: *Polym. Prep.*, **31,** 599.

[67] **Greszta, D., Mardare, D. And Matyjaszewski, K.**, 1994: Living radical polymerization. 1. Possibilities and limitations, *Macromolecules*, **27**, 638-644.

[68] **Goto, A. and Fukuda, T.**, 2004: Kinetics of living radical polymerization. *Prog. Pol. Sci.*, **29,** 329-385.

[69] **Fischer, H.**, 2001: The Persistent Radical Effect: A Principle for Selective Radical Reactions and Living Radical Polymerizations. *Chem. Rev.*, **101,** 3581-3610.

[70] **Georges, M.K., Veregin, R.P.N., Kazmaier, P.M. and Hamer, G.K.**, 1993: Narrow molecular weight resins by a free-radical polymerization process Macromolecules, **26,** 2987-2988.

[71] **Wayland, B. B., Poszmik, G., Mukerjee, S. L. and Fryd, M.**, 1994: Living Radical Polymerization of Acrylates by Organocobalt Porphyrin Complexes. *J. Am. Chem. Soc.*, **116,** 7943-7944.

[72] **Wang, J.-S. and Matyjaszewski, K.**, 1995: Controlled/"living" radical polymerization. atom transfer radical polymerization in the presence of transition-metal complexes. *J. Am. Chem. Soc.*, **117,** 5614-5615.

[73] **Matyjaszewski, K. and Xia, J.**. 2001: Atom Transfer Radical Polymerization. *Chem. Rev.*, **101**, 2921-2990.

[74] **Peng, C.-H., Scricco, J., Li, S., Fryd, M. And Wayland, B.B.**, 2008: Organo-Cobalt Mediated Living Radical Polymerization of Vinyl Acetate. *Macromolecules*, **41,** 2368-2373.

[75] **Gridnev, A.A. and Ittel, S.D.**, 2001: Catalytic Chain Transfer in Free-Radical Polymerizations, *Chem. Rev.*, **101**, 3611-3660.

[76] **Moad, G., Rizzardo, E. And Thang, S. H.**, 2005: Living Radical Polymerization by the RAFT Process, *Aust. J. Chem.*, **58**, 379-410.

[77] **Perrier, S. and Takolpuckdee, P.**, 2005: Macromolecular design via reversible addition–fragmentation chain transfer (RAFT)/xanthates (MADIX) polymerization. *J. Polym. Sci., Part A: Polym. Chem.*, **43**, 5347-5393.

[78] **Moad, C. L., Moad, G., Rizzardo, E. and Thang, S. H.**, 1996: Chain Transfer Activity of ω-Unsaturated Methyl Methacrylate Oligomers, *Macromolecules*, **29,** 7717-7726.

[79] **Chiefari, J., Chong, Y. K., Ercole, F., Krstina, J., Jeffery, J., Le, T. P. T., Mayadunne, R. T. A., Meijs, G. F., Moad, C. L., Moad, G., Rizzardo, E. and Thang, S. H.**, 1998: Living Free-Radical Polymerization by Reversible Addition−Fragmentation Chain Transfer: The RAFT Process**,** *Macromolecules*, **31,** 5559-5562.

[80] **Favier, A. and Charreyre, M.-T**., 2006: Experimental Requirements for an Efficient Control of Free-Radical Polymerizations via the Reversible Addition-Fragmentation Chain Transfer (RAFT) Process, *Macromol. Rapid Commun.*, **27,** 653-692.

[81] **Buchmeiser M. R**, 1997: Synthesis of Polyenes That Contain Mesogenic Side Chains via the Living Polymerization of 4-(Ferrocenylethynyl)-4'-ethynyltolan, *Macromolecules*, **30**, 2274-2277.

[82] **Buchmeiser M. R., Schuler N., Kaltenhauser G., Ongania K-H, Lagoja I., Wurst K., Schottenberger H.**, 1998: Living Polymerization of Novel Conjugatively Spaced Ferrocenylacetylenes, *Macromolecules,* **31,** 3175-3183.

[83] **Buchmeiser M. R, Schuler N., Schottenberger H., Kohl I., and Hallbrucker A.**, 2000: Ferrocenyl- and octamethylferrocenyl-substituted phenylenevinylene-, thienylenevinylene-, and 1,1′-ferrocenylenevinylene spaced ethynes: Synthesis, metathesis polymerization, and polymer properties, *Des Monomers Polymers* **3,** 421-445.

[84] **Trnka T. M., and Grubbs R. H.**, 2001: The Development of $L_2X_2Ru{=}CHR$ Olefin Metathesis Catalysts: An Organometallic Success Story, *Acc Chem Res.,* **34,** 18-29.

[85] **Matyjaszewski K**., 1993: Ranking living systems, *Macromolecules,* **26**, 1787-1788.

[86] **Schrock R. R**., 1993: In: **Brunelle D.J.** (Ed.), *Ring-opening polymerization*, Hanser, Munich, p, 129.

[87] **Schrock R. R**., 1995: The Alkoxide Ligand in Olefin and Acetylene Metathesis Reactions, *Polyhedron,* **14,** 3177.

[88] **Ivin K. J., and Mol J. C**., 1997: *Olefin metathesis and metathesis polymerization*, Academic, San Diego, CA.

[89] **Weskamp T., Kohl F. J. and Herrmann W. A**., 1999: *N*-heterocyclic carbenes: novel ruthenium–alkylidene complexes. *J Organomet Chem*, **582,** 362-365.

[90] **Bielawski C. W. and Grubbs R. H**., 2000: Highly Efficient Ring-Opening Metathesis Polymerization (ROMP) Using New Ruthenium Catalysts Containing N-Heterocyclic Carbene Ligands, *Angew Chem*., **112,** 3025-3028.

[91] **Lynn D. M., Kanaoka R. H. and Grubbs R. H**., 1996: Living Ring-Opening Metathesis Polymerization in Aqueous Media Catalyzed by Well-Defined Ruthenium Carbene Complexes, *J Am Chem Soc.* **118,** 784-790.

[92] **France M. B., Grubbs R. H., and McGrath D. V. and Paciello R. A**., 1993: Chain transfer during the aqueous ring-opening metathesis polymerization of 7-oxanorbornene derivatives, *Macromolecules* **26**, 4742-4747.

[93] **Mohr B., Lynn D. M. and Grubbs R. H**., 1996: Synthesis of Water-Soluble, Aliphatic Phosphines and Their Application to Well-Defined Ruthenium Olefin Metathesis Catalysts, *Organometallics*, **15**, 4317-4325.

[94] **Liu X., Guo S., Mirkin C. A**., 2003: Surface and Site-Specific Ring-Opening Metathesis Polymerization Initiated by Dip-Pen Nanolithography, *Angew Chem*., **42**, 4785-4789.

[95] **Klavetter F. L, Grubbs R. H**., 1988: Polycyclooctatetraene (polyacetylene): synthesis and properties, *J Am Chem Soc.* **110,** 7807-7813.

[96] **Cabrera K., Lubda D., Eggenweiler H. M, Minakuchi H., and Nakanishi K**., 2000: *J High Res Chromatogr*., **23**, 93.

[97] **Schrock R. R**., 1990: Living ring-opening metathesis polymerization catalyzed by well-characterized transition-metal alkylidene complexes, *Acc Chem Res.,* **23,** 158-165.

[98] **Bairoch A**, 2000: "The ENZYME database in 2000" Nucleic Acids Research **28,** 304–305

[99] **Radzicka A., and Wolfenden R**., 1995: A proficient enzyme, *Science* **6, 267,** 90–93.

[100] **Dennison C.,** 2002: *A Guide to Protein Isolation*, Kluwer Academic Publishers, Newyork, p3.

[101] **Amersham Biosciences Corp.,** *Affinity Chromatography, Principles and Methods,* 2002: Amersham Biosciences Corp., 800 Centennial Avenue, PO Box 1327, Piscataway NJ 08855, USA, p.7

[102] **Amersham Biosciences Corp.,** *Ion Exchange Chromatography Principles and Methods*, 2002: Amersham Biosciences Corp., 800 Centennial Avenue, PO Box 1327, Piscataway NJ 08855, USA, p.10

[103] **Himmelhoch, S. R.,** 1971: Chromatography of proteins on ion-exchange adsorbents, *Meth. Enzymol.*, **22,** 273—286,

[104] **Ochoa, J. L.,** 1978: Hydrophobic (interaction) chromatography, *Biochimie*, **60,** 1-15.

[105] **Andrade J. D., in Andrade J. D. (ed.),** 1985: *Surface and Interfacial Aspects of Biomedical Polymers. Volume 2; Protein Adsorption*, Plenum Press, New York, p. 1–80.

[106] **Norde W.,** 1986: Adsorption of proteins from solution at the solid-liquid interface. *Adv. Colloid Interface Sci*. **25,** 267–340.

[107] **Horbett T.A. and Brash J.L.** in J.L. Brash and T.A. Horbett (Eds**.),** 1987: *Proteins at Interfaces: Physicochemical and Biochemical Studies*, *ACS Symp. Series 343*, American Chemical Society, Washington, D.C., p. 1–35.

[108] **Brash J.L. and Horbett T.A. in** Horbett T.A. and Brash J.L. (Eds.), 1995: *Proteins at Interfaces II: Fundamentals and Applications*, *ACS Symp. Series 602*, American Chemical Society,Washington, D.C., p. 1–23.

[109] **Andrade J.D., Hlady V., Feng L., and Tingey K. in** Brash J.L. and Wojciechowski P.W. (Eds.), 1996: *Interfacial Phenomena and Bioproducts*, Dekker, New York, p. 19–56.

[110] **Duke C.B.,** 1984: *J. Vac. Sci. Technol.*, *A 2,* 139–143.

[111] **Absolom D., Lamberti F., Policova Z., Zingg W., Oss C. V., and Neumann A.,** 1983: Surface thermodynamics of bacterial adhesion. *Appl. Environ. Microbiol.,* **46,** 90–97.

[112] **Absolom D.R., Hawthorne L.A. and Chang G.,** 1988: Endothelialization of polymer surfaces. *J. Biomed. Mater. Res.* **22**, 271–285.

[113] **Lee S. and Ruckenstein E.,** 1988: Adsorption of proteins onto polymeric surfaces of different hydrophilicities—a case study with bovine serum albumin. *J. Colloid Interfac. Sci.* **125,** 365– 379.

[114] **Norde W. and Lyklema J**., 1978: The adsorption of human plasma albumin and bovine pancreas ribonuclease at negatively charged polystyrene surfaces : I. Adsorption isotherms. Effects of charge, ionic strength, and temperature. *J. Colloid Interfac*. Sci. **66,** 257– 265.

[115] **Bagchi P., Birmbaum S.,**1981: Effect of pH on the adsorption of immunoglobulin G on anionic poly(vinyltoluene) model latex particles. *J. Colloid Interfac. Sci*. **83,** 460– 478.

[116] **Kondo A., Higashitani K.,** 1992: Adsorption of model proteins with wide variation in molecular properties on colloidal particles, *J. Colloid Interfac. Sci.* **150,** 344–351.

[117] **Luey J., McGuire J. and Sproull R .D.,** 1991: The effect of pH and NaCl concentration on adsorption of β-lactoglobulin at hydrophilic and hydrophobic silicon surfaces. *J. Colloid Interface Sci.* **143,** 489–500.

[118] **Kondo A., Oku S., Higashitani K.,** 1991: Structural changes in protein molecules adsorbed on ultrafine silica particles. *J. Colloid Interface Sci*. **143,** 214–221.

[119] **Kondo A., Murakami F. and Higashitani K.,** 1992: Circular dichroism studies on conformational changes in protein molecules upon adsorption on ultrafine polystyrene particles. *Biotechnol. Bioeng*. **40,** 889–894.

[120] **Norde W. and Favier J.P.**, 1992: Structure of adsorbed and desorbed proteins. *Colloids Surf*. **64,** 87–93.

[121] **Bohnert J. L. and Horbett T. A.**, 1986: Changes in adsorbed fibrinogen and albumin interactions with polymers indicated by decreases in detergent elutability. J. *Colloid Interface Sci*. **111,** 363–377.

[122] **Lu D. R., Park K.**, 1991: Effect of surface hydrophobicity on the conformational changes of adsorbed fibrinogen. *J. Colloid Interface Sci*. **144,** 271–281.

[123] **Elwing H., Welin S., Askendal A. and Lundstrom I.**, 1988: *J. Colloid Interface Sci*. **123,** 306–308.

[124] **McGuire J., Wahlgren M. C. and Arnebrant T.**, 1995: Structural Stability Effects on the Adsorption and Dodecyltrimethylammonium Bromide-Mediated Elutability of Bacteriophage T4 Lysozyme at Silica Surfaces. *J. Colloid Interface Sci*. **170,** 182–192.

[125] **Ho Y. S. and McKay G.**, 1999: Pseudo-second order model for sorption processes, *Process Biochemistry*, **34**, 451–465

[126] **Cheng Z., Zhu X., Shi Z. L., Neoh K. G. and Kang E. T.**, 2005: Polymer Microspheres with Permanent Antibacterial Surface from Surface-Initiated Atom Transfer Radical Polymerization**.** *Ind. Eng. Chem. Res*. **44**, 7098-7104.

[127] **Sidney S.**,1967: *Quantitative Organic Analysis*, third ed., Wiley, New York.

[128] **Bradford M. M.**, 1976: A rapid and sensitive method for the quantitation of microgram quantities of protein utilizing the principle of protein-dye binding. Anal. Biochem. **72,** 248-254.

[129] **Arica M. Y., Bayramoglu G.**, 2006: Invertase reversibly immobilized onto polyethylenimine-grafted poly(GMA–MMA) beads for sucrose hydrolysis. *J. Mol. Catal. B,* **38**, 131-138.

[130] **Langmuir I.**, 1918: The adsorption of gases on plane surfaces of glass, mica and platinum, *J Am. Chem. Soc*. **40**, 1361–1403.

[131] **Scatchard G.**, 1949: The attractions of proteins for small molecules and ions, *Ann. N.Y. Acad. Sci*. **51**, 660–673.

[132] **Freundlich H. M. F.**, 1906: Over the adsorption in solution. *J. Phys. Chem*. **57,** 385–391.

[133] **Dubinin M. M., Radushkevich L. V., 1947:** Equation of the characteristic curve of activated charcoal. *Chemisches Zentralblatt,* **1**, 875–882.

[134] **Bayramoglu, G., Arica, M. Y**., 2004:   Polyethyleneimine-grafted poly(hydroxyethyl methacrylate-co-glycidyl methacrylate) membranes for reversible glucose oxidase immobilization. *Biochem Eng J*., **20,** 73-77.

[135] **Senkal B. F., Bicak N.,** 1997: Aldehyde separation by polymer-supported oligo(ethyleneimines. *Polym. Sci. Part A: Polym. Chem.* **35**, 2857-2864.

[136] **Vicente C., Sebastian B., Fontaniella B., Marquez A., Filho L. X. and Legaz M. E.,** 2001: Bioskin as an affinity matrix for the separation of glycoproteins. *J. Chromatogr. A,* **917**, 55-61.

[137] **Johansson B. L., Belew M., Eriksson S., Glad G., Lind O., Maloisel J. L. and Norrman N.,** 2003: *J. Chromatogr. A*: Preparation and characterization of prototypes for multi-modal separation media aimed for capture of negatively charged biomolecules at high salt conditions. **1016,** 21-33.

[138] **Blanco R., Arai A., Grinberg N., Yarmush D. M. and Karger B. L.,** 1989: Role of association on protein adsorption isotherms. β-Lactoglobulin A adsorbed on a weakly hydrophobic surface, *J. Chromatogr.* **482,** 1–12.

[139] **Suen S. Y., Etzel M. R.,** 1992: A mathematical analysis of affinity membrane bioseparations, *Chem. Eng. Sci.* **47**, 1335–1364.

[140] **Kahraman M. V., Bayramoglu G., Kayaman-Apohan, N. and Gungor A., 2007:** UV-curable methacrylated/fumaric acid modified epoxy as a potential support for enzyme immobilization**,** *React Funct Polym**,*** **67,** 97-103.

[141] **Mateo C., Palomo J. M., Fernandez-Lorente G., Guisan J. M. and Fernandez-Lafuente R.,** 2007: Improvement of enzyme activity, stability and selectivity via immobilization techniques, *Enzyme Microb Technol,* **40,** 1451-1463.

[142] **Bayramoglu G., Arica M. Y. and Bicak N.,** 2004: Characterisation of tyrosinase immobilised onto spacer-arm attached glycidyl methacrylate-based reactive microbeads, *Process Biochem*, **39**, 2007-2017.

[143] **Sanjay, G. and Sugunan, S.,** 2008: Acid activated montmorillonite: an efficient immobilization support for improving reusability, storage stability and operational stability of enzymes, *J Porous Mater,* **15**, 359-367.

[144] **Neri D. F. M., Balcao V. M., Carneiro-da-Cunha M. G., Carvalho, Jr L. B. and Teixeira, J. A.,** 2008: Immobilization of a galactosidase from Kluyveromyces lactis onto a polysiloxane-polyvinyl alcohol magnetic (mPOS-PVA) composite for lactose hydrolysis. *J. A. Catal Commun*, **9**, 2334-2339.

[145] **Nestorson A., Neoh K. G., Kang E. T., Jarnstrom L. and Leufven A**., 2008: Enzyme immobilization in latex dispersion coatings for active food packaging. *Packag Technol Sci*, **21,** 193-205.

[146] **Bayramoglu G., Kaya B., Arica, M. Y.**, 2005: Immobilization of *Candida rugosa* lipase onto spacer-arm attached poly(GMA-HEMA-EGDMA) microspheres. *Food Chem*, **92,** 261-268.

[147] **Arica, M. Y.,** 2000: Immobilization of polyphenol oxidase on carboxymethylcellulose hydrogel beads: preparation and characterization, *Polym Int*, **49,** 775-781.

[148] **Arica M. Y., Yilmaz M. and Bayramoglu, G.,** 2007: Chitosan-grafted poly(hydroxyethyl methacrylate-*co*-glycidyl methacrylate) membranes for reversible enzyme immobilization, *J Appl Polym Sci*, **103,** 3084-3093.

CURRICULUM VITAE

Candidate's full name: Erdem YAVUZ

Place and date of birth: Yalova 22/06/1975

Permanent Address: Fatih Mah. Adnan Kahveci Cad. Ankara Sit. C Blok D:16
Büyük Çekmece-İstanbul

**Universities and
Colleges attended:**

Istanbul Technical University (Chemical Engineering)

Istanbul Technical University (Polymer Science and Technology)

Publications:

- Preparation of pyridine sulphonamide resin for the removal of dyes from aqueous solutions , Bahire Filiz Senkal, Emir Tugrul Tekin, **Erdem Yavuz**, Polymers For Advanced Technologies 2009, 20 (3), 308-311

- Thiol Containing Sulfonamide Based Polymeric Sorbent for Mercury Extraction, **Yavuz E**, Barim G, Senkal BF, Journal of Applied Polymer Science, 2009, 114(3), 1879-1883

- Glycidyl methacrylate grafted on p(VBC) beads by SI-ATRP technique: Modified with hydrazine as a salt resistance ligand for adsorption of invertase, Bayramoglu G, **Yavuz E**, Senkal BF, Arica MY, Colloids And Surfaces A-Physicochemical And Engineering Aspects, 2009, 345(1-3), 127-134

- Poly(vinylbenzylchloride) Beads Grafted with Polymer Brushes Carrying Hydrazine Ligand for Reversible Enzyme Immobilization, **Yavuz E**, Bayramoglu G, Senkal BF, Arica MY, Journal Of Applied Polymer Science, 113, 4, 2661-2669

- Poly(glycidylmethacrylate) brushes generated on poly(VBC) beads by SI-ATRP technique: Hydrazine and amino groups functionalized for invertase adsorption and purification, **Yavuz E**, Bayramoglu G, Senkal BF, Arica MY, Journal Of Chromatography B-Analytical Technologies In The Biomedical And Life Sciences, 2009, 877(14-15), 1479-1486

- The synthesis of new polymeric sorbent and its application in preconcentration of cadmium and lead in water samples, B. Filiz Senkal, Muharrem Ince, **Erdem Yavuz**, Mehmet Yaman, Talanta 72 (2007) 962–967

- Preparation of poly(glycidyl methacrylate) grafted sulfonamide based polystyrene resin with tertiary amine for the removal of dye from water, Bahire Filiz Senkal, Fatih Bildik, **Erdem Yavuz** , Ayfer Sarac, Reactive & Functional Polymers 67 (2007) 1471–1477

- Sulfonamide based polymeric sorbents for selective mercury extraction, Bahire Filiz Senkal, **E. Yavuz**, Reactive & Functional Polymers 67 (2007) 1465–1470

- Removal of dyes from water by poly(vinyl pyrrolidone) hydrogel, Senkal BF, Erkal D, **Yavuz E**, Polymers For Advanced Technologies 17 (11-12): 924-927 Nov-Dec 2006

- Preparation of poly(vinyl pyrrolidone) grafted sulfonamide based polystyrene resin and its use for the removal of dye from water, Senkal BF, **Yavuz E,** Polymers For Advanced Technologies 17 (11-12): 928-931 Nov-Dec 2006

- Ureasulfonamide polymeric sorbent for selective mercury extraction, Senkal BF, **Yavuz E,** Monatshefte Fur Chemie 137 (7): 929-934 Jul 2006

- Preparation of a new polymeric surfactant for emulsion polymerization, Sarac A, Senkal BF, **Yavuz E**, Gursel YH, Journal of Applied Polymer Science 101 (1): 348-352 Jul 5 2006

- Crosslinked poly(glycidyl methacrylate)-based resin for removal of mercury from aqueous solutions, Senkal BF, **Yavuz E**, Journal Of Applied Polymer Scıence 101 (1): 348-352 Jul 5 2005

- Poly(acrylamide) grafts on spherical polyvinyl pyridine resin for removal of mercury from aqueous solutions, **Erdem Yavuz,** Bahire Filiz Şenkal , Niyazi Bicak, Reactive & Functional Polymers 2005, 65, 121–125

- Poly (Acrylamide) Grafts On Spherical Polymeric Sulfonamide Based Resin For Selective Removal of Mercury Ions From Aqueous Solutions, B. F. Senkal, **E. Yavuz**, N. Bicak, Macromol. Sym. 2004, 217, 169-178